

The isolation of new tissue polarity genes in *Drosophila* and the genetic analysis of *Rab23* involved in the regulation of the number and planar organization of the adult cuticular hairs

Ph. D. Dissertation

Andreea Csilla Pataki

Supervisor: Dr. József Mihály

Institute of Genetics
Biological Research Center of the
Hungarian Academy of Sciences

University of Szeged

2010

„Az utakat sokáig nem érti meg az ember. Csak lépdél az utakon és másra gondol. Néha széles az egyik út, aszfaltos, néha rögös, barázdás, meredek. Az utakat sokáig csak alkalomnak tekintjük, lehetőségnek, melynek segítségével elmehetünk a hivatalba vagy kedvesünkhöz vagy a rikkantó tavaszi erdőbe. Egy napon megtudjuk, hogy az utaknak értelmük van: elvezetnek valahová. Nemcsak mi haladunk az utakon, az utak is haladnak velünk. Az utaknak céljuk van. Minden út összefut végül egyetlen közös célban. S akkor megállunk és csodálkozunk, tátott szájjal báméskodunk, csodáljuk azt a rejtelmes rendet a sok út szövevényében, csodáljuk a sugárutak, országutak és ösvények sokaságát, melyeken áthaladva végül eljutottunk ugyanahhoz a célhoz. Igen, az utaknak értelmük van. De ezt csak az utolsó pillanatban értjük meg, közvetlenül a cél előtt.”

(Márai Sándor)

TABLE OF CONTENT

Introduction.....	3
Planar cell polarity.....	3
Definition and short history.....	3
Model systems for PCP studies.....	4
<i>Drosophila</i> PCP genes and their phenotypes.....	8
The PCP regulatory hierarchy and a general model of PCP establishment in <i>Drosophila</i>	12
Asymmetric localization of the PCP proteins during development.....	14
Cell shape and planar polarity.....	17
Membrane trafficking and wing morphogenesis.....	17
Vesicular transport/ membrane traffic.....	18
Rab proteins.....	19
Rab protein family members.....	22
The mouse and <i>Drosophila</i> Rab proteins.....	23
Aims of the thesis.....	27
Materials and methods.....	28
Fly strains and genetics.....	28
Isolation of PCP mutants- mutagenesis screen.....	28
Isolation of new <i>Rab23</i> mutants.....	30
Determination of the lethal phase.....	30
DNA techniques.....	30
DNA preparation from single flies.....	31
Analysis of planar polarity in adult wings and notum.....	32
Analysis of planar polarity in adult eye.....	32
Analysis of planar polarity in the adult abdomen.....	32
Analysis of planar polarity in legs.....	33
Rab23 antibody production.....	33
Tissue culture.....	33
Immunohistochemistry.....	33
Immunoprecipitation and Western-blot analysis.....	34

Image acquisition.....	35
Statistical analysis.....	35
Results.....	37
Isolation of new PCP genes.....	37
Mapping of the new PCP mutants.....	37
Phenotypic characterization and mapping of the complementation group with five members.....	39
Mapping of the 82.1.4.1 mutant.....	42
Isolation and characterization of new <i>Rab23</i> alleles.....	45
<i>Drosophila Rab23</i> impairs hair polarity and number on the adult cuticle.....	47
<i>Drosophila Rab23</i> has no role in Hedgehog signaling and CNS development in flies.....	49
<i>Rab23</i> influences the place of prehair initiation and acts cell autonomously in <i>Drosophila</i> pupal wings.....	49
<i>Rab23</i> is required for hexagonal packing of the wing epithelium.....	51
The <i>Rab23</i> - induced multiple hair phenotype is not correlated with the packing defects.....	51
<i>Rab23</i> is required for the late cortical polarization of the PCP proteins and In.....	53
The subcellular localization of <i>Rab23</i> in the developing pupal wing cells.....	56
<i>Rab23</i> associates with the Pk protein.....	59
Dominant genetic interactions between <i>Rab23</i> and other PCP genes.....	62
Double mutant analysis of <i>Rab23</i> with core genes, In group genes and <i>mwh</i>	66
Discussion.....	70
List of abbreviations.....	77
References.....	81
List of publications.....	93
Acknowledgements.....	94
Summary.....	95
Összefoglalás.....	101

INTRODUCTION

Planar cell polarity

Definition and short history

In tissues, cells show coordinated properties and are polarized along different axes. Well known examples include the *Drosophila* ovary and embryo where all major body axes are determined in a single cell, the oocyte, neuronal cells that typically exhibit axonal-dendritic polarity and epithelial cells that are polarized in multiple ways. Apical-basolateral polarity (perpendicular to the plane of the epithelial sheet) enables a cell to directionally transport molecules across a cell layer (e.g. in the gut, kidney and glandular tissues) or to selectively secrete extracellular components from the basal lamina (Eaton and Simons, 1995). In many instances, however, tissue differentiation also requires the coordination of cell polarity within the plane of the tissue - a feature referred to as planar cell polarization (PCP) or tissue polarity, for short.

PCP was first recognized in 1975 in the eye and the cuticular bristle pattern of the insect *Oncopeltus fasciatus* (large milkweed bug) (Lawrence and Shelton, 1975), although it is now obvious that PCP can be observed throughout the nature. In plants it is studied mainly in *Arabidopsis* where the position of the root hairs is directed toward a concentration maximum of the hormone auxin in the root tip (Grebe, 2004; Fischer et al., 2006; Ikeda et al., 2009). In vertebrates it is evident in the ordered arrangement of fish scales or bird's feathers, hairs of the mammalian skin, cilia of the respiratory tract and the oviduct, or the stereocilia of the sensory epithelium of the inner ear. The detailed genetic and molecular dissection of what is now referred to as PCP, began 28 years ago with David Gubb's and Antonio Garcia-Bellido's observations that a small set of genes controls the polarity of cuticular hairs and bristles in *Drosophila* (Gubb and Garcia-Bellido, 1982). This was later accompanied by the detailed genetic analysis of several PCP genes (Gubb, 1993) and the molecular cloning of *frizzled*, a key PCP gene from *Drosophila* (Vinson et al., 1989). These initial insights were followed by systematic genetic screens in the fruitfly by several research teams and the subsequent molecular cloning and analysis of the identified PCP factors. Finally, in the last several years it has become clear that the basic mechanisms of PCP establishment are highly conserved from insects to vertebrates (Wang and Nathans, 2007; Roszko et al., 2009; Lai et al., 2009).

The analysis of PCP generation is now an important feature of developmental biological studies in many organisms. Despite the fact that the phenomenon of planar

polarization is widespread in nature, to date it has remained best studied in the *Drosophila* model system.

Model systems for PCP studies

PCP is evident in various body regions of *Drosophila* from which the most heavily studied are the wing, the eye and the epidermis. The simplest and best-understood model system is offered by the organization of wing hairs. The surface of the *Drosophila* wing is covered by a well organized epithelium of about 30.000 hexagonal cells, each of which displays a single protrusion, called trichome or hair (Figure 2. A). Wing hairs are formed during pupal life when each cell produces a single microvillus-like prehair stiffened by actin and microtubules. In wild type wing cells prehairst form at the distal vertex of the cells and extend distally as they grow (Figure 1. A) (Wong and Adler, 1993). In the adult wing all hairs align coherently along the proximal-distal axis, pointing towards the distal direction. The regulation of wing hair orientation and the hexagonal packing of these epithelial cells appear to be under PCP control (Classen et al., 2005).

The compound eye of *Drosophila* has emerged as another important model system to study planar cell polarity. The adult *Drosophila* eye is a highly organized neurocrystalline lattice consisting of about 800 unit eyes, called ommatidia. Each ommatidium is composed of 20 cells, including eight photoreceptor neurons, four lens-secreting cone cells, seven optically insulating pigment cells and one mechanosensory bristle cell. PCP in the eye is manifested in the mirror-symmetric arrangement of the ommatidial clusters (Figure 2. E). The rhabdomeres (R) are membrane- dense extensions of the photoreceptor cells that contain the light gathering rhodopsin molecules. The rhabdomeres of the outer photoreceptor cells (R1-R6) are grouped around the inner rhabdomeres, R7 and R8, in a way that R7 lies on the top of R8. Because the R3 and R4 rhabdomeres acquire an asymmetrical position within the photoreceptor cluster, the ommatidia obtains a chiral structure (Figure 1. E). Interestingly, ommatidia display a different chirality in the dorsal and ventral halves of the eye and are arranged in mirror image symmetry as compared to the dorso-ventral midline, also called equator. The mirror image orientation of the ommatidia is the direct consequence of ommatidial rotation during development (Figure 1. C) (Wolff and Ready, 1993). At the beginning of photoreceptor differentiation, each developing ommatidial cluster (precluster) consists of five cells, the precursors of the R8, R2/R5 and R3/R4 cells (Figure 1. C). Initially, these preclusters are symmetric with respect to the equator, subsequently however, the preclusters start to rotate and at the same time, the R3 and R4 photoreceptors are displaced from each other and acquire

an asymmetrical position within the cluster (Figure 1. C). Strikingly, although each ommatidia rotates about 90° , the distal and ventral clusters rotate in the opposite directions. Ultimately, the opposite direction of rotation leads to mirror-symmetric dorsal and ventral halves of the adult eye with asymmetric positioning of the R3 (anterior, polar) and R4 cells (posterior, more equatorial) within the trapezoid formed by the six outer photoreceptors (Figure 1. C, D) (Jenny and Mlodzik, 2006).

On the thorax and abdomen of *Drosophila*, sensory bristles are aligned along the anterior-posterior axis and point toward the rear end of the fly body. These bristles develop during the pupal stage and consist of four different cells that originate from a single sensory organ precursor (SOP) cell in two rounds of asymmetric division (Bardin et al., 2004). First, the SOP cell divides into a smaller anterior (pIIa) and a larger posterior (pIIb) cell. Next, the pIIa cell gives rise to the externally visible hair and the socket cell, whereas the pIIb cell generates the neuron and the sheath cell which are not visible from outside. In this process, PCP signaling is required to orient the mitotic spindle during asymmetric cell divisions that will determine the orientation of the future bristle cell (Gao et al., 2000; Roegiers et al., 2001; Le Borgne et al., 2003).

The abdomen of *Drosophila* represents a continuous epithelium that is subdivided into a succession of anterior (A) and posterior (P) compartments. Bristle pattern is organized by signaling across these compartment boundaries (Lawrence et al., 2004). The dorsal surface of the abdomen includes the pigmented tergites as well as regions of flexible cuticle. Most tergites are decorated with polarized hairs and bristles. From landmarks, it is possible to estimate positions of the cells vis-à-vis the compartments and their boundaries. The ventral surface consists of the sternites and the pleura. The latter is a flexible cuticle covered by polarized hairs, whereas the sternites are covered by bristles and hairs. Both the hairs and bristles originate from the histoblast nest cells that, during the pupal stage, propagate and migrate to replace the larval epidermis. As they migrate, some of the epidermal cells in the A compartment become selected as SOPs (Fabre et al., 2008). Both on the dorsal and ventral epidermal regions, bristles and hairs point posteriorly, indicating the polarity of the epidermal cells (Struhl et al., 1997; Lawrence et al., 2004).

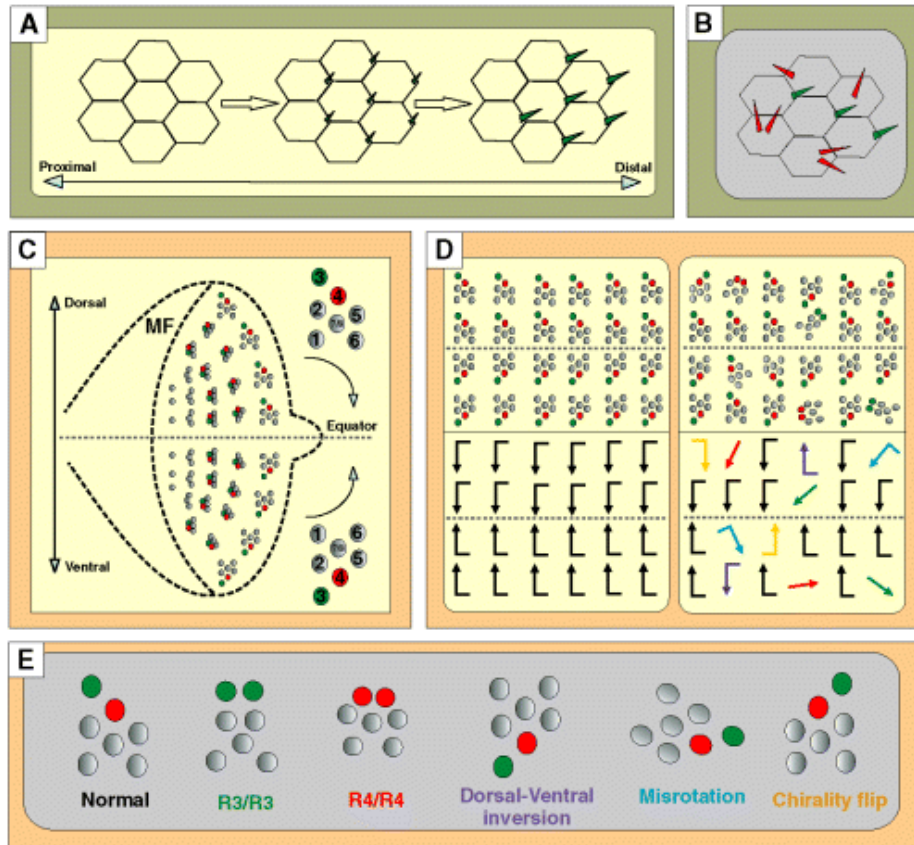


Figure 1. Planar polarity and PCP phenotypes in the *Drosophila* wing and eye. (A) The establishment of PCP in the wing begins with actin accumulation at the distal vertex (middle cartoon) that will subsequently lead to the formation of a distally pointing hair (shown in green). (B) The absence of PCP genes can affect hair formation in different ways. Hairs are sometimes disoriented, and the site of hair outgrowth is often not restricted to the distalmost part of the cell, or multiple hairs form in a single cell (mutant forms are indicated in red). (C) Ommatidial preclusters emerge from the morphogenetic furrow (MF) of the eye disc and initially form symmetric structures. As eye development proceeds, preclusters rotate 90° towards the equator, i.e. dorsal clusters rotate clockwise, while ventral ones rotate counterclockwise. At the end of this process the R3/R4 cell pair acquires an asymmetric position within the cluster, and thus chirality also becomes established (R3 cells are highlighted in green, R4 cells in red). (D) The mirror symmetric structure of an adult eye can be disrupted by PCP mutations that can cause rotation defects, dorsal-ventral inversions, and loss of chirality resulting in symmetrical ommatidia with either R3/R3 or R4/R4 cell pairs (see enlarged on E). (Mihály et al., 2005)

In vertebrates, the most widely used PCP model systems include the processes of convergent extension (CE), neural tube closure and eyelid closure, the determination of hair bundle orientation in the cochlea and follicle orientation in the mammalian skin. Convergent extension is a polarized cell movement during early embryogenesis whereby cells converge medially toward the axial midline, intercalate and extend the embryonic axis along the

anterior-posterior direction (Figure 2. I) (Wallingford et al., 2002). The cell types of the early vertebrate embryo that undergo this type of morphogenetic cell movements include mesodermal cells, and cells of the middle ectoderm of the neural plate where medial convergence is essential for neural tube closure (Figure 2. I-L) (Wallingford and Harland, 2001; Wallingford and Harland, 2002). In order to migrate during CE, cells elongate along the axis of migration and become polarized. Eyelid closure normally occurring in E16 (16 days old) developing mouse embryo is similar to neural tube closure; it involves CE of a pair of flanking epithelial sheets (Wang and Nathans, 2007).

The best studied vertebrate PCP model beyond CE is provided by the sensory epithelia of the inner ear. Cells of the sensory epithelia of the Corti- organ generate an array of uniformly orientated stereociliary bundles on their apical surface (Figure 2. G). The precise orientation of these stereociliary bundles is absolutely critical for both hearing and balance (Yoshida, 1999). The inner ear sensory epithelium is clearly an important model system for vertebrate PCP studies, with the unique advantages that the PCP phenotypes can be quantitatively scored at single cell resolution (Wang and Nathans, 2007), and that the developing epithelium from the Corti- organ can be cultured *in vitro* for at least one week during which time the hair bundles refine their orientations (Dabdoub et al., 2003).

The mammalian PCP phenomenon, that most closely resembles the oriented patterning of hairs and bristles on the *Drosophila* cuticle, is the regular arrangement of the epidermal hairs (Figure 2. C). Hair follicles make up accurate angle with the skin, and therefore each follicle and its associated hair has a defined orientation with respect to the body axis. A major difference between the mammalian hair follicles and the *Drosophila* hairs and bristles is that in *Drosophila* each wing epithelial cell makes a single hair, whereas each mammalian hair follicle is composed of hundreds of cells and is separated from the neighboring follicles by tens of cell diameters. Nevertheless, such as hair or bristle orientation in flies, hair follicle orientation in mammals is clearly coordinated as compared to the major body axes and the neighboring follicles (Wang and Nathans, 2007).

Despite the fact that the precise molecular mechanisms of PCP establishment in these different model systems are not entirely understood, recent findings revealed that PCP regulation is highly conserved from flies to human (Seifert and Mlodzik, 2007; Wang and Nathans, 2007; Simons and Mlodzik, 2008). Most of the current evidences indicate that tissue polarity is regulated by a very similar set of genes in all tissues and organisms examined. Thus, the core cassette of PCP genes is conserved across tissues and species, even though the cellular readouts of this conserved signaling cassette must be highly variable.

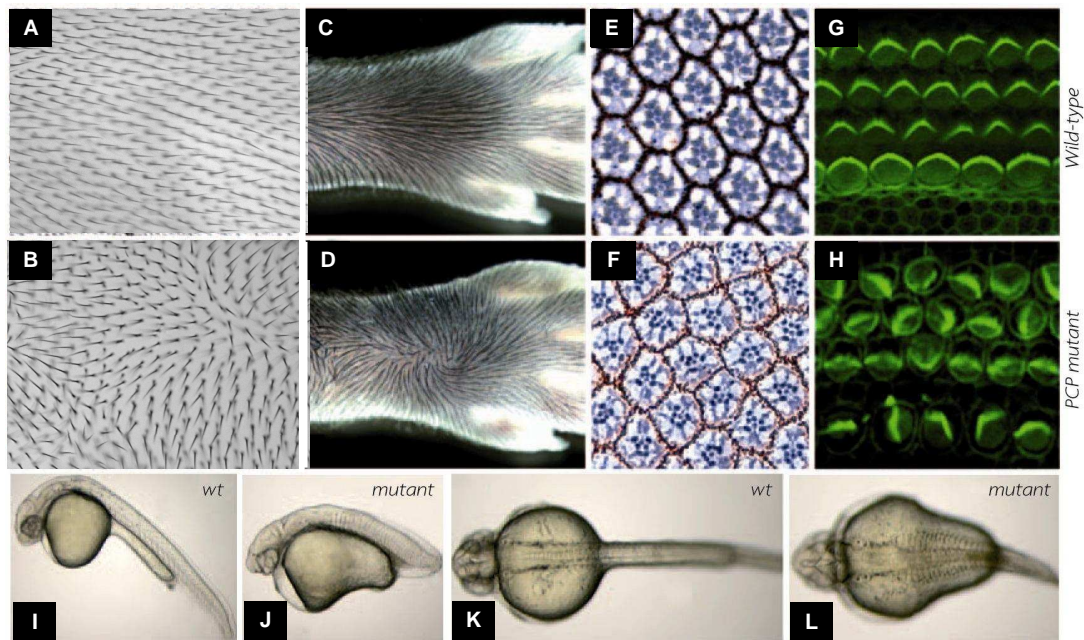


Figure 2. Characteristics of PCP pathway are conserved between flies and vertebrates. (A-D) Proximo-distal orientation of hairs on appendages in *Drosophila* and mouse. (A) Each wing cell of *Drosophila* generates a single distally pointing hair. (B) Mutations in PCP genes disrupt this orientation and instead, wing hairs create swirls and waves (*fz* mutant). (C, D) The pattern of mammalian fur/hair, similarly to *Drosophila*, is regulated by Fz/PCP signaling. In *fz* mutants the hairs do not point uniformly distally, swirls, waves appear (D-Fz6 mutant mouse). (E-F) PCP aspects of unit eye orientation in the *Drosophila* compound eye. The ommatidia are composed of photoreceptors arranged in precisely oriented trapezoids. In PCP mutants both the arrangement of photoreceptors in each ommatidium and the arrangement of ommatidia with respect to the whole eye become disorganized (F- *Stbm* mutant). (G-H) The sensory epithelia of the mouse inner ear. Individual sensory hairs of the cochlea generate polarized bundles of actin-based stereocilia (green). In PCP mutants these bundles still form but their orientation becomes randomized (G- wild type mouse; H- *Vangl2* mutant mouse). (I-L) PCP effects on convergent extension during vertebrate gastrulation and neurulation. Zebrafish embryos from PCP mutants fail to extend their antero-posterior axis as cells do not migrate distally nor intercalate medially in a coordinated manner. This leads to a shortened and broadened embryo (I, J- lateral and dorsal view of zebrafish embryos) and K, L- *trilobit* /*Stbm* mutants).

***Drosophila* PCP genes and their phenotypes**

Genetic studies in *Drosophila* led to the identification of a number of genes (now referred to as PCP genes) mutations of which impair tissue polarity. In the wing, mutations of PCP factors generally do not cause a complete randomization of hair orientation. Rather, hairs

tend to be roughly aligned with their immediate neighbors, leading to a large-scale pattern in which many hundreds of hairs create swirls and waves (Figure 1. B and Figure 2. B). In the eye the PCP mutations can lead to very diverse alterations in the polarity of the ommatidia. Ommatidia can be flipped along the D-V (dorsal-ventral) axis (e.g. for a dorsal ommatidia the adoption of ventral chirality) or along the A-P (anterior-posterior) axis. They can lose their polarized trapezoid form resulting in symmetric ommatidia and can display both under- and over-rotation defects (Figure 1. F and Figure 2. E). On the epidermis, in the absence of PCP signaling, the SOP cells still divide asymmetrically. However the axis of division is randomly chosen, and thus the bristles become randomly oriented (Fanto and McNeill, 2004).

Based on their phenotypic effects, PCP genes can be classified in different ways. For example, some of the PCP genes appear to affect polarity in all tissues examined and therefore these are often referred to as primary polarity genes, whereas some other genes act tissue-specifically and are placed into the group of the secondary polarity genes. Another classification relies on genetic epistasis analysis and the careful comparison of the phenotypic details. Below, I will introduce all major polarity genes according to the latter classification with focus on the wing phenotypes they cause when mutated.

The first group (upstream elements) includes two atypical cadherins, *dachsous* (*ds*) and *fat* (*ft*) as well as *four-jointed* (*ff*) encoding a type II transmembrane protein, and the transcriptional co-repressor *atrophin* (*atro*) (Adler et al., 1998; Zeidler et al., 2000; Strutt and Strutt, 2002; Ma et al., 2003; Fanto et al., 2003). Mutations of this group (often called the Ft/Ds group) exhibit two major phenotypic effects: polarity inversions and non-cell-autonomous effect (Adler et al., 1998; Zeidler et al., 2000; Ma et al., 2003). These genes have a role in PCP establishment in all tissues examined.

The second group of PCP genes consists of the core elements. Mutations in this group of genes impair hair orientation to various degrees, often causing a swirling pattern, while some cells display double hairs. In wing cells carrying these mutations pre-hairs typically form in the center of the cells (Figure 3.) (Wong and Adler, 1993). The core PCP gene to be cloned first was *fz* (*frizzled*) which was found to encode a seven-pass transmembrane protein (Vinson et al., 1989). Although Fz can act as a redundant receptor for the Wingless (Wg) ligand during canonical Wnt signaling (Bhanot et al., 1996), during PCP signaling *fz* is thought to act through a non-canonical Wnt pathway (Wong and Adler, 1993). Other members of the core group are the four-pass transmembrane protein Strabismus (Stbm), also known as Van Gogh (Vang) (Wolff and Rubin, 1998), the seven-pass transmembrane cadherin Flamingo (Fmi), also known as Starry night (Stan) (Chae et al., 1999; Usui et al., 1999), and the cytoplasmic

proteins Dishevelled (Dsh) (also involved in canonical Wg signaling) with three conserved domains (DIX, PDZ, DEP), Prickle (Pk), that contains three LIM domains and a PET domain (Tree et al., 2002b) and the ankyrin repeat protein Diego (Dgo) (Axelrod, 2001; Das et al., 2004). They all have intrinsic roles in polarizing individual cells, but some of them display non- cell- autonomous functions in polarizing neighboring cells. Both *fz* and *stbm* have long been implicated in transmitting polarity information to neighboring cells. Clones of cells mutant for *fz* often disrupt the polarity of neighboring wild type cells (Gubb and Garcia-Bellido, 1982). This non-autonomy can be observed on the distal side of wing clones and the polar side of eye clones (Zheng et al., 1995). Similarly, loss- of- function mutations in *stbm* revealed non- autonomous functions in opposite directions as compared to *fz* (Taylor et al., 1998). Mutations of *dsh* or *pk* affect cells within the clones primarily, and thus act in cell autonomous manner (Adler et al., 2000; Lim and Choi, 2004).

The third group of PCP genes (In group) includes Inturned (In) coding for a cytoplasmic protein with a putative PDZ domain (Adler et al., 2004), Fuzzy (Fy) a putative four- pass transmembrane protein (Park et al., 2006), and the WD40 repeat protein Fritz (Frtz) (Collier et al., 2005). Mutations of these genes cause the formation of multiple (mostly two) hairs per cell that are roughly equal in size, slightly misoriented and derive from prehairst formed around the cell cortex in abnormal positions (Figure 3.) (Adler et al., 2004). These genes act cell- autonomously, whereas in regard to tissue specificity, *in* affects the polarity of wing hairs, sensory bristles and weakly the ommatidia, while *fy* and *frtz* have roles in the establishment of hair and bristle polarity (Adler, 2002).

The fourth group (Mwh group) includes Multiple wing hairs (Mwh), a GBD-FH3 domain containing protein (Yan et al., 2008; Strutt and Warrington, 2008). The mutant of *mwh* is characterized by the presence of four or more hairs of different size in each cell, initiated from the cell periphery. *mwh* is known to act cell autonomously, and it is specific to the wing (Yan et al., 2008; Strutt and Warrington, 2008).

Apart from *mwh*, there are several other genes that affect wing hair number, many of which encode cytoskeletal regulators like the small GTPase family members: *RhoA* and *Drok* (*Rho associated kinase*) that appears to regulate wing hair number without major effects on hair orientation (Figure 3.) (Winter et al., 2001; Ma et al., 2003). Besides *RhoA* and *Drok*, additional small GTPase family members have also been shown to regulate hair formation. Cells lacking the activity of the actin polymerization regulator Cdc42 often fail to generate hair outgrowth or show multiple and short hairs, while cells expressing the dominant negative form of *Rac1* (small GTP binding protein) fail to restrict hair outgrowth to a single location

resulting in multiple wing hairs (Eaton et al., 1996). Furthermore, mutants of *tricornered* (*trc*) and *furry* (*fry*) show clustered and split hairs, while *misshapen* (*msn*), that is part of the Jun-N-terminal kinase pathway, also shows multiple hair phenotype (Adler et al., 2002).

Beside the core and wing-specific genes, there are several PCP factors that are responsible for correct PCP establishment in the *Drosophila* eye. This eye-specific effector group includes *nemo* (*nmo*), *roulette* (*rtl*) (Choi and Benzer, 1994), *lamininA* (*lamA*) (Henchecliffe et al., 1993), *scabrous* (*sca*) (Chou and Chien, 2002), Notch signaling elements such as the Notch (N) transmembrane receptor and its ligand Delta (Dl) (Cooper and Bray, 1999; Fanto and Mlodzik, 1999); the Janus kinase *hopscotch* (*hop*), and *Stat92E/marelle* involved in Jak-Stat pathway, the Wnt ligand, Wingless (Wg), the glycosyl-transferase Fringe (Fng) and the homeobox transcription factor, Mirror (Mirr) (Adler et al., 2002).

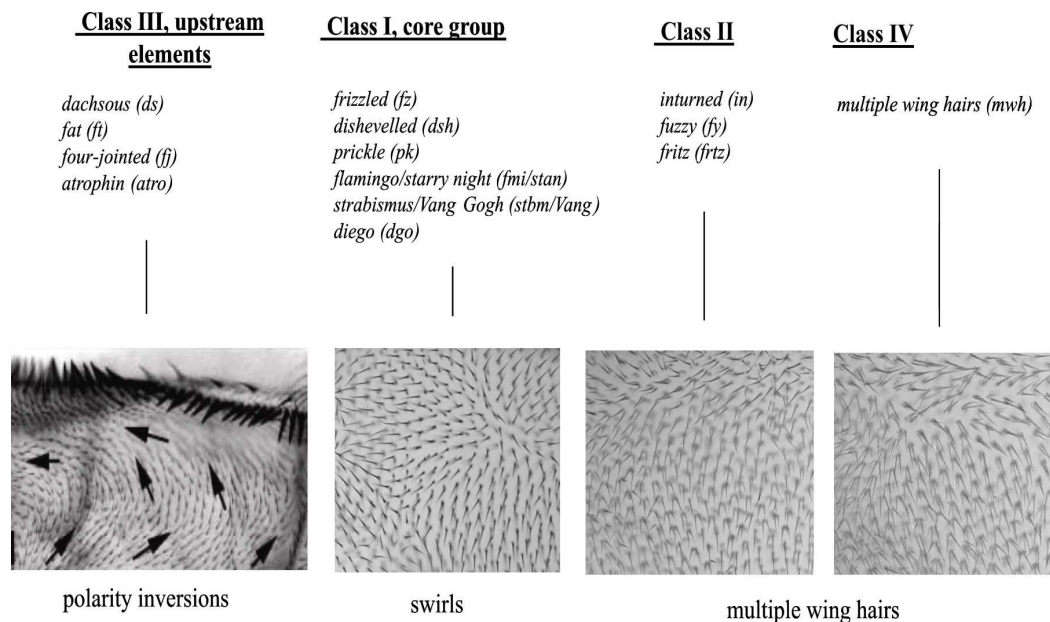


Figure 3. The four major groups of PCP genes based on their mutant wing phenotype. Mutations in the Ft/Ds group (Class III.) results in reversed polarity of the wing hairs; the core mutations (Class I.) mainly impair hair orientation, often swirls form; mutations affecting Class II and Class IV genes cause the formation of multiple wing hairs.

One of the most striking recent finding of the PCP field was that PCP regulation in vertebrates depends on a very similar set of genes as in *Drosophila*. It has been shown that the vertebrate homologs of *fz* (Fz3 and Fz6), *dsh* (Dvl1 and Dvl2), *stbm* (Vangl2), *fmi* (Celsr1-3), and *pk* (Prickle1 and Prickle-like2) have important roles in the establishment of correct

polarity during CE or inner ear development. When mutated alone or in combination, they give rise to PCP phenotypes (Figure 2. D, H, J, L) (Wang et al., 2006; Montcouquiol et al., 2006; Wang and Nathans, 2007; Roszko et al., 2009) indicating that the molecular mechanism of PCP establishment is highly conserved throughout evolution.

The PCP regulatory hierarchy and a general model of PCP establishment in *Drosophila*

Double mutant analysis demonstrated that the tissue polarity phenotypic groups summarized above, also represent epistatic groups of which *mwh* is epistatic to all the other groups. The In group is epistatic to the Ft/Ds group and the core group, and the core group is epistatic to the Ft/Ds group. These data together suggested that the PCP genes may act in a regulatory hierarchy where the Ft/Ds group is on the top followed downstream by the core, than the In and Mwh groups. Although the existence of such a linear hierarchy is debated (Casal et al., 2006; Lawrence et al., 2007), it has been proposed that polarity genes regulate PCP establishment through a multi- tier mechanism (Tree et al., 2002a). According to this view, in response to a graded ligand (first tier), a gradient of Fz activity (second tier) determines the direction of polarization and activates the cell type- specific tissue polarity effectors (third tier) (Lawrence et al., 2004). Although, this is clearly an attractive hypothesis that is in agreement with most published data, the source and nature of the polarity signal remained elusive, including the basic question whether it is a long or a short range signal.

Models counting with the long range possibility propose that polarity is established as a result of interpreting the concentration of a long-range signal, probably a secreted factor, present in a concentration gradient across the tissue. Despite the fact that the molecular nature of the polarity cue (often called factor X) is not known, several genes acting upstream of Fz have recently been implicated in long-range signaling. It has been shown that the activity gradients of Ft, Ds and Fj generate or modulate the activity of a long-range polarity signal (Zeidler et al., 1999; Simon, 2004; Mihály et al., 2005). Whether the activity of the Ft/Ds/Fj module will ultimately lead to the secretion of a Fz ligand or coordinate PCP in a different way, is still an open question. So far, experiments have provided evidences that Ft acts through the transcriptional corepressor Atro (Atrophin) (Fanto et al., 2003); supports for the *in vivo* existence of the Ft-Ds heterophilic interaction (Matakatsu and Blair, 2004); and proved that Fj is a Golgi-associated protein (Strutt et al., 2004). Strutt et al. also demonstrated that Fj is a signaling molecule present in a gradient on the proximal- distal axis of the wing and proposed that Fj most likely acts by modulating the activity of other proteins involved in intercellular signaling (Strutt et al., 2004). The best candidates for being the targets of Fj are

Ds and Ft which have been shown to act downstream of Fj (Yang et al., 2002). Additionally Fj may regulate cell adhesion by modulating Ds/Ft heterophilic interactions (Strutt and Strutt, 2002; Ma et al., 2003; Matakatsu and Blair, 2004) although the molecular mechanism of this modulation remains to be discovered.

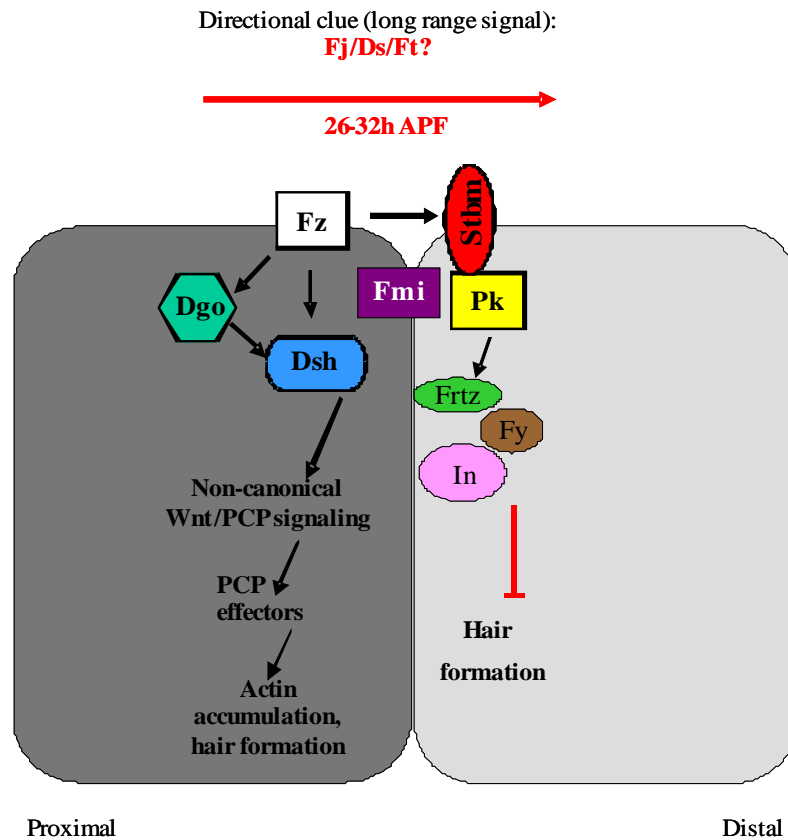


Figure 4. A model for PCP signaling in wing cells. First a directional clue that is provided by the Fj, Ds and Ft proteins determines the axis of polarization. This somehow initiates the asymmetric relocalization of the core PCP proteins that is enlarged by feedback mechanisms between the core elements themselves. This will lead to high Fz signaling activity on the distal side of the cell, which will subsequently activate the polarity effector proteins in the distal vertex where they initiate actin accumulation or with other words prehair formation. Additionally, it is believed that the Inturned complex prevents hair formation on the proximal side of the cell.

Based on the short range models, cells may not respond to a global directional cue (present in a concentration gradient), but instead, polarity information is only relayed to the neighboring cells through an asymmetric distribution of the PCP proteins. The asymmetric localization of the PCP complexes in one cell alters localization of these complexes in an adjacent cell through Fz-dependent feedback cycles (Tree et al., 2002b). It has been suggested

that a gradient of Ft activity controlled by Ds and Fj expression sets up an initial weak bias along the proximal-distal axis (Ma et al., 2003), which subsequently initiates a weak asymmetrical distribution of the PCP proteins, and that is finally stabilized by Fz-dependent interactions between neighboring cells (Figure 4.). How Ft activity would alter the asymmetric localization of PCP proteins is unclear, at present.

Asymmetric localization of the PCP proteins during development

Although the precise molecular mechanism of how PCP is established in different tissues still remains elusive, an important set of observations revealed that the core PCP proteins adopt a proximo- distally polarized subcellular localization in critical periods of PCP establishment, e.g. when prehairst form in the *Drosophila* wing cells (Usui et al., 1999; Axelrod, 2001; Shimada et al., 2001; Strutt, 2001; Tree et al., 2002; Bastock et al., 2003; Das et al., 2004). Significantly, the polarized enrichment of the core PCP proteins is critical for proper trichome placement in the wing, and polarity establishment in other tissues (Zallen, 2007). These initial studies suggested that during pupal wing development, the core PCP proteins are recruited into apico-lateral junctional complexes that are symmetrical until 24 hours after puparium formation (APF). However, at around 24 hours APF these complexes relocate into asymmetrical complexes in a way that asymmetry is evident until prehair initiation at about 32 hours APF. Subsequently, the polarized accumulation is lost again in few hours and by 36 hours APF it can hardly be detected. Between 24-32 hours APF Fz, Dsh and Dgo accumulate in distal junctional complexes (Axelrod, 2001; Strutt, 2001; Das et al., 2004), Pk and Stbm enrich in proximal complexes (Tree et al., 2002a; Bastock et al., 2003) (Figure I5. A), whereas Fmi is found on both sides of the membrane (Usui et al., 1999; Shimada et al., 2001). This polarized distribution of the core PCP proteins has been shown in other epithelial tissues as well, including the *Drosophila* eye and the dividing SOP cells (Mihály et al., 2005; Jenny and Mlodzik, 2006). Also, recent work revealed that some of the vertebrate PCP proteins display a polarized distribution suggesting that the polarized distribution is a key property of PCP function in epithelia, although differences do exist between different tissues.

Importantly, it has been demonstrated that all the core PCP proteins are required for the correct localization of each of the others (Zallen, 2007), suggesting that these proteins act together in multiprotein complexes. However, detailed phenotypic analysis revealed that the different proteins might play different roles in the process of PCP protein localization. In the

wing, for instance, some PCP mutations (e.g. *fmi*, *fz* and *stbm*) impair the apical localization of the other proteins, whereas others (e.g. *dsh*, *dgo* and *pk*) merely affect the asymmetric enrichment of PCP proteins without disrupting their apical localization. Regarding the potential physical association between the core PCP proteins, Fz has been reported to interact directly with Dsh (Wong et al., 2003; Strutt and Strutt, 2007), Stbm can associate with Pk (Bastock et al., 2003; Jenny et al., 2003), whereas Dgo can bind Pk and Stbm (Das et al., 2004). Together, these observations suggest that PCP protein localization can be divided into two main phases: proteins first become localized to adherens junctions, and in the second stage they become asymmetrically distributed. According to this model, the transmembrane proteins, Fz, Fmi and Stbm, are required for the membrane recruitment of the cytoplasmic proteins, Dsh, Dgo and Pk that are in turn involved in the formation and/or maintenance of polarized complexes.

Although the existence of polarized core PCP protein complexes is well established, recent studies challenged the view that PCP protein polarization is limited to 24-32 hours APF. Instead, it has been suggested that at least a partial proximal-distal polarization is already evident at the end of larval life and during the prepupal stages (6 hours APF). Polarity is then largely lost at the beginning of the pupal period, but becomes evident again in several hours until hair formation begins (Classen et al., 2005). Thus, molecular asymmetries are clearly revealed during wing hair formation, yet the molecular mechanisms that contribute to the establishment of these asymmetrical core PCP protein patterns are not well understood.

While much attention has recently been paid to the asymmetric localization of the core PCP proteins, novel studies on the planar polarity effector genes *in*, *fy*, *frtz* and *mwh* led to the discovery that these elements exhibit a polarized accumulation as well. The first study towards this direction revealed that the In protein becomes preferentially accumulated at the proximal edge of the pupal wing cells under the control of the core PCP genes in a *fy* and *frtz* dependent manner (Adler et al., 2004). *fy* encodes a transmembrane protein that could recruit In directly (Collier and Gubb, 1997), and single or double mutants of *fy*, *frtz* and *in* display almost identical wing hair phenotypes suggesting that these genes function together in PCP and might interact with each other directly (Wong et al., 1993; Lee and Adler, 2002). Very recent findings demonstrate that Fy and Frtz also show a proximal enrichment in a Stbm dependent manner, and together with In activate Mwh that is enriched on the proximal side of the wing cell (Yan et al., 2008; Strutt and Warrington, 2008).

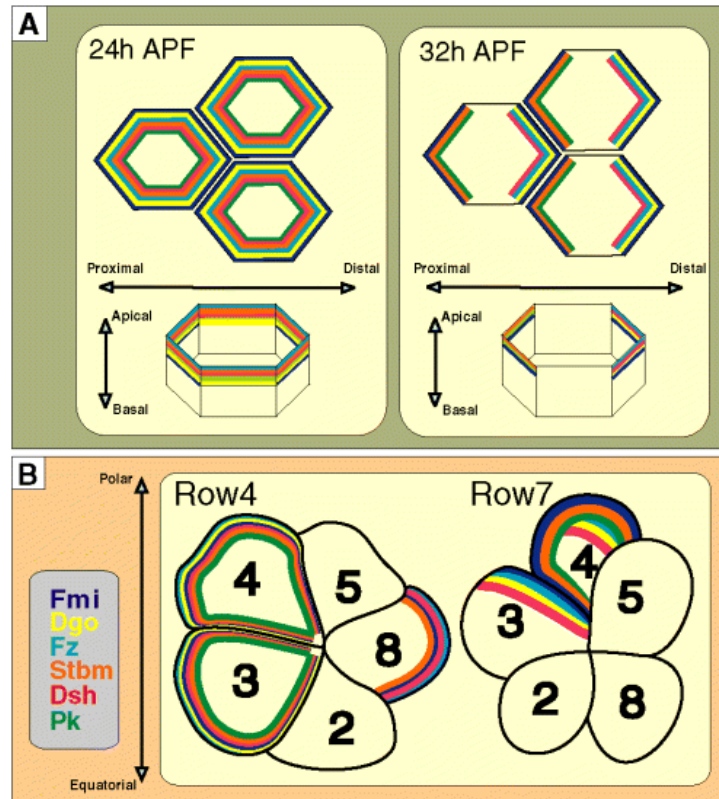


Figure 5. Core PCP protein localization in the developing wing and eye. (A) During the initial phase of pupal wing development [up to ≈ 24 h after prepupa formation (APF)] the protein products of the core PCP genes are found in apically localized symmetric complexes (shown on the left). However, at ≈ 24 h APF they redistribute into asymmetric complexes that are present transiently until actin accumulation begins at ≈ 32 h APF. Between 24 and 32 h APF Fz, Dsh and Dgo are enriched on distal cell membranes, Stbm and Pk accumulate on proximal membranes, while Fmi is found on both sides (right panel). (B) Although core PCP protein localization in the eye is somewhat more complicated than in the wing, it appears that PCP protein distribution across the R3/R4 cell boundary is remarkably similar to that of the distal–proximal cell boundaries in the wing. Notably, after the initial phases of ommatidia differentiation when PCP proteins do not show polarized accumulation, five or six rows behind the morphogenetic furrow Fz, Dsh and Dgo begin to preferentially accumulate on the R3 side, whereas Stbm and Pk accumulate on the R4 side, and Fmi becomes enriched on both sides of the R3/R4 interface. Developing ommatidia are shown in five-cell precluster stages before and after asymmetric redistribution takes place, in Row 4 and Row 7, respectively. Color code of the PCP proteins is identical in both (A) and (B). Numbers on (B) indicate the identity of the photoreceptor precursor cells. (Mihály et al., 2005)

Adler et al. hypothesized that In might function as an inhibitor of hair initiation on the proximal side of the wing cell (Adler et al., 2004). This information together with the recent finding that the site of prehair initiation is influenced by both proximal and distal protein

complexes, led to a model in which Fz/Dsh promotes hair formation at the distal-most part of the cell but only there, while at the same time Stbm/Pk inhibits hair formation in the proximal part acting through an In complex and Mwh (Strutt and Warrington, 2008).

Cell shape and planar polarity

The function of some epithelial tissues depends on the exact geometry of the constituent cells. The *Drosophila* wing for example consists of a hexagonally packed array of cells, each of which produces a single hair. Regular hair spacing and orientation have been proposed to guide air flow over the surface of the wing during flight (Wootton, 1992). Wing epithelial cells are irregularly packed during the larval and prepupal stages. In this period less than half of the cells are hexagonal. Subsequently however, by the time of prehair formation, the epithelium is repacked into a quasihexagonal array of cells (Classen et al., 2005) which involves the rearrangement of many of the cellular junctions.

Interestingly, it has been shown that the PCP proteins play important role in generating hexagonal packing of the wing epithelium (Classen et al., 2005). However, defects in packing geometry do not appear to directly perturb hair polarity in core PCP mutant wing cells (Classen et al., 2005). The possible exception to this rule is *pk* that exhibits very strong hair orientation defects and induces the strongest packing defects within the core PCP group (Classen et al., 2005; Lin and Gubb, 2009). Additionally, another study revealed that irregularities in cell geometry are associated with polarity defects in the case of *ft* mutant wing clones (Ma et al., 2008). Thus, cell geometry is not the direct determinant of cell polarity, but in some instances cell packing seems to have an impact on PCP signaling and hair orientation.

The cellular mechanisms of hexagonal packing, and the way how PCP proteins are transported to the proper membrane domains during formation of the asymmetric complexes, are equally elusive. However, it is conceivable that both of these processes include membrane trafficking that might help protein translocation and plasma membrane remodeling as well.

Membrane trafficking and wing morphogenesis

Upon activation by Wnt, the Fz receptor is internalized in a process that requires the recruitment of Dsh. Yu et al. (2007) have shown that the direct interaction of Dvl2 with Ap-2 is important for Fz internalization and Fz/PCP signaling. Internalization of Fz is likely to proceed by clathrin-mediated endocytosis (Chen et al., 2003; Yu et al., 2007). In addition, it has been shown that during wing PCP development, Fmi and Fz containing vesicles are

transported along microtubules that are approximately oriented along the A- P axis of the cell (Shimada et al., 2005). Thus, these results demonstrated that membrane transport plays a role during PCP signaling.

It has also been shown that during hexagonal packing of *Drosophila* wing epithelium, cellular junctions are rearranged and this requires extensive endocytosis and recycling of the adhesion molecule E-cadherin through endosomes containing Rab11. PCP proteins polarize trafficking of E-cadherin containing vesicles during junction remodeling (Fmi can recruit Sec5-positive vesicles containing E-cadherin). These observations indicate that PCP proteins may promote hexagonal packing by polarizing membrane trafficking.

Since cell fate determination is often dependent on precise levels of extracellular ligands, endocytic trafficking of these ligands and their receptors provides an important mechanism for communication between cells during development. The best evidence of a role for endocytic trafficking in PCP signaling is the Wnt/Wg signaling regulation in *Drosophila*. The Wg protein can be detected in cytoplasmic puncta in wing imaginal disc (van der Heuvel et al., 1989; Marois et al., 2005). It seems likely that Wg enters the cell by receptor-mediated endocytosis since both its receptor DFrizzled-2 (DFz2) and its coreceptor Arrow (Arr) contain putative endocytic sorting signals (Marois et al., 2005; Rives et al., 2006). Thus, the regulation of the distribution of the Wg morphogen is another important aspect of wing development that is controlled by membrane trafficking.

Together, these results underlined the importance of vesicle transport in several different aspects of wing development. Nevertheless, our understanding of membrane trafficking during PCP signaling has just begun, and further work is required to shed light on this process.

Vesicular transport/membrane traffic

The compartmentalization of the eukaryotic cells requires the constant transport of lipids and proteins between distinct organelles. To maintain the characteristic structure, biochemical composition and function of different organelles represents a formidable challenge for the organelles of the exocytic and endocytic pathways given the continuous flow of protein and membrane along these pathways. The exocytic pathway sorts newly synthesized proteins from the endoplasmic reticulum, through the Golgi apparatus to their final destination at the plasma membrane or lysosome vacuole. Conversely, the endocytic pathway is required for the uptake of nutrients and for the internalization of receptors. Newly internalized material is transported to the early endosome, a tubulo-vesicular network

localized to the cell periphery. Proteins destined for recycling are sorted to recycling endosomes and then to the plasma membrane, whereas proteins destined for degradation are transported to late endosomes (also called prelysosomes) and subsequently to the lysosome vacuole (Grosshans et al., 2006).

The mechanisms underlying membrane traffic can be divided into four essential steps. 1. Cargo is selected, and transport intermediates in the form of vesicles or tubules are formed. 2. These vesicles are delivered to their target membrane, often using molecular motors for transport along the microtubule or actin filament systems. 3. Tethering then brings the vesicle and the target membrane into close proximity. 4. The final step is the fusion of vesicles with the target membrane (Kartberg et al., 2005).

Rab proteins

Rab (Ras associated binding) proteins are ubiquitously expressed family of small (20-29 kDa) monomeric Ras-like GTPases (Chavier and Goud, 1999), that play a fundamental role in the regulation of vesicular membrane traffic (Touchot et al., 1987). They regulate vesicle transport by the association of motor and other proteins with the vesicles, and by docking and fusion of vesicles at defined locations (Chavier and Goud, 1999). Several subfamilies of closely related Rab GTPases share 75-95% sequence identity and overlapping functions, therefore many Rab GTPase genes are thought to be the product of gene duplications. Generally, Rab GTPases consist of a large GTPase and small N- and C- terminal domains. They differ mostly in their C- terminal domain's sequence, which is involved in subcellular targeting, whereas the regions involved in nucleotide binding are highly conserved (Echard et al., 2000).

Rab proteins closely resemble other Ras- related GTPases regarding their structure. They contain five parallel β - sheet strands plus one in anti parallel orientation flanked by five α - helices (Pfeffer, 2005). In this structure the elements responsible for guanine nucleotide and Mg^{2+} binding, as well as GTP hydrolysis, are located in five loops that contain the α - helices and β - strands (Figure 6.) These structures are highly conserved within the entire Ras superfamily, and therefore they can be used as landmarks to recognize any small GTPase family member (Stenmark and Olkkonen, 2001). Extensive sequence-analysis studies revealed the presence of five distinct amino-acid stretches that are characteristic for Rab GTPases. These so-called RabF regions cluster in and around Switch regions I and II, and are suggested to be characteristic to Rab proteins. In addition, four regions named RabSF can be

used to define the subfamilies of Rab GTPases, they probably allow the specific binding of downstream effectors (Figure 6.).

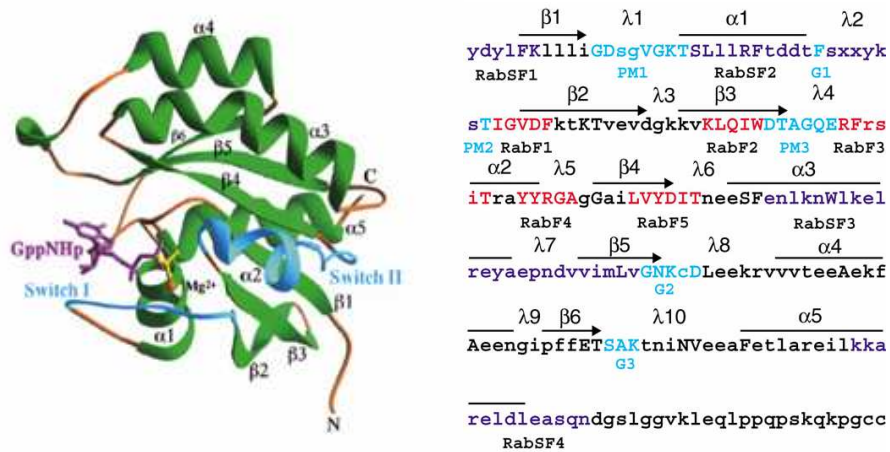


Figure 6. Structural features of Rab GTPases. On the left: Ribbon drawing of Rab3A complexed with the GTP analogue GppNHp. Purple, bound nucleotide; orange shore, Mg^{2+} ion; blue, switch I and II regions; green, α - helices and β - sheets; yellow loops. On the right: a profile amino-acid sequence of the Rab GTPase subfamily generated using the Markov model (HMM) method. Uppercase characters, residues found in the profile with a probability of $p > 0,5$; red, Rab-specific residues (RabF1-5); dark blue, subfamily-specific motifs (RabSF1-4); cyan, highly conserved nucleotide-binding motifs; G, guanine-base-binding motif; PM, phosphate/magnesium-binding motif. The secondary structure units: α helices, β - strands, and λ - loops are indicated above the sequence. (Stenmark and Olkkonen, 2001)

Crystallographic analysis has shown that Rab proteins adopt two different conformations (Ostermeier and Brunger, 1999). The GDP-bound form of the protein is complexed to a so-called GDP dissociation inhibitor (GDI) that complexes the isoprenoid functions of the Rab C-terminus, thereby enabling cytosolic localization of the protein. Upon contact with a donor membrane, a GDI displacement factor (GDF) initiates release of Rab from the Rab-GDI complex and promotes Rab membrane anchoring via the geranylgeranyl groups. Rab now can interact with membrane localized guanine nucleotide exchange factors (GEF) that catalyze GDP-GTP exchange. In the GTP-bound state Rab now does sense effector proteins that are connected with the target membrane, thereby participating in membrane fusion. Subsequently, a GTPase activating protein (GAP) catalyses GTP hydrolysis by Rab, and enables binding of RabGDI, that brings the Rab protein back to the cytosol, where a new transport cycle may start (Figure 7.) (Behnia and Munro, 2005; Pechlivanis and Kuhlmann, 2006).

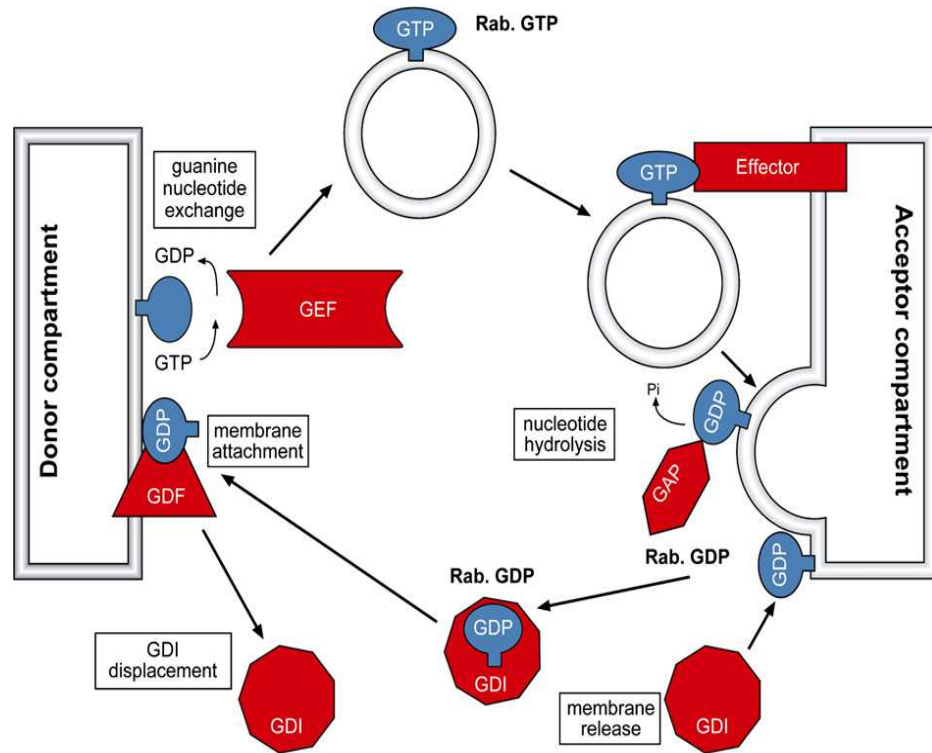


Figure 7. The Rab GTPase cycle. The Rab GTPase switches between GDP-bound inactive and GTP-bound active form. The conversion from the GDP- to GTP-bound forms is catalyzed by the guanosine-nucleotide-exchange factor (GEF), while the opposite change is by GTPase activating protein (GAP). The GTP-bound form interacts with effector molecules, while the GDP-bound form interacts with Rab escort proteins (REP) and GDP dissociation inhibitors (GDI), Pi-inorganic phosphate.

The Switch sequences of the Rab proteins are involved in the transition between the GDP and GTP bound conformation (Zhang et al., 2007). Mutations affecting these regions can lead to GTP-bound constitutively active (CA) or GDP-bound dominant negative (DN) forms (the well conserved Threonine or Serine amino acids are changed in the DN, Glutamine amino acid is changed in the CA forms) (Zhang et al., 2007).

In order to fulfill their functions, Ras GTPases undergo hydrophobic modifications. First, a common sequence motif at the C-terminus of the protein is recognized by a soluble isoprenyl transferase. Ras proteins with amino-acid CAAX box (Cysteine-aliphatic-aliphatic-arbitrary) are either farnesylated by the farnesyl transferase (FTase) or geranylgeranylated by the geranylgeranyl transferase (GGTase I) enzyme (Zhang and Casey, 1996; Roskoski and Ritchie, 1998). Rab proteins also contain isoprenylation motifs in their C-terminal xxxCC, -

xxCxC, -xxCCx, -xCCxx, or -Ccxxx pattern. Here a second geranylgeranyl transferase (GGTase II or RabGGTase) does catalyze the introduction of the hydrophobic side chain (Zhang and Casey, 1996). In addition to Ras family motifs, Rab family members require a helper protein, the Rab escorting protein (Grosshans et al., 2006), to be efficiently isoprenylated (Pereira-Leal et al., 2001).

Rab protein family members

Rab GTPases have been found in all eukaryotes investigated, including *Saccharomyces cerevisiae* (11 members), *Caenorhabditis elegans* (29 members) (Bock et al., 2001), *Drosophila melanogaster* (33 members) (Zhang et al., 2007) and mammals including human (63 members) (Zerial and McBride, 2001; Nishimura and Sasaki, 2008), some of which have been intensively studied for their roles in endosome and synaptic vesicle trafficking. Bioinformatical analysis has revealed that Rab genes exhibit a rather strict phylogeny of homology and function (Pereira-Leal and Seabra, 2001; Buvelot et al., 2006). Although Rab proteins are themselves highly homologous, their GEFs and GAPs that are specific for a particular Rab protein or related Rab protein, share very little structural or sequence homology among each other (Ng and Tang, 2008).

The first member of the Rab subfamily to be studied, Sec4p, was identified in yeast as an essential protein required for secretory vesicle exocytosis (Salminen and Novick, 1987). Mammalian relatives of Sec4p were identified and found to be specifically associated with distinct subcellular membrane compartments, some of them being considered as standard markers for these compartments. For example Rab1 is primarily enriched in the endoplasmic reticulum, Rab3 in synaptic vesicles, Rab5 in early endosomes, Rab6 and Rab10 in the Golgi, Rab7 and Rab9 in late endosomes, Rab8 in post-Golgi exocytic vesicles, and Rab11 in the recycling endosomes (Figure 8.) (Pfeffer, 2001; Pfeffer and Aivazian, 2004; Ali and Seabra, 2005; Jordens et al., 2005; Pfeffer, 2005).

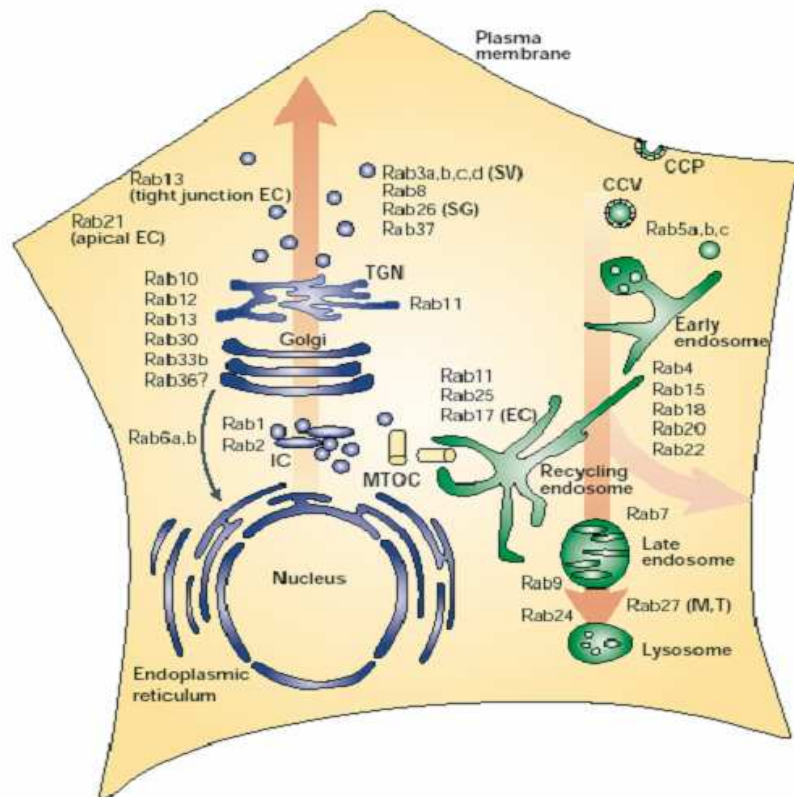
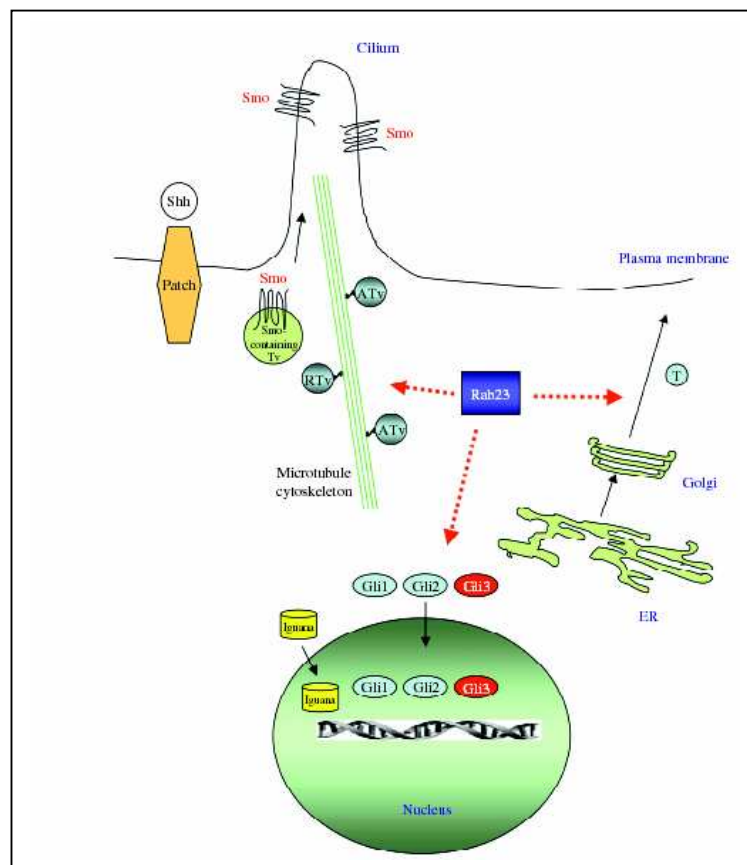


Figure 8. The intracellular localization of Rab proteins in mammalian cells. Some proteins are cell (for example Rab3a in neurons) or tissue specific (like Rab11 in tight junctions), others are localized on endomembranes. (CCV, clathrin-coated vesicles; CCP, clathrin-coated pits; EC, epithelial cells; IC, ER-Golgi intermediate compartment; M, membranes; MTOC, microtubule organizing center; SG, sensory granules; SV, synaptic vesicles; T, T-cell granules; TGN, trans Golgi network). (Zerial and McBride, 2001)

The mouse and *Drosophila* Rab23 proteins

Rab23 has been first described in 1994 as a novel small GTPase expressed predominantly in the mouse brain (Olkkonen et al., 1994). Later it has been shown that the mouse *open brain (opb)* gene (encoding *Rab23*) is cell autonomously required to define dorsal and lateral cell fates during mouse neural tube development (Eggenchwiler and Anderson, 2000). In the caudal spinal cord of E10.5 day *opb*¹ embryos, markers of dorsal cell types are reduced or absent and ventral markers are expanded. Eggenchwiler and coworkers have identified an *opb*² mutation that exhibited ventralization of neural cell fates in the spinal cord posterior to somite 17. This phenotype is similar to that described previously for *opb*¹ but significantly stronger. In *opb*² mutant neural tubes the Shh-responsive early markers of ventral neural progenitors were expressed in the same nested order as seen in wild-type embryos, but all the domains were expanded dorsally (Eggenchwiler and Anderson, 2000,

Guo et al., 2006). These results suggested that Rab23 is an essential negative regulator of the mouse Sonic-hedgehog (Shh) signaling pathway. It is required for the specification of dorsal cell fate in the spinal cord, that is an opposing role in neural patterning as compared to *Shh* required for ventral cell fate determination in the spinal cord (Eggenchwiler et al., 2001). The organization of ventral cell types in *opb*, *Shh* double mutants revealed that Shh-independent mechanisms can pattern the neural tube along its dorsal-ventral axis. This shows that dorsalizing signals activate transcription of *opb* (*Rab23*) in order to silence the Shh pathway in dorsal neural cells (Eggenchwiler et al., 2001), and it has also been revealed that *opb* acts downstream of *Shh*. In the chick, *Rab23* was found to be expressed asymmetrically in the Hensen's node, and to play a role in the dorsoventral patterning of the neural tube. It



acts in **Figure 9. Schematic diagram depicting signaling components of the Sonic hedgehog (Shh) pathway that may be subject of regulation by Rab23.** Solid arrows indicate various trafficking processes associated with Shh signaling components. Dotted-lined arrows indicate the possible influence by Rab23. Although Smo has been shown to translocate to the cilium from the cytoplasm, it is less likely to be a Rab23 target as it functions upstream of Rab23. On the other hand, some other cilia proteins carried by anterograde vesicles (ATv) and retrograde vesicles (RTv) may conceivably be regulated by Rab23. Rab23 may also influence the exocytosis of Tectonic (T), or the nucleocytoplasmic transport of Gli proteins or Iguana. (Wang et al., 2006a)

the same manner as described for the spinal cord in mouse, but unlike in mouse, it is already expressed asymmetrically during gastrulation (Li et al., 2008).

The Rab23 protein was first linked to vesicular trafficking and endocytosis in 2003 by Evans et al. They revealed that Rab23 is localized to plasma membrane and shows colocalization with the early endosomal marker Rab5, but not with the late endosomal marker LBPA (lysobisphosphatidic acid) (Evans et al., 2003). To investigate Rab23 with respect to members of the Shh signaling pathway, Rab23-GFP was coexpressed with either Patched (Ptc) (Shh receptor) or Smoothed (Smo) a transmembrane protein required to transduce the

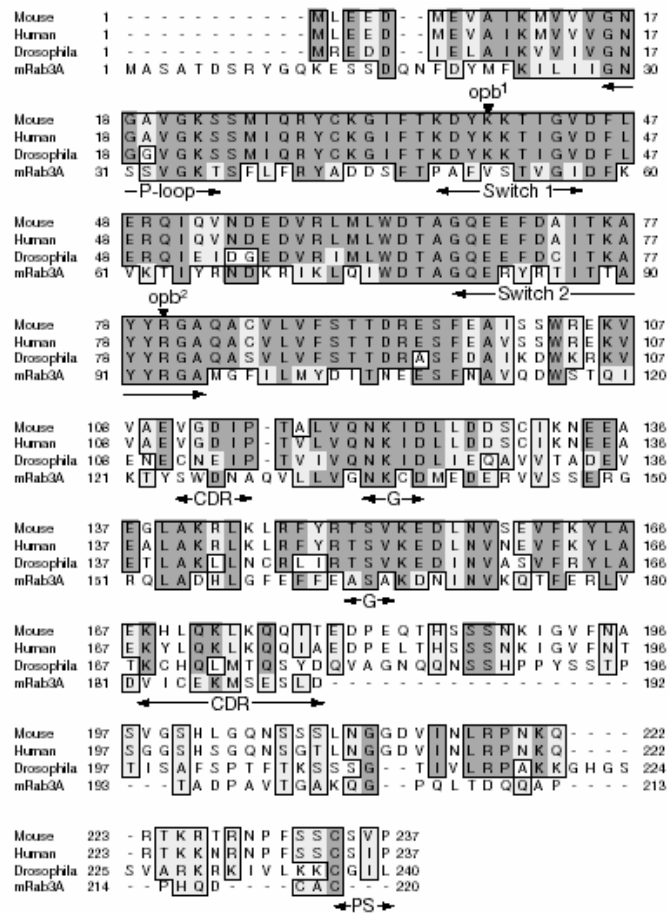


Figure 10. Alignment of mouse, human and *Drosophila* Rab23 and mouse Rab3a sequences. Positions of stop codons in *opb*¹ and *opb*² alleles (mouse orthologues) are indicated above the sequence. Functional domains defined in other Rab family proteins are indicated below the sequence: P-loop, phosphate binding loop; Switch1 and 2, conformational switch regions; CDR, Rab effector binding regions; G, guanosine nucleotide-binding residues; PS, prenylation site. The WDTAGQE (red line) *Drosophila* amino acid sequence before the switch II region is responsible for nucleotide binding and hydrolysis. The Q96L change results in a constitutively active form. (Eggenschwiller et al., 2001)

Shh signal. Ptc colocalized with intracellular Rab23-GFP but Smo did not. Analysis of Patched distribution by light and immunoelectron microscopy revealed that it is primarily localized to endosomal elements, including transferrin receptor-positive early endosomes and putative endosome carrier vesicles and, to a lesser extent, with LBPA positive late endosomes. Neither Ptc nor Smo distribution was altered in the presence of wild-type or mutant Rab23-GFP, suggesting that despite the endosomal colocalization of Rab23 and Patched, Rab23 acts independently and downstream of Ptc in regulating Hh signaling (Evans et al., 2003). Later genetic analysis has shown that Rab23 functions downstream of Smo and affects the function of the Shh regulated Gli family of transcription factors (Figure 9.) (Eggenchwiller et al., 2006; Wang et al., 2006a). In addition to these observations, another study has shown that Rab23 controls phagosome maturation modulated by *Salmonella typhimurium*, as DN mutants of *Rab23* interfere with phagosome-lysosome fusion in HeLa cells (Smith et al., 2007).

In contrast to other organisms, the knowledge about the *Drosophila Rab23* orthologue remained very poor. According to FlyBase (an integrated *Drosophila* Genome database), the *Drosophila Rab23* gene is located on the right arm of the third chromosome in the 83B9 cytological region. It encodes a 268 amino acids long polypeptide with the characteristic GTPase domain, and overall the predicted protein is 55% identical to mouse *Rab23* (Figure 10.) (Eggenchwiller et al., 2001). However, prior to our work, functional or phenotypic data were not available.

AIMS OF THE THESIS

Tissue polarity or planar cell polarity is a widespread and conserved phenomenon in nature. The detailed genetic and molecular dissection of PCP began 28 years ago by the identification of a small set of genes that controls the polarity of cuticular hairs and bristles in *Drosophila* (Gubb and Garcia-Bellido, 1982), and subsequently, *Drosophila* has become one of the best-studied model organism of this field.

Although by now much has been learned about the genes and pathways contributing to PCP establishment in flies, many fundamental questions remained unanswered. What is the ligand of the Fz receptor in the Fz/PCP pathway? The mechanistic details of protein localization are largely missing or just poorly understood. The link between Fz signaling and asymmetric localization of the core PCP proteins and In is not understood, and it remains a mystery how upstream elements are coupled to the asymmetric enrichment of the PCP proteins. Furthermore the tissue- specific downstream components or their way of action is still an open problem.

The major aim of this work was to answer part of these questions by isolating new PCP genes and by studying their role during PCP signaling and development.

We have successfully isolated new PCP mutations by conducting out a large scale mutagenesis screen. Later on, we have molecularly mapped two novel PCP complementation groups identifying the *Drosophila Kuzbanian-like* and *Rab23* genes. For detailed functional analysis we have chosen *Rab23* which encodes a putative membrane transport protein and addressed the following specific questions:

- What is the role of *Rab23* during PCP establishment?
- Where does Rab23 fit into the PCP pathway?
- What is the regulatory relationship between *Rab23* and the known PCP proteins?
- What is the mechanism through which Rab23 acts at the cellular and molecular level?

MATERIALS AND METHODS

Fly strains and genetics

Flies were grown on cornmeal-yeast food at 25°C. We used *OregonR*, and *w*¹¹¹⁸ as wild type strains. Fly strains carrying the *ru*, *cu*, *ca* mapping chromosome and the deletions were obtained from the Bloomington and Szeged stock centers, except for the different *Rab23* alleles (see below), and the *Ubx-Flp* stocks (Emery et al., 2005) which was a generous gift from J. Knoblich (IMBA, Vienna). Other stocks used: *P{RS5}5-SZ-3123* (DrosDel), *Rab23* RNAi line (c2L 54F9 8178) has been provided by the VDRC RNAi Center (IMP-IMBA, Vienna), whereas the *w; UASp-YFP::Rab23* lines were generous gifts from M. Scott (Stanford University, Stanford).

The following mutant alleles were used in interaction studies: *fz*²¹, *dsh*¹, *fmi*^{fz3}, *dgo*³⁸⁰, *pk*^{pk-30}, *pk*^{pk-sple-13}, *stbm*⁶, *frtz*¹, *in*¹, *fy*³, *mwh*¹.

Mitotic clones were generated using the FRT/Flp system (Xu and Rubin, 1993). Flip-out clones of *UASp-YFP::Rab23* were generated using *w,hsFLP;ActP-FRT-y+-FRT-Gal4,arm-lacZ,FRT40A* by applying 2 hours heat shock at 37°C during the early third instar larval stage. For overexpression studies we used *Act5C-Gal4* or *Sal-Gal4* drivers.

Isolation of PCP mutants, mutagenesis screen

In order to isolate new PCP genes, we mutated the second chromosome and the right arm of the third chromosome taking advantage of the FRT/Flp mosaic recombination system (Xu and Rubin, 1993). As a Flp source, we used *Ubx-Flp* which is expressed at the highest level in the wing imaginal discs (Pirrotta et al., 1995) (Figure 11. B), and thus induces recombination in the presumptive wing and notum cells where polarity in adults can easily be followed under normal stereomicroscopes. The large clone size is partly ensured by the fact that *Ubx-Flp* is expressed from early stages of development and in addition, mutant clones are induced on a genetic background where the so called twin-spot cells are eliminated by the cell lethal technique (Newsome et al., 2000). To further increase the sensitivity and reliability of the screen, we performed an F₂ screen (Figure 11.) that offered the advantage of recognizing even the weak and low penetrance phenotypes, and eliminated the sterility problems of F₁ screens.

In the first step of the screen we mutagenized 4 days old male flies carrying the appropriate FRT chromosome. As a mutagenic agent we either used EMS (ethyl

methanolsulphonate) in 30mM concentration or ENU (N-ethyl-N-nitrosourea) in 1,6mM concentration both in 1% sucrose solution. After feeding 4x100 males with the mutagen agent, these were crossed to 4x80 females in each experiment. All crosses were transferred in new bottles two times in three days intervals. The unused mutagen and the contaminated tools were neutralized in 20% Na-tiosulphate and 0,1N NaOH solution. The dosage of used mutagen was reported to induce an average of one hit per chromosome. The male progeny of crossed males carrying the mutated chromosome (F1) (FRT42 on 2R, FRT40 on 2L, FRT82 on 3R) were then crossed individually to females carrying the appropriate balance chromosome. For example, for the right arm of the second chromosome the male progeny of this cross (F2 males) were crossed to *y w Ubx-Flp; FRT42, arm-lacZ, l(2R)3.7/CyO, y+* females, and siblings of this cross were analyzed for PCP phenotypes on the wing and notum. After that, we established stable stocks from the mutant lines that exhibited PCP defects.

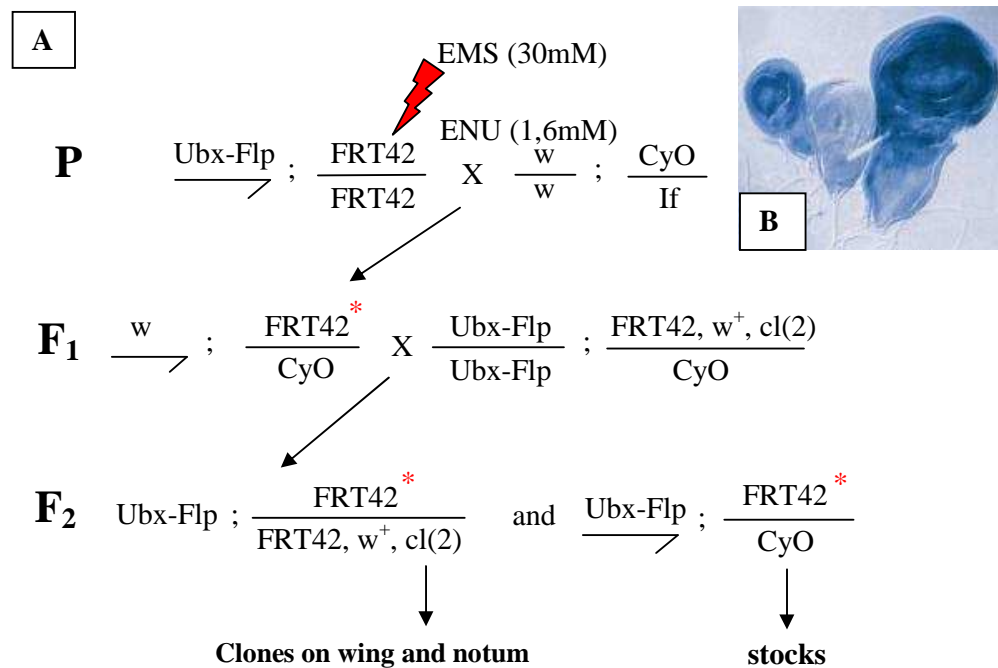


Figure 11. Generation of new PCP mutants. (A) Crossing scheme for the right arm of the second chromosome. At the beginning of the screen mutagenized males were crossed with double- balanced females. F₁ males carrying the mutagenized chromosome over a balancer were crossed to Ubx-Flp females also carrying an FRT *cell lethal* chromosome over balancer. In the second generation we observed the mutant clones on the notum and wings. Before establishing the stocks, in order to check our mutants, we back crossed the males with the Ubx-Flp carrying females. (B) Ubx-Flp expression in L3 wing disc.

Isolation of new *Rab23* mutants

In order to generate new *Rab23* alleles, we used the P-element excision technique. The P- element *P{RS5}5-SZ-3123* (DrosDel) inserted into the first intron of the *Rab23* gene was remobilized using a *Sb/Tm3,Δ2-3* transposase source. Candidates carrying potential imprecise excisions were tested with PCR analysis using the Rab23F1 and Rab23R1 primers (see below) to detect the potential deletions. Successful candidates were later tested with other primer pairs to determine more precisely the place of the deletion and to check if the excision alleles contain P- element residues.

Determination of the lethal phase

We established stocks carrying the mutant *Kul* and *Rab23*^{T69A} chromosomes over a *TM6,Tb,Ubi-GFP* balancer chromosome. This allowed us to select homozygous embryos from the stocks that did not express the GFP marker. By monitoring the development of these animals we could determine till what developmental stage they survive. In each case 100-100 homozygous mutant embryos were collected and observed.

DNA techniques

DNA constructs for transgenic flies and transfection experiments were made with standard cloning techniques and the *Drosophila* Gateway system (Hartley et al., 2000).

For transfection vectors the *Rab23* coding region was PCR amplified from a *Rab23* cDNA clone (RH23273) using the Rab23pF1 and Rab23pR1 primer pairs. The EcoRI fragment was introduced into pJET1 cloning vector (Gene JET Fermentas kit) and the resulting clone was sequenced with the pJET primers. Then the Rab23 coding region was ligated into EcoRI- digested pENTR3C Gateway vector. Later on the pENTR3C-Rab23 clone was introduced into different destination vectors by LR reaction using the Gateway LR ClonaseII Enzyme mix (Invitrogen).

To create a *Rab23* genomic rescue construct, the gene has been amplified from the BACRO03P13 genomic clone (BACPAC Resources). The 12,3 kbs Xba1 restriction fragment carrying the gene has been inserted first into a pBS KS+ vector, and after that recloned into the pCaSpeR4 *Drosophila* transformation vector. To clone the *Rab23*⁵¹ transcript, total RNA was isolated from homozygous mutant adults with Trizol reagent (Invitrogen), cDNA was synthesized with Revert Aid (Fermentas), RT-PCR was carried out with primers specific to the first and third exon of *Rab23*, respectively Rab23Ex3 and Rab23Ex1.

The *Kul* genomic rescue construct was cloned out from the BACRP98203 genomic clone (BACPAC Resources). For the rescue experiments the 8,4 kbs BglIII- EcoRV fragment, including the entire gene with 5' regulatory region was subcloned into pCaSpeR4 after multiple cloning steps.

Primer sequences:

Pry4	CAA TCA TAT CGC TGT CTC ACT CA
Rab23F1	CTG CAG AAA GAC ACA TTC GG
Rab23R1	AAA CCC GTT CAC ATC GAA GC
Rab23pF1	GGG AAT TCA TGC GTC TAA TCC AAA CGG C
Rab23pR1	GGG AAT TCC AAT ATT CCG CAT TTC TTG AGC
Rab23Ex3	CCC GGC CAC AAC ATC ATT AG
Rab23Ex1	TCA AAT TTC GAT CGC GAC GAG

For transfection experiments the following constructs were built: pAVW-Rab23, pPHW-Rab23, pPVW-Rab23, pPMW-Rab23, BLMT-RFP-Rab23, pAVW-Rab23^{Q96A}, pPVW-Rab23^{Q96A}, BLMT-Rab23^{T69A}, BLMT-Rab23^{Q96A}-EGFP, pAC5.1-Fz-Myc, pAC5.1-Dsh-EGFP, pAC5.1-HA-Dgo, pAC5.1-6xMyc-Pk, pRME-Stbm-HA (a kind gift from T. Wolff, Washington University). When necessary, pActin5c-Gal4 has been cotransfected to drive expression from UAS promoters. Expression from the BLMT vectors was induced by 1mM CuSO₄ for 4 hours or 500µM CuSO₄ ON (overnight).

DNA preparation from single flies

Single flies were placed into 0,5ml Eppendorf tubes, and mashed with a pipette tip containing 50µl SB buffer (10mM Tris-Cl pH=8.2, 1mM EDTA, 25mM NaCl, and 200µg/ml ProteinaseK, with the enzyme diluted freshly each day). After breaking the fly body the SB buffer was expelled from the pipette tip. Preparations were then incubated at 37°C for 30 minutes, followed by an incubation of 1-2 minutes at 95°C in order to inactivate the ProteinaseK. Preparations were then stored at 4°C.

Analysis of planar polarity in adult wings and notum

For microscopic analysis of the wings, flies were stored in glycerol-ethanol 3:1 solution for at least 1 hour. After that, the wings were collected, washed in distilled water and mounted in Hoyer's solution (Sullivan et al., 2000) on microscopic glass plates and incubated overnight at 60°C. For genetic interaction studies, wing hairs were counted on the dorsal side of the wing in the proximal half of the A region. Statistical analysis was done with the Microsoft Office Excel2003 program. The sensory bristles and trichomes on fly notums were observed under stereomicroscopes in Voltalef oil.

Analysis of planar polarity in adult eyes

In order to analyze the *Kul* LOF clones in eyes, fly heads were dissected and after a cut on one of the eyes (to expose the inside of the head to the fixative), the heads were placed into 2% glutaraldehyde in PBS in Eppendorf tube on ice. After 15 minutes the eyes were collected by centrifugation and incubated for 1 hour in 1:1 mixture of OsO₄ and glutaraldehyde. After the solution mixture was replaced with OsO₄, heads were incubated for another 1-6 hours and were dehydrated successively in 30%, 50%, 70%, 90% and 100% ethanol for 10 minutes each. After dehydration, the ethanol was replaced with propylene-oxide for 10 minutes and incubated overnight in equal volumes of propylene- oxide and resin mixture at room temperature. Next day the solution was removed and heads were incubated 4 hours in resin. After they were transferred into molds in Durcupan resin (Fluka), positioned and incubated at 70°C overnight, the excess of resin around the eyes was trimmed and the embedded eyes sectioned horizontally with microtome. Sections were collected on microscope slides in a drop of water, and dried at 65°C for 2 minutes. Afterwards, in order to get a clearer image, we stained the sections with a mixture of 1% borax and 1% toluidine-blue for 1-5 minutes at 65°C. In case of sections of clonal eyes we didn't stain the slides as the clone border (the border of w^+/w and w/w tissues) on these sections are visible only on unstained sections.

Analysis of planar polarity in the adult abdomen

For abdomen analysis, flies were stored in glycerol-ethanol 3:1 solution for 2-3 days. After removing the head and thorax, the abdomens were placed into 96% ethanol for 20 minutes and a cut was made on the dorsal side of abdomen. Cut abdomens were placed into glycerol for 10 minutes and after cleaning, they were mounted in 10% KOH solution and

incubated for 30 minutes at 51°C. Abdomens were then washed away from the cover slips, mounted in Hoyer's solution (Sullivan et al., 2000) and incubated ON at 60°C.

Analysis of planar polarity in legs

Adult flies were boiled in 10% KOH for 10 minutes and washed several times with distilled water. Legs were mounted in Hoyer's medium (Sullivan et al., 2000) and incubated ON at 60°C.

Rab23 antibody production

To produce Rab23 antibody, pDEST17-Rab23-His (His-tagged full length Rab23 protein) expressing BL21 (codon+) cells were lysed and the His- tagged transgenic protein was purified using BD-Talon beads (Clontech). The purified protein was tested with Co²⁺-conjugated HRPO (horseradish peroxidase) (Pierce) on Western blot. The purified protein was then injected subcutaneously into Balb/c 3 month old female mice. After four boosts, the crude serum was used for immunostainings and Western-blot analysis (1:100 dilution).

Tissue culture

Drosophila S2 cells were cultured at 25°C in Schneider's *Drosophila* medium (Sigma or in the case of induction in Lonza or GYBCO) supplemented with 10% FBS and 1% antibiotic mix (Penicilline 106 IU, Streptomycine 1g/100ml).

Immunohistochemistry

For pupal wing analysis white puparia were collected and kept at 25°C. At 6, 30, 31, 32, 36 hours APF (after puparium formation) pupae were removed from their pupal case, cut at both ends, cleaned, and then fixed in 4% formaldehyde in PBS solution for 30 minutes at room temperature. For In staining fixation was made in 4% para-formaldehyde (30 minutes at 4°C) (Adler et al., 2004). After fixation wing sacs were peeled off from the wing and free wings still attached to the body were washed three times in PBS-T (PBS+0,1% Triton-X100) at intervals of 5 minutes. Then they were blocked in PBS-BT (0,1% BSA in PBS-T) for 20 minutes and stained with primary antibody in PBS-BT overnight at 4°C. Next day the wings were washed six times with PBS-T at 10 minutes intervals, and incubated with the secondary antibody in PBS-BT for 2 hours at room temperature. After washing six times at 10 minutes intervals in PBS-T, the wings were removed and mounted in PBS: Glycerol- 1:1 mixture.

Drosophila S2 cells were transfected with different expression vectors (100ng/ μ l concentration) using Effectene transfection kit (Qiagene) and transferred to Petri dishes of 35mm diameter (about $2,2 \times 10^6$ cells) on 4-5 round- shape cover slips. After 24 hour incubation, cells were washed one time with PBS and fixed in 4% formaldehyde in PBS solution for 10 minutes. After that cells were washed 3 times with PBS at intervals of 5 minutes and permeabilized with PBS-T for 3 minutes followed by a wash with PBS 3 times, 5 minutes each. Cells were blocked for 1 hour at room temperature (RT) with 5% FBS in PBS (PBS-FBS) solution and incubated for 1 hour at room temperature with primary antibody in PBS-FBS. After 3 times washing with PBS at 5 minutes each, cells were incubated 1 hour at room temperature with the secondary antibody in PBS-FBS followed by 3 times washing with PBS. The coverslips were mounted on slides in PBS:Glycerol 1:1 solution and analyzed with Olympus SV1000 LSM confocal microscope.

For immunostaining we used the following primary antibodies: mouse anti-Rab23 1:100 (our laboratory), mouse anti- β -gal 1:1000 (Promega), rabbit anti- β -gal 1:1000 (Molecular Probes), mouse anti-GFP 1:200 (DSHB), rabbit anti-GFP 1:1000 (Santa-Cruz Biotechnology), rabbit anti-Dgo 1:200 (Feiguin et al., 2001), rabbit anti-Stbm 1:500 (Rawls et al., 2003), mouse anti-In 1:1000 (Adler et al., 2004), rabbit anti-Pk 1:2000 (Tree et al., 2002b), mouse anti-Myc 1:400 (Roche), mouse anti-HA 1:400 (Roche), mouse anti-Fz 1:10 (DSHB), mouse anti-Fmi 1:10 (DSHB). For secondary antibodies we used the appropriate Alexa-488, Alexa-546 or Alexa-647, all in 1:500 (Molecular Probes). Actin was stained with Rhodamine-Phalloidine 1:100 (Molecular Probes).

Immunoprecipitation and Western-blot analysis

For immunoprecipitation experiments 100 pupae (28-30 hours APF) were homogenized and lysed in 1ml Lysis buffer (0,1% SDS, 0,2% NaDoc, 0,5% NP-40, 150mM NaCl, 50mM TrisHCl, pH=8.0) for 1 hour at 4°C. Insoluble materials were pelleted with centrifugation (15000 rpm, 15 minutes at 4°C) and the clear supernatant was used for further studies. 1/10 volume of clear lysate was used as control in Western-blot. The remaining lysate was then preincubated with 100 μ l IgG free Protein-A Sepharose (CL-4B, Pharmacia) beads for 1 hour at RT to deplete non-specific bindings. For immunoprecipitation 60 μ l of CL-4B Sepharose beads were incubated with 30 μ l anti-Rab23 antibody for 2 hours at room temperature in 1ml final volume in Lysis buffer (precomplex). The precomplex was washed briefly 3 times with Lysis buffer and was added to the lysate. A portion of the precomplex was saved as bead (IgG) control. Immunoprecipitation was carried out ON at 4°C. Beads were

then washed 3 times with Lysis buffer and proteins were eluted with 2x Laemmli buffer. Primary antibodies- mouse α -Rab23: 1:100, rabbit α -Pk: 1:1000, mouse α -Fmi: 1:10 and rabbit α -Stbm: 1:500- were applied ON at 4°C. Secondary antibodies were α -rabbit-HRPO (1:10000, Sigma) and α -mouse-HRPO (1:5000, DAKO). For chemiluminescent detection we used a Millipore Immobilon™ kit.

To test the specificity of the α -Rab23 antibody produced in our laboratory, HA-tagged full-length Rab23 was transiently expressed in cultured S2 cells. Non-transfected S2 cells were used as negative control. Aliquots of 10^6 cells were lysed in 80 μ l Lysis buffer for 1 hour at 4°C and, after addition of 20 μ l 5x Laemmli buffer, the samples were boiled for 10 minutes. SDS-PAGE and Western-blot analysis were done as described above. Primary antibodies were: mouse α -Rab23 (our laboratory) (1:100) and mouse α -HA (Roche) (1:400).

Image acquisition

Bright field and Nomarski images were collected using Zeiss Axiocam MOT2, with Axiocam HR, we used a 40x plan-neofluar (NA=0.75) objective. Confocal images were collected with Olympus FV1000 LSM microscope. Images were edited with Adobe Photoshop 7.0CE and Olympus Fluoview1000.

Statistical analysis

Pairs with different number of samples ($n \neq m$)

In each case pairs of standard deviations (s_1 and s_2) were calculated with Microsoft Excel, and compared with Fisher F -probe to decide if the difference between them had been statistically significant or not, using the following formula:

$$F = \frac{s_1^2}{s_2^2}$$

The calculated F -value was then compared to a table containing the critical F -values with at least 95% confidence level.

Pairs with different standard deviations

If the difference between the standard deviations was significant, then the t' -test (a modified two-tailed t -probe) was used to calculate the t' value using the following formula:

$$t' = \frac{w_1 t_1 + w_2 t_2}{w_1 + w_2} \quad \text{where } w_1 = \frac{s_1^2}{n} \quad \text{and } w_2 = \frac{s_2^2}{m}$$

t_1 and t_2 are t values from the t -table, where freedom of degree (FG) of t_1 is $n-1$ and FG of t_2 is $m-1$. The t' value was then compared to a t value calculated with the following formula:

$$t = \frac{\bar{X}_1 - \bar{X}_2}{s_d}, \text{ where } \bar{X}_1 \text{ and } \bar{X}_2 \text{ are the averages of measured mwh numbers and } s_d \text{ is the deviation of difference between standard deviations: } s_d = \sqrt{\frac{s_1^2}{n} + \frac{s_2^2}{m}}$$

If the $t' > t$, then we stated with at least 95% confidence level ($P < 0,05$) that the difference between \bar{X}_1 and \bar{X}_2 was not significant. On the other hand if the $t' < t$, we stated with at least 95% confidence level ($P < 0,05$), that the difference between the two phenotypes was significantly different.

Pairs with equal standard deviations

If the difference between standard deviations was not significant (based on F -probe data), then the t value was calculated with the $t = \frac{\bar{X}_1 - \bar{X}_2}{s_d}$ formula, and the t value was compared to the values of t -table with at least 95% confidence level.

Pairs with equal number of samples (n=m)

The calculation was basically the same as before with the following modifications.

$$t = \frac{\bar{X}_1 - \bar{X}_2}{s_d} \text{ where } s_d = \sqrt{\frac{s_1^2 + s_2^2}{n}}$$

Pairs with different standard deviations

The calculated t value was compared with values of t -table at $FG = n-1$

Pairs with equal standard deviations:

The calculated t value was compared with values of t -table at $FG = 2(n-1)$
 In each case we used t -tables with the highest available confidence level (from 95% to 99,99%).

RESULTS

Isolation of new PCP genes

In order to gain a better understanding of PCP in *Drosophila* and to identify new PCP genes, we have initiated a large-scale mutagenesis screen using the FRT/Flp mosaic recombination system (Xu and Rubin, 1993) which was employed for the first time in *Drosophila* to identify PCP mutants. As mutagenic agents, we used EMS (ethyl methanolsulphonate) in 30mM concentration or ENU (N-ethyl-N-nitrosourea) in 1,6mM concentration. To increase the sensitivity and reliability of the screen, we performed a two generation (F2) screen (Figure 11. A) that offers the advantage of recognizing even the weak phenotypes and phenotypes with low penetrance, and eliminates the sterility problems often occurring in one generation (F1) screens. There are at least two important requirements for the success of such an approach: a Flp source expressed at appropriately high levels in the tissues where polarity phenotypes can easily be recognized; and the ability to induce large mutant clones. To meet the first requirement we were using an Ubx-Flp transgene that is expressed at high levels in wing imaginal discs (Figure 11. B) (Pirrotta et al., 1995), and thus induces recombination in the presumptive wing and notum cells where polarity phenotypes can easily be followed under normal stereomicroscopes. The large clone size was partially ensured by the fact that the Ubx-Flp is expressed from the early stages of development. In addition, mutant clones were induced in a genetic background where the so-called twin-spot cells are eliminated by the cell lethal technique (Newsome et al., 2000). We mutated the left and right arms of the second chromosome (2L and 2R) and the right arm of the third chromosome (3R). We analyzed about 23.000 crosses based on notum and wing phenotypes, and isolated 23 mutants on the 2R, 8 on the 2L and 27 on the 3R chromosomes (Table 1.) that exhibited tissue polarity phenotypes. The high number of the isolated mutants demonstrated that our strategy was an adequate and powerful tool to isolate new tissue polarity genes.

Mapping of the new PCP mutants

In order to map our mutants, we employed different types of mapping techniques. The first step was to decide whether the newly isolated mutants are allelic to the already known PCP genes or they identify new PCP genes. Therefore the new candidates were crossed to alleles of already known PCP genes. The results of these tests have shown that on 2R we have isolated 18 *fmi*, 1 *stbm* and 1 *pk* alleles and 3 new PCP genes. The high number of new *fmi* alleles could be explained by the fact that *fmi* is a large gene (encodes a polypeptide with

3579 amino acids) thus offering a larger target site for the mutagen. The allelic complementation of new mutants obtained from the mutagenesis of the 2L has shown that we have obtained 1 *ds*, 4 *frtz* alleles and 3 new alleles. No PCP genes have been located so far to the 3R chromosome, therefore all 27 mutants isolated in our screen and located to this arm can be considered new (Table 1.).

The next step was to determine the number of complementation groups among new PCP mutants. Because the chromosomes carrying the novel PCP mutations were lethal in homozygous state, the cross- complementation analysis was a lethality/viability test. Viable combinations were checked for adult PCP phenotypes too. These experiments revealed that the 6 new alleles isolated on the second chromosome fall into 6 independent complementation groups, while the mutants on 3R can be classified into 22 complementation groups: one with 5 members, one with 2 members and 20 individual alleles (Table 1.).

Having these results in our hands and after the phenotypic characterization of our new candidates, we selected two complementation groups for further mapping and detailed analysis.

Known PCP genes		
2R (7300X)	2L (7400X)	3R (8100X)
<i>fmi</i> (18)	<i>ft</i>	
<i>stbm</i> (1)	<i>ds</i> (1)	
<i>dgo</i>	<i>fy</i>	
<i>RhoA</i>	<i>frtz</i> (4)	
<i>pk</i> (1)	<i>bsk</i>	
<i>fj</i>		
<i>jun</i>		
New PCP genes		
3 independent complementation groups	3 independent complementation groups	1 complementation group (5 members) 1 complementation group (2 members) 20 independent complementation groups

Table 1. Summary of the results of the mutagenesis screen. In the columns are shown the number of crosses made for each chromosome, the known genes on the respective chromosome and in brackets the number of alleles isolated by us for the known genes. Below, the number of new alleles are represented in red.

Phenotypic characterization and mapping of the complementation group with five members

The PCP mutants of the complementation group with five members isolated from the mutagenesis of the 3R were originally designated as 82.1.T.4, 82.1.T.2, 82.3.4.5, 82.6.7.1 and 82.4.2.1. These mutants exhibit PCP phenotypes that are characteristic to the primary polarity genes, as they are manifested in all tissues examined so far. On the notum we detected shorter and misoriented sensory bristles (Figure 12. B'), on the wing they exhibited multiple wing hairs and weak hair orientation defects (Figure 12. A'), whereas in the eye misrotated and symmetrical ommatidia can be observed (Figure 12. C').

All members of this complementation group were homozygous lethal, and the transheterozygous combinations were lethal as well. Because in mutant clones these 5 alleles displayed very similar PCP phenotypes, it seemed likely that the lethal hits on these chromosomes are mutations of the same gene that is responsible for the PCP defects. If it was not the case, we should assume the very unlikely situation that we hit the same gene five times and additionally, we induced an independent PCP mutation on the same arm in every case. Therefore, to map this complementation group we mapped the lethality by deficiency mapping. For this purpose we used deletions uncovering most of the 3R chromosomal arm. This analysis led to the conclusion that all five lethal alleles map to the 99B7-B10 chromosomal region (Figure 13.).

The 99B7-B10 chromosomal region contains 12 genes. Most of them are described as housekeeping genes or having roles in olfaction. Although we could not formally exclude the possibility that such genes play role in PCP, we thought that out of the 12 genes the best candidate for being affected by our mutations is *Kuzbanian-like (Kul)* because it has recently been reported that RNAi mediated silencing of this gene leads to the formation of multiple hairs on the wing (Sapir et al., 2005). To test this hypothesis, rescue experiments were carried out with a genomic rescue construct containing the full length *Kul* gene. The presence of one copy of this construct was able to rescue the lethality of our mutants therefore we concluded that our mutants are indeed new *Kul* alleles.

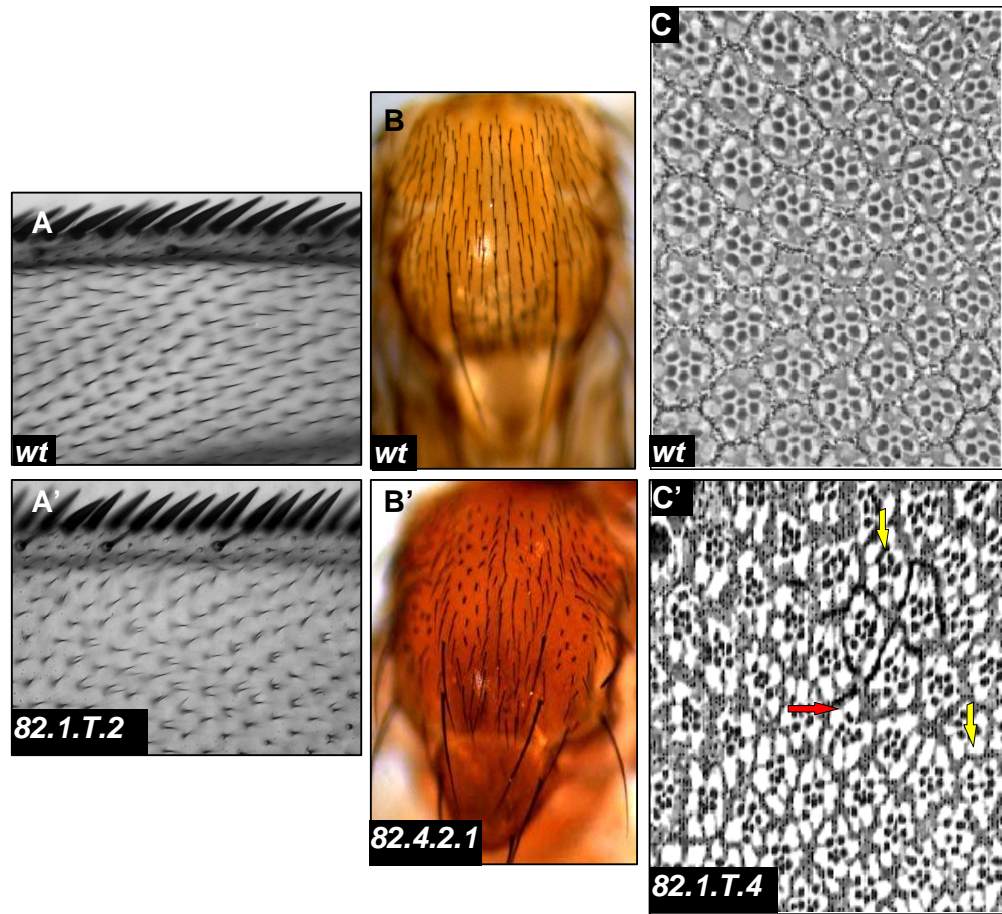


Figure 12. PCP phenotypes of the 3R complementation group with five members (A, A') wild type (A) and *82.1.T.2* (A') mutant wings (A region). Note the multiple hair phenotype and hair orientation defects on mutant wing (A'). On the *82.4.2.1* mutant notum (B') the bristles are shorter and misoriented compared to the wild type (B). (C') In *82.1.T.4* mutant's compound eye misoriented ommatidia (red arrows) and symmetrical ommatidia (blue arrows) appear (in comparison with the upper wild type C).

The *Drosophila Kul* gene encodes a polypeptide with 1534 amino-acids that show a significant homology with the human ADAM10 metalloprotease (Sapir et al., 2005) consisting of several conserved domains: SP domain, Pro- domain, metalloprotease, desintegrin homology, cystein rich transmembrane and intracellular domains (Figure 14.) In order to determine the precise place of the mutations in our newly isolated *Kul* mutants, we cloned and sequenced them. We found that our mutants could be classified into two groups. In the *Kul*^{82.1.T.4}, *Kul*^{82.1.T.2}, *Kul*^{82.3.4.5} and *Kul*^{82.6.7.1} alleles, a Cysteine amino-acid in position 481 was changed to Arginine; while in the *Kul*^{82.4.2.1} mutant a Valine residue in position 603 was changed to Alanine (Figure 14.). Given that these are conserved residues within the functionally important metalloprotease domain, our results suggest that we have isolated LOF alleles of *Kul* with reduced protease activity.

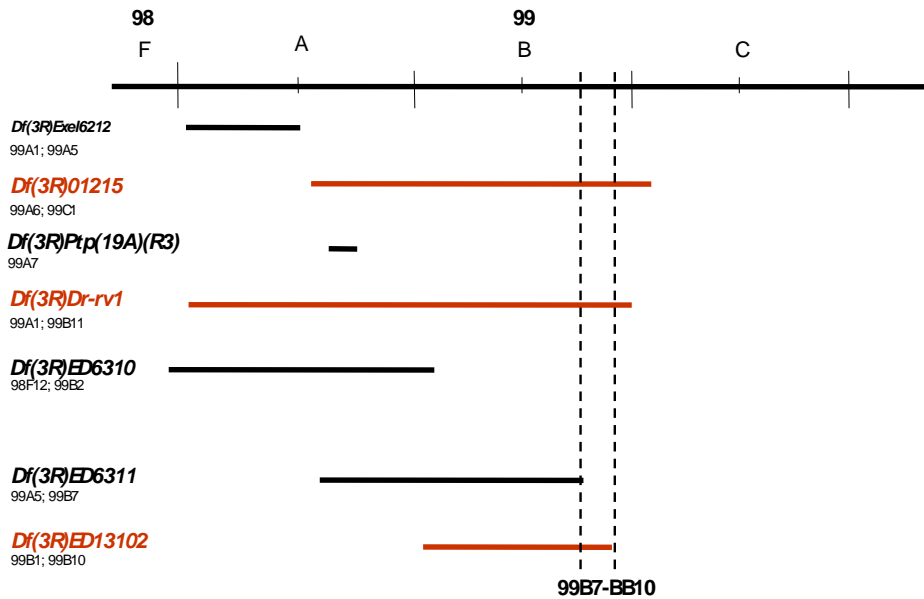


Figure 13. Deletion- based mapping of the complementation group with five members. The red lines represent deletions that do not complement our mutants, while the black lines the deletions that complement the lethality of our mutants. Based on genetic mapping our mutants carry the mutation in the 99B7-B10 chromosomal region.

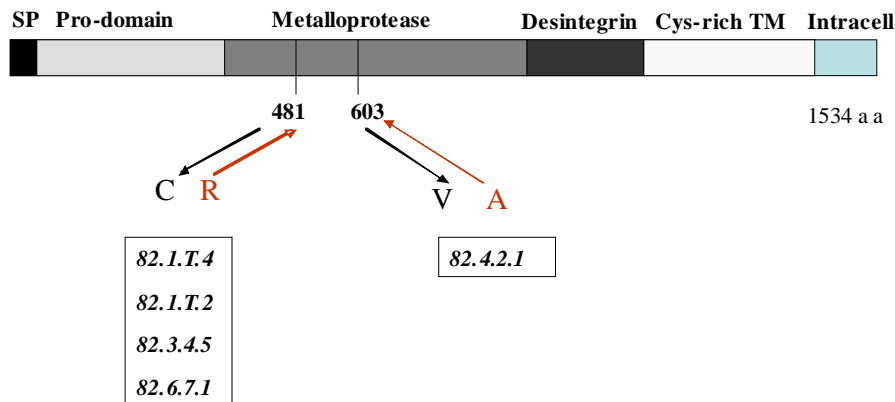


Figure 14. The domain structure of the *Drosophila* Kul protein, and the position of the mutations induced in *Kul*. In the upper part of the figure the domain structure of the Kul protein is shown. Four of our *Kul* alleles carry a C481R mutation, while one of the mutants carries the mutation in the 603rd position where V was changed to A. Both mutations occur in the metalloprotease domain of the 1534 amino acid long polypeptide.

Previous work demonstrated that *Drosophila Kul* plays a role in the cleavage of the Notch ligand Delta both in cultured cells and in the wing (Sapir et al., 2005). The double stranded RNA (dsRNA) "knock down" construct of *Kul* (*dsKul*) resulted in the appearance of

multiple hairs and partial vein loss when expressed in the wing (Sapir et al., 2005). Despite the intensive former studies, the Notch pathway has not been linked to multiple hair formation in the wing. Conversely, the Notch pathway is known to play role in the regulation of ommatidial polarity (Baonza and Garcia-Bellido, 2000). However, unlike for the case of *Kul*, the loss of Notch or Delta in the eye has minor effect on ommatidial rotation. Taken together, these results suggest that *Kul* regulates planar polarity establishment in a Notch/Delta independent way and we have therefore revealed a previously unknown link between the ADAM metalloprotease family and PCP establishment in *Drosophila*. What is the substrate of *Kul* during PCP signaling, is a critical question to address however, for the moment it awaits future investigations.

Mapping of the 82.1.4.1 mutant

The other complementation group chosen for detailed analysis was identified by the 82.1.4.1 mutant, isolated from the mutagenesis of 3R. This mutant displayed weakly misoriented and multiple hairs on the wing in mutant clones, was homozygous lethal, and the cross- complementation analysis demonstrated that it does not complement any of the other newly isolated alleles on 3R. To determine if the lethality is associated with the PCP phenotype, we used a recombination- based mapping strategy. During this experiment we found that the PCP phenotype is not associated with the lethality, as we isolated 3 independent recombinants (later we designated them as T69A) that still exhibited the PCP defects but lost the lethal mutation. The lethal allele has turned out to be a second site mutation on 3L, while the polarity mutation was mapped to the genomic region between 82D and the recessive marker gene *curled* (*cu*) located in 86D. For our further studies we only used the T69A recombinants that lost the second site lethal mutation. Subsequently, we delimited the position of the T69A allele to the 83B8-C1 chromosomal region by deficiency mapping (Figure 15.).

for the latter two (VDRC- Vienna Drosophila RNAi Center), we first tested these and found that the wing- specific silencing of CG2108 induced the formation of multiple hairs (Figure 17. J), whereas silencing of CG2104 had no phenotypic effect (not shown). These observations made CG2108 (*Rab23*) the best candidate to be affected by the *82.1.4.1* polarity mutation. Indeed, sequence analysis revealed that the *82.1.4.1* allele carries a point mutation in the Switch1 region of the GTPase domain of *Rab23*, a Threonine to Alanine transition affecting an amino acid residue that is invariant in the whole small GTPase superfamily (Figure 16.) (Vetter and Wittinghofer, 2001). Therefore this allele was named *Rab23^{T69A}*.

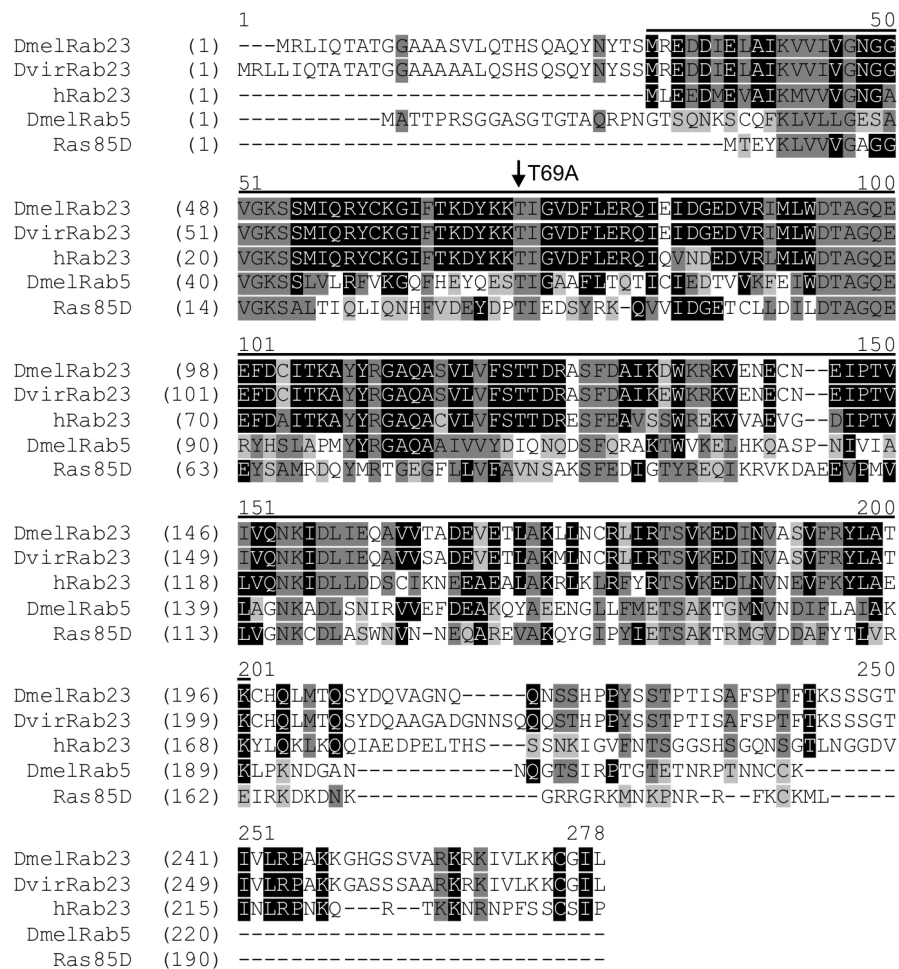


Figure 16. The position of the *Rab23^{T69A}* mutation. Multiple alignments of different Rab family members reveal a high level of conservation in the GTPase domain indicated with a black line above the alignment. The *Rab23^{T69A}* mutation affects a threonine residue (T69A) that is invariant in the whole small GTPase superfamily (arrow).

The *Rab23*^{T69A} allele is semilethal (the lethal phase of most of the homozygous animals is between late L2 and early L3 larval instars) but homozygous animals occasionally survive to adulthood and display a strong multiple hair phenotype and mild hair orientation defects on the wing (Figure 17. C, D, F). Although these trichome orientation defects are relatively mild compared to *fz* and *dsh*, they are exhibited in every *Rab23* mutant wing. Whereas in wing sectors B and C (Figure 17. A) hair orientation is mildly affected, the deflection from wild type orientation is obvious in sectors A, D and E (Figure 17. A-B and not shown), clearly indicating a requirement for hair orientation.

Isolation and characterization of new *Rab23* alleles

To test our point mutant allele and to increase the number of independent *Rab23* alleles for further experiments, we generated new *Rab23* alleles by remobilizing the P-element line *P{RS5}5-Sz-3123* residing in the first intron of the *Rab23* gene (Figure 18.). PCR analysis of the P element excision candidates has shown that we have isolated two deletion mutants (50/3, 51/1) (data not shown) but according to their phenotypic analysis only one of them, named *Rab23*⁵¹ was homozygous viable and displayed a strong multiple hair phenotype (Figure 17. G), therefore we have used this allele for further experiments.

Further, we tested the new *Rab23*⁵¹ allele in combination with our point mutants. *Rab23*⁵¹ is viable over *Rab23*^{T69A} and this combination displays a strong multiple hair phenotype. Similarly, both mutations are viable over deficiency chromosomes uncovering *Rab23* and both exhibit multiple wing hair phenotypes on such a genetic background (Figure 17. H, I). Because the severity of the PCP phenotype is almost identical in these mutant combinations, our *Rab23* alleles genetically behave as strong loss-of-function (LOF) or null. In agreement with this, it has already been reported that impairment of the Threonine residue (T69 in Rab23) in other small GTPases leads to loss of function (Vetter and Wittinghofer, 2001) (Figure 16.). With respect to the excision allele, we revealed by molecular cloning that *Rab23*⁵¹ encodes a hybrid transcript consisting of the first (non coding) exon of *Rab23*, part of the first intron of *Rab23*, followed by 443 base pairs from the 5' end of the *P{RS5}5-Sz-3123* transposon spanning from 5' ITR until the end of ORF0 (O'Hare and Rubin, 1983) that is fused to the third exon of *Rab23* (Figure 18.). If translation from this fusion transcript begins with the ATG of ORF0, the predicted fusion protein is entirely devoid of *Rab23* sequences because ORF0 and the third exon of *Rab23* are not in the same phase. If a downstream ATG would be used, according to our sequence analysis, M53 (Methionine) of

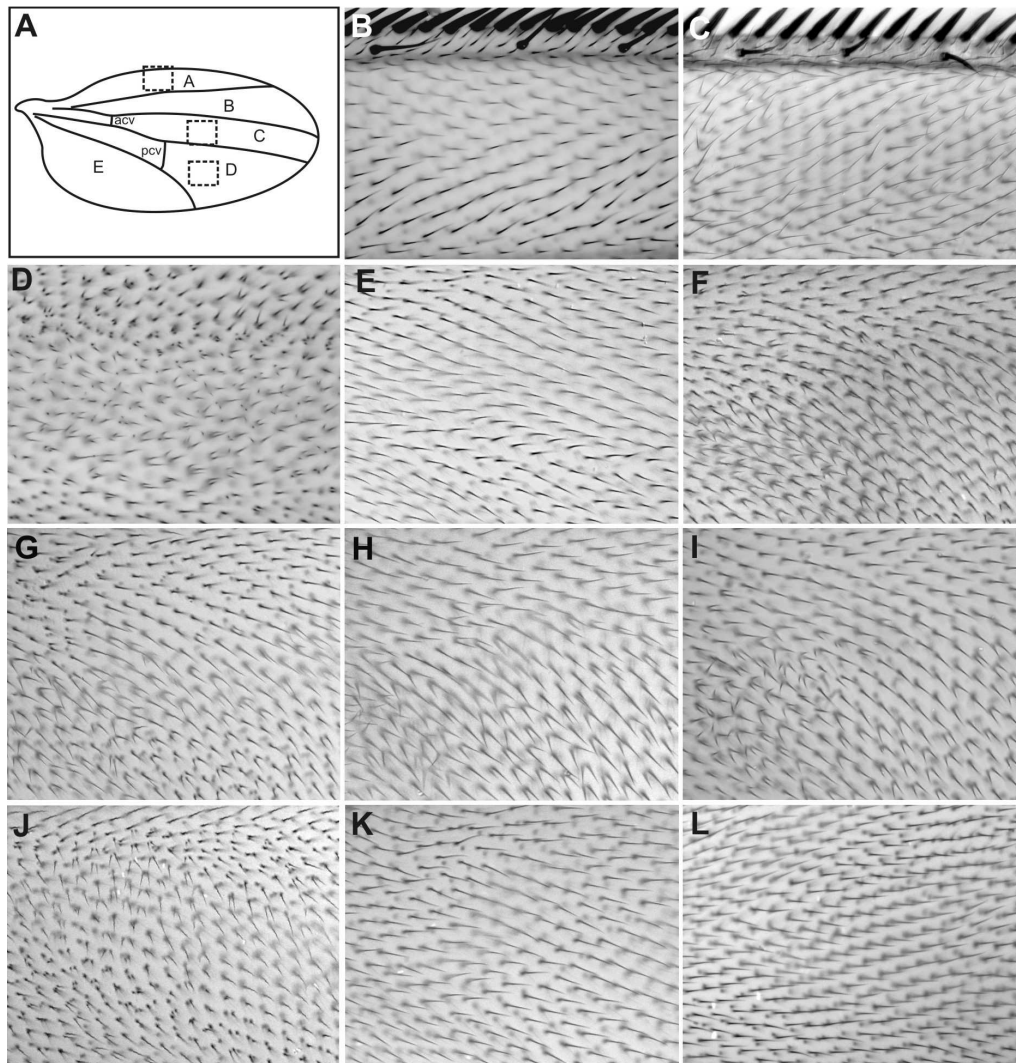


Figure 17. *Rab23* mutant wings display PCP defects. (A) A schematized wing indicating the main wing blade regions (A-E) and the two cross-veins (acv: anterior cross vein, pcv: posterior cross vein). Distal is on the right and anterior is on top on all panels. Wild type wing cells exhibit a single, distally pointing hair (B, E), whereas *Rab23^{T69A}* (C, D, F) and *Rab23^{S1}* (G) mutant wings exhibit multiple hairs and orientation defects in every wing regions. Photomicrographs were taken from the A region (B, C), the C region (D) and the D region (E-L) of the wing (dashed areas in panel A). Wings of *Rab23^{T69A}/Df(3R)BSC47* (H), *Rab23^{S1}/Df(3R)BSC47* (I), and wings in which *Rab23* is silenced by RNAi (J), also display multiple hairs and hair orientation defects. (K-L) The wing PCP phenotypes induced by *Rab23* can be fully rescued by a single copy of the *Rab23* genomic rescue construct (*Rab23-GR*) (K), and by *Act-Gal4* driven expression of *UAS-YFP::Rab23* (L).

Rab23 is a potential alternative starting point, however, translational initiation from here would result in a mutant *Rab23* protein that is lacking 52 N-terminal amino acids, including 15 from the highly conserved and functionally essential part of the GTPase domain (Santos

and Nebreda, 1989). Thus, these results suggests that *Rab23*⁵¹ encodes a functionally strongly if not entirely impaired protein.

The multiple hair phenotype of the *Rab23* alleles can be fully rescued by providing a single wild type copy of the *Rab23* gene, whereas the semilethality of the *Rab23*^{T69A} allele could not be significantly rescued probably due to a nearby second site mutation on the chromosome (Figure 17. K). The LOF analysis and the rescue experiments together show that *Drosophila Rab23* is not essential for fly viability, but, it is involved in the regulation of wing hair number, and to a lesser degree, wing hair orientation.

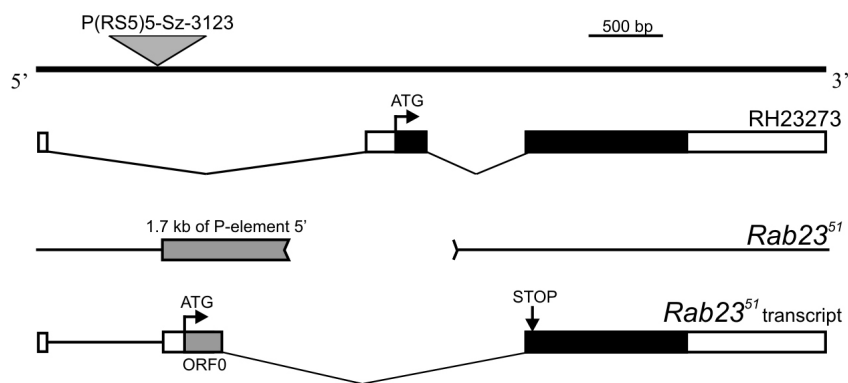


Figure 18. Isolation of new *Rab23* alleles. The upper line indicates the *Rab23* genomic region and the position of the *P{RS5}5-Sz-3123* P-element (triangle) insertion line that was used to generate the *Rab23*⁵¹ allele (bottom line). The structure of the RH23273 EST clone, corresponding to the full length *Rab23* cDNA, is shown in the second row, black color indicates the coding region; white color indicates the untranslated regions. The possible transcript from the *Rab23*⁵¹ deletion- carrying gene is shown at the bottom of the panel.

***Drosophila Rab23* impairs hair polarity and number on the adult cuticle**

Because PCP appears also in tissues other than the wing, we examined the eyes, notum, legs and abdomen of *Rab23* mutants. We found that ommatidial polarity and the orientation and number of the epidermal bristles on the notum (not shown), legs and abdomen are the same as in the wild type and these mutants also lack the duplicated dorsal joint phenotype typical for the core PCP mutants (Figure 19.). Conversely, *Rab23* affects the orientation and number of the trichomes covering the legs and abdomen. The orientation defects are equally evident on the tergites, sternites and pleural regions of the abdominal cuticle, and also on the leg (Figure 19. B, D, F, H). Interestingly, hair polarity looks randomized all over the tergites (Figure 19. F), that is different from other PCP mutations

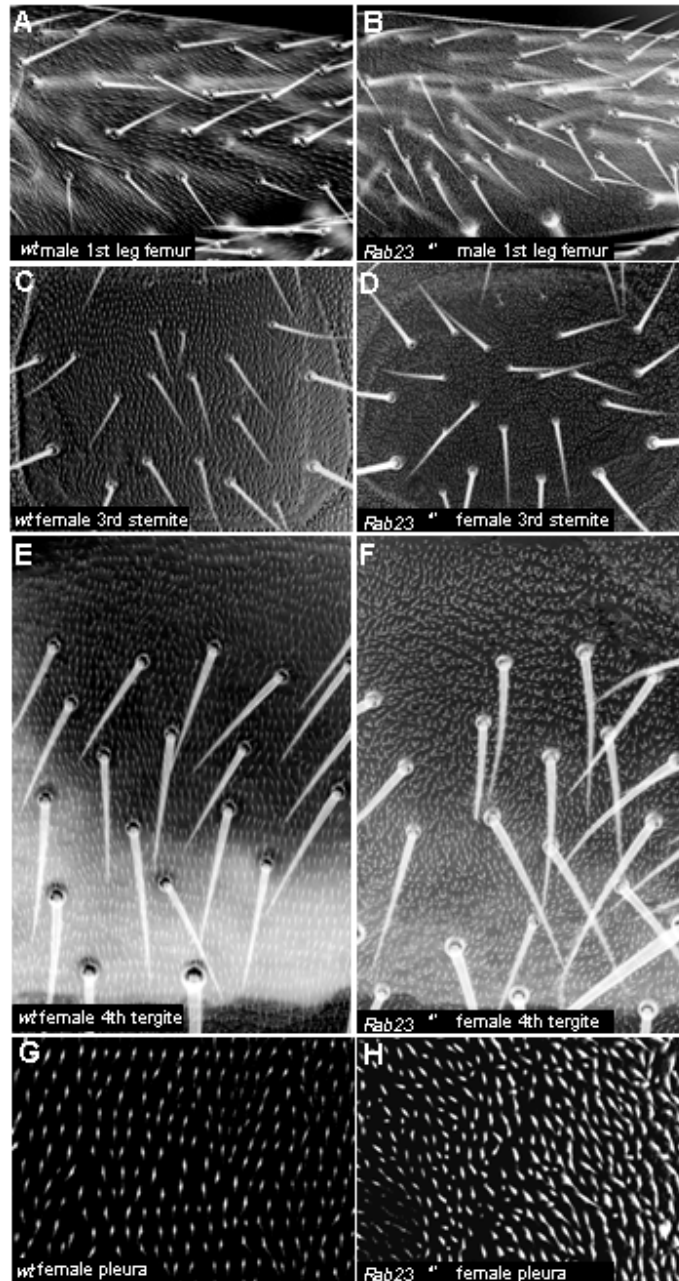


Figure 19. *Rab23* affects hair polarity on the leg and the abdominal cuticle. (A-B) Photomicrographs taken from the femur (male first leg), the third sternite (female) (C-D), the fourth tergite (female) (E-F), and pleural regions of the adult cuticle (G-H). Proximal is on left, distal is on right on A-B, anterior is on top, posterior is on bottom on C-F. (A) A wild type leg exhibiting distally pointing hairs and bristles. (B) A *Rab23* mutant leg is covered by distally pointing bristles, however, trichome orientation defects, and occasionally the formation of multiple hairs are evident. (C) Hairs and bristles of a wild sternite, (E) tergite, and pleura (G) point posteriorly. In *Rab23* mutant sternite (D), tergite (F), and pleura (H) hairs display largely randomized orientations and the appearance of multiple hairs is also evident whereas, bristle orientation is not significantly altered.

exhibiting polarity reversions or orientation defects affecting only certain areas along the anterior-posterior axes of the tergites (Casal et al., 2002; Lawrence et al., 2004). Additionally, the formation of multiple hairs is also obvious on the leg and the abdominal cuticle (Figure 19. B, F). Together, these findings suggest that *Rab23* identifies a unique class of PCP genes that is specifically required for the regulation of trichome orientation and number in different body regions without affecting the polarization of the multicellular structures such as ommatidia and sensory bristles.

***Drosophila Rab23* has no role in Hedgehog signaling and CNS development in flies**

Because former work revealed that the mouse *Rab23* orthologue (*open brain2*) is an essential negative regulator of *Sonic-hedgehog* (*Shh*) signaling during neuronal patterning of the mouse embryo (Eggenchwiler et al., 2001), we were curious whether it has the same role in *Drosophila*. However, we found that *Rab23* is not expressed in the *Drosophila* embryonic CNS (central nervous system) (data not shown), likewise, CNS defects were not detected in *Rab23* mutant embryos and therefore, *Rab23* is unlikely to play a role in any aspects of neuronal development in flies. Nevertheless, *Drosophila hedgehog* (*hh*) is required for the proper development of many different tissues from embryonic stages to the adulthood (Ingham and McMahon, 2001). Thus, to determine if *Drosophila Rab23* plays a role in Hh signalling in tissues other than the CNS, we analyzed *Rab23* homozygous mutant embryos and adult tissues. We found no evidence for a *Rab23* requirement in Hh signaling, as for example the embryonic cuticle pattern or anterior-posterior patterning of the wing remained normal in our mutants (data not shown). Moreover, if *Rab23* were a negative regulator of Hh signal transduction in flies, the loss of *Rab23* should activate the Hh pathway (such as the loss of *patched* does) and would lead to similar phenotypic effects as the overexpression of Hh. In case of the abdominal cuticle Hh overexpression induces reversed hair polarity (Struhl et al., 1997, Lawrence et al., 1999) which is clearly distinct from the effect of *Rab23* that induces randomized polarity and multiple hairs (Figure 19. F). Thus, our findings indicate that although the *Rab23* protein has been highly conserved throughout evolution (Guo et al., 2006), its role in Hh signaling is likely to be restricted to vertebrates.

***Rab23* influences the place of prehair initiation and acts cell autonomously in *Drosophila* pupal wings**

To investigate *Rab23* function at the cellular level, we examined prehair initiation in *Rab23*⁵¹ homozygous pupal wings at 31 hours APF. We observed that- similarly to mutations

of the In group genes- in the absence of *Rab23*, presumably as a consequence of the failure to restrict the site of actin accumulation, many cells develop more than one prehair in abnormal positions around the cell periphery (Figure 20. B', B''). We observed an increased amount of

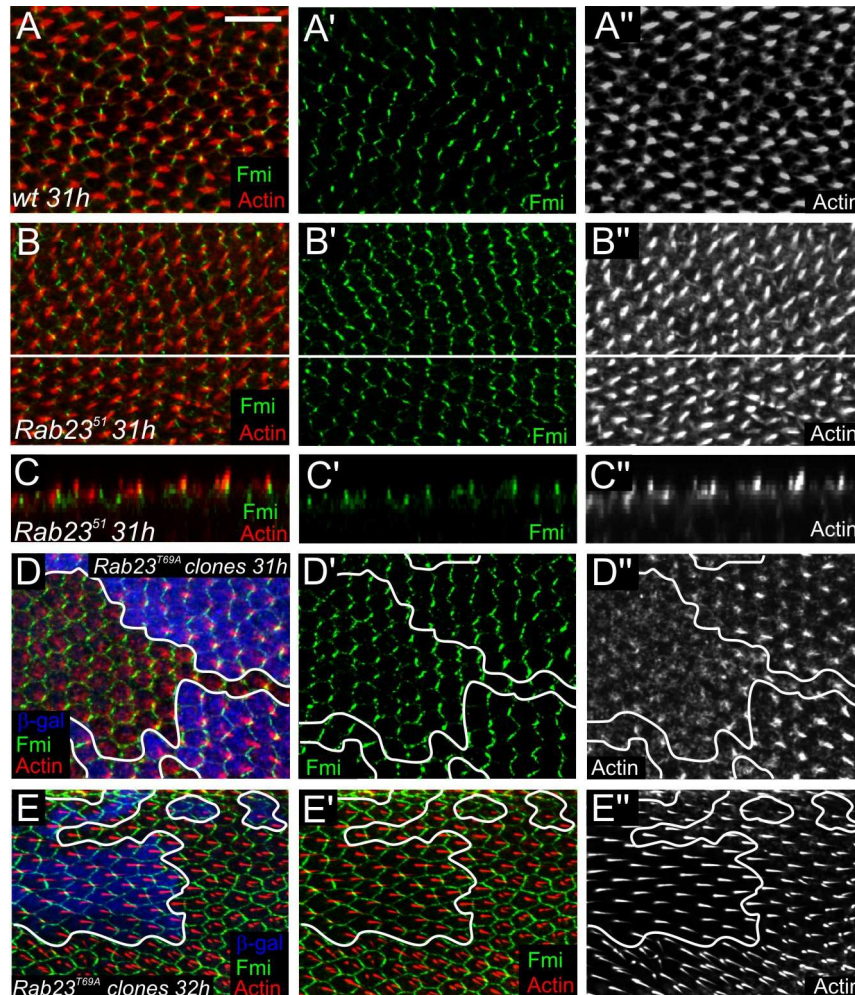


Figure 20. Rab23 impairs prehair initiation. (A-A'') Prehair initiation in wild type pupal wings at 31 hours APF. Note that each wing cell develops an actin-rich prehair at its distal vertex. (B-B'') Apical actin level is increased in *Rab23*⁵¹ mutant pupal wing cells, many of which fail to restrict prehair initiation to a single site. (C-C'') Z axis projections of the wing shown in panel B, projection is shown along the white line indicated on B-B''. Note that Fmi and actin are accumulated near the apical cell surface. (D-D'') Prehair initiation is delayed in a *Rab23*^{T69A} mutant clone (derived from the proximal half of wing sector C, and marked by the absence of β -gal staining, in blue) as prehairst are shorter in the mutant tissue than in the surrounding wild type tissue. Note that some cells initiate multiple hairs that form around the cell periphery. Moreover, the P-D accumulation of Fmi is partly impaired within the mutant tissue. (E-E'') Multiple hairs are not seen outside of *Rab23*^{T69A} mutant clones indicating that *Rab23* acts cell-autonomously. In all panels, cell borders are labeled with Fmi staining (green in A,A',B,B',C,C',D,D',E and E'), actin is labeled in red in A,B,C,D,E and E', and in white in A'',B'',C'',D'' and E''. Scale bar: 10 μ m. Proximal is on left, distal is on right on all panels.

disorganized apical actin filaments in mutant tissues (Figure 20. B', C'). The above-mentioned phenotype is also present in *Rab23*^{T69A} mutant clones (Figure 20. C- C'', D- D''). This clone analysis demonstrated that actin accumulation is somewhat delayed in the *Rab23* mutant tissue (Figure 20. C' - C''). This delay is particularly obvious in clones induced in the proximal half of the wing sector B and C (in 85,7% of the clones, n=23), conversely the delay is less frequent in clones from distal B and C sectors (25%, n=20). Clones with delayed prehair initiation are more randomly distributed in wing sectors D and E in about 50% of clones examined (n=36). Beyond these effects, *Rab23* acts in a cell autonomous manner (Figure 20. D-D''), as the presence of the multiple hair outgrowth was always restricted to the mutant area.

***Rab23* is required for hexagonal packing of the wing epithelium**

Recent studies uncovered that the wing epithelial cells are irregularly shaped throughout larval and early pupal stages but most of them become hexagonally packed shortly before prehair formation (Classen et al., 2005). It has also been shown that the core PCP proteins partly interfere with normal cellular packing (Classen et al., 2005). While analyzing *Rab23* mutant wings, we noticed that some of the *Rab23* mutant wing cells also fail to adopt a hexagonal shape at around 30-32 hours APF (Figure 21. B). We quantified this effect in the D intervein region of the wing (Figure 21. C), and found that in wild type wings the ratio of non-hexagonal cells is about 11%, whereas in the *Rab23*^{T69A} homozygous mutant wings this ratio is increased to 27% (Figure 21. C). As a comparison, we measured the packing defects in two core PCP mutants, *stbm*⁶ and *dsh*¹, where the ratio of the non hexagonal cells was 30% and 28%, respectively (Figure 21. C). Because the strength of the *Rab23*- induced packing defects is comparable to the effect of the core mutations, these data suggest that *Rab23* might also be an important determinant of cellular packing.

The *Rab23* induced multiple hair phenotype is not correlated with the packing defects

To address whether the multiple hair phenotype and/or the hair orientation problems induced by *Rab23* correlates with the packing defects, we compared the average prehair number of hexagonally and non-hexagonally packed *Rab23* mutant wing cells. However, we failed to reveal any correlation between the presence of multiple hairs and the cellular packing defects (Figure 21. D). To extend this analysis, we investigated the packing defects of other mutations causing multiple hairs such as *in*, *frtz* and *mwh*. These mutants exhibit weak packing defects (Figure 21. C), and similarly to the case of *Rab23*, the formation of multiple

hairs does not appear to correlate with irregular cell shape (Figure 21. D). Taken together, these results demonstrate that cell packing has no direct effect on the number of prehair initiation sites in the wing epithelial cells.

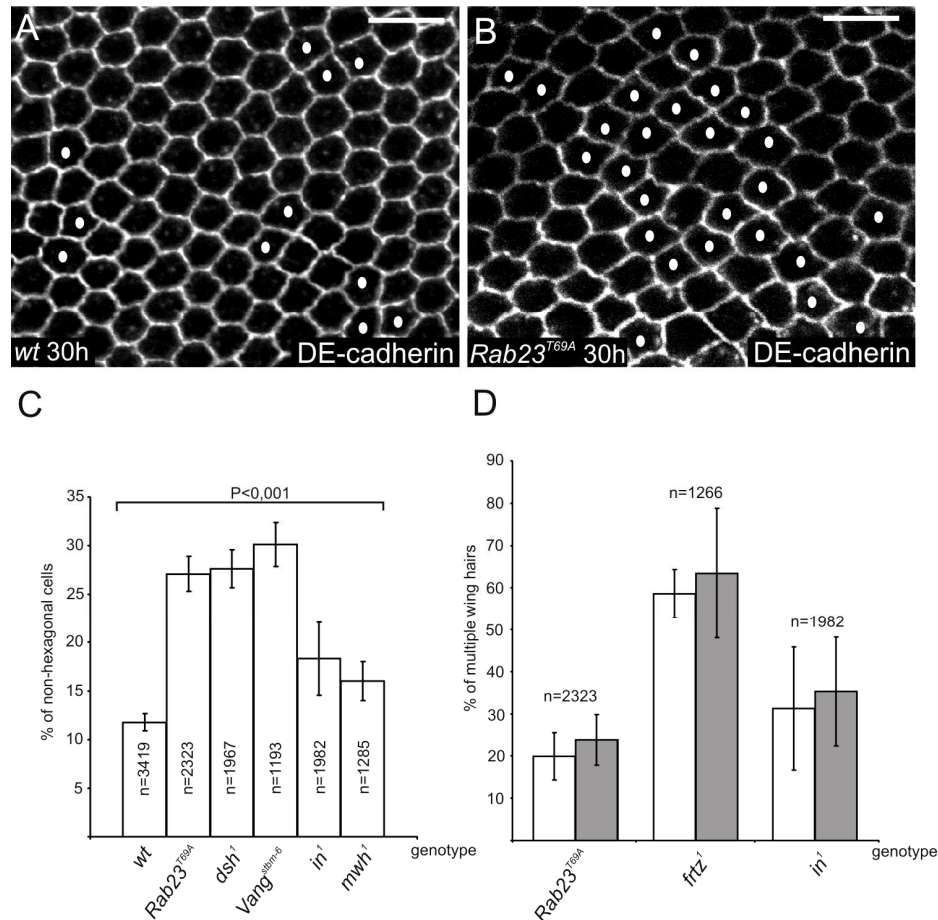


Figure 21. *Rab23* impairs hexagonal packing of the pupal wing cells, but packing defects do not correlate with the formation of multiple hairs. (A) DE-cadherin staining in wild type and (B) *Rab23⁵¹* mutant pupal wings at 30h APF. In wild type wings by this stage of development most cells acquire a hexagonal shape, whereas *Rab23* wings display an increased ratio of non hexagonal cells (indicated with white dots). (C) Quantification of the ratio of the non-hexagonally shaped cells in wild type, *Rab23* mutant and other PCP mutant wings. We examined 10-25 wings for each genotype and counted at least 100 cells per wing. To test for significance we applied the *t*-test as a statistical method, P indicates probability. (D) Quantification of the ratio of cells that exhibit multiple hairs in hexagonal (white columns) and in non hexagonal (gray columns) cells in *Rab23⁵¹*, *in¹* and *frtz¹* mutants. Scale bars: 5 μ m. On A and B panels proximal is on the left, distal is on the right.

***Rab23* is required for the late cortical polarization of the core PCP proteins and In**

We demonstrated that *Rab23* has a role in hexagonal packing of the wing epithelium. Because this process depends on correct asymmetrical localization of the core PCP proteins (Classen et al., 2005), we were curious if *Rab23* influences the asymmetric localization of these proteins in pupal wing cells. To this end, we first examined the localization pattern of the core PCP proteins in *Rab23*⁵¹ homozygous mutant pupal wings. We found that by 24-30 hours APF core PCP proteins accumulate into apico-lateral complexes however, they fail to polarize properly in a *Rab23* mutant tissue where the PCP complexes are not efficiently removed from the anterior-posterior cell membranes of many of the wing cells (Figure 20. B, and not shown). We obtained similar results when we looked at PCP protein localization in *Rab23*^{T69A} mutant clones (Figure 22. A-C'). Moreover, we noticed that in *Rab23*^{T69A} mutant clones that exhibited a delay in actin accumulation, mislocalization was always evident (n=26) in most part of the mutant tissue independent of the wing region the clone was formed. In clones that did not exhibit a delay in actin accumulation, localization was strongly affected in the distal C region in every case (n=70). In other wing sectors the effect was restricted to a smaller region within the clones (n=24). Thus instead of a regional specificity, it appears that altered PCP protein localization correlates with the delay of actin accumulation. In agreement with this, we were unable to find a regional specificity in *Rab23*⁵¹ homozygous mutant wings. Instead, smaller or larger areas in which the “zigzag” pattern was altered were evident in all wing sectors (n=25).

It has been shown previously that In localization depends on the correct localization of core PCP proteins (Adler et al., 2004), so we assumed that the asymmetric localization of In might also be altered in *Rab23* mutant wing cells. Indeed, the analysis of *Rab23*⁵¹ homozygous mutant wings and *Rab23*^{T69A} mutant clones strengthened our assumption, as we found that the lack of *Rab23* impairs In localization as well (Figure 22. D, D').

Recent data suggested that asymmetric PCP protein accumulation is not restricted to the period of 24-32 hours APF but it is also visible in early pupal wings until 6 hours APF (Classen et al., 2005). Therefore, we decided to investigate if *Rab23* affects the early polarization of the PCP proteins. When we examined Fmi distribution in early, 6 hours- old *Rab23*⁵¹ mutant pupal wings, we failed to detect any problem in Fmi distribution (Figure 23. A-B').

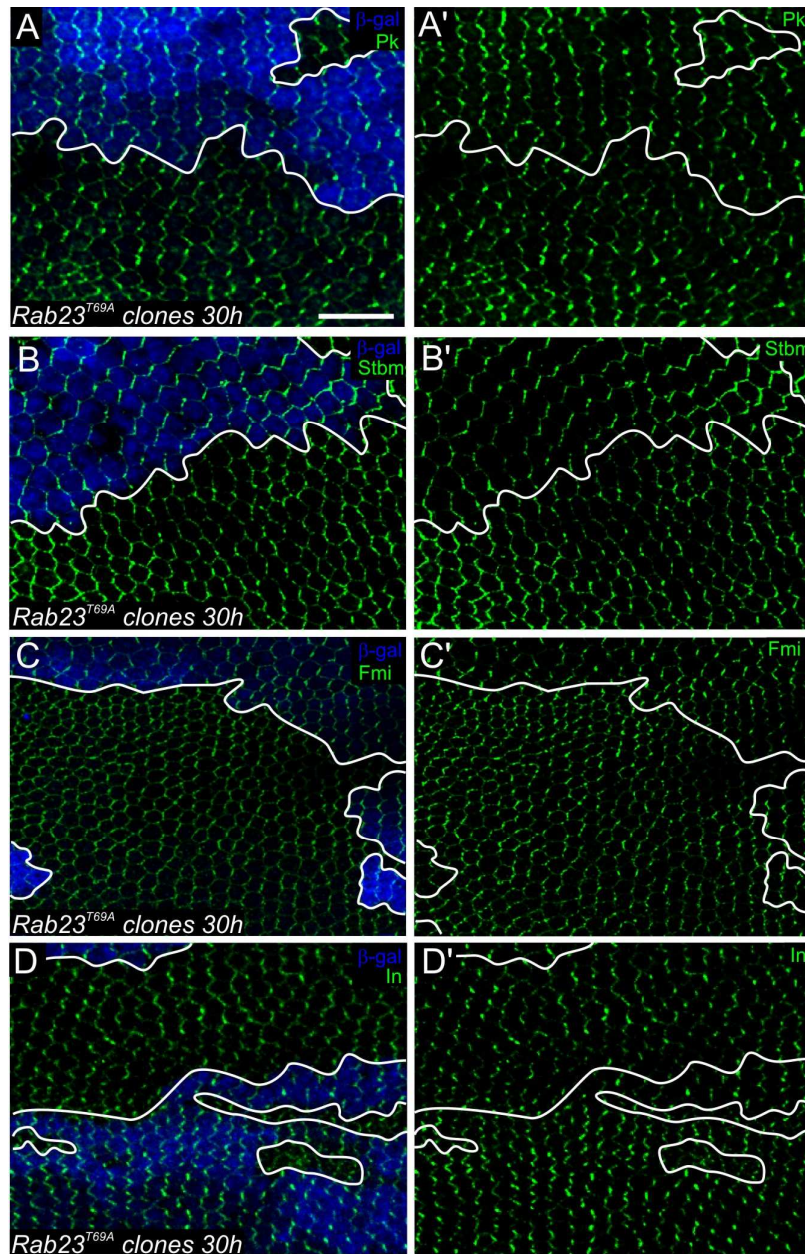


Figure 22. Rab23 is required for correct localization of the PCP proteins. (A-D') *Rab23^{T69A}* mutant clones at 30 hours APF, marked by the absence of β -gal staining (blue). The proximal-distal polarization of Pk (in green) (A, A'), Stbm (in green) (B, B'), Fmi (in green) (C, C') and In (in green) (D, D') is impaired in many of the mutant cells. Sometimes the angle of polarity is not well correlated from cell to cell (best visible in A', D'), or the PCP protein complexes are not efficiently removed from the anterior-posterior cell boundaries and the “zig-zag” pattern is lost (obvious in B', C'). Photomicrographs were taken from the C region (B, C) and the D region (A, D) of the wing. A', B', C' and D': single images of the green channel of A, B, C and D. Scale bar: 10 μ m.

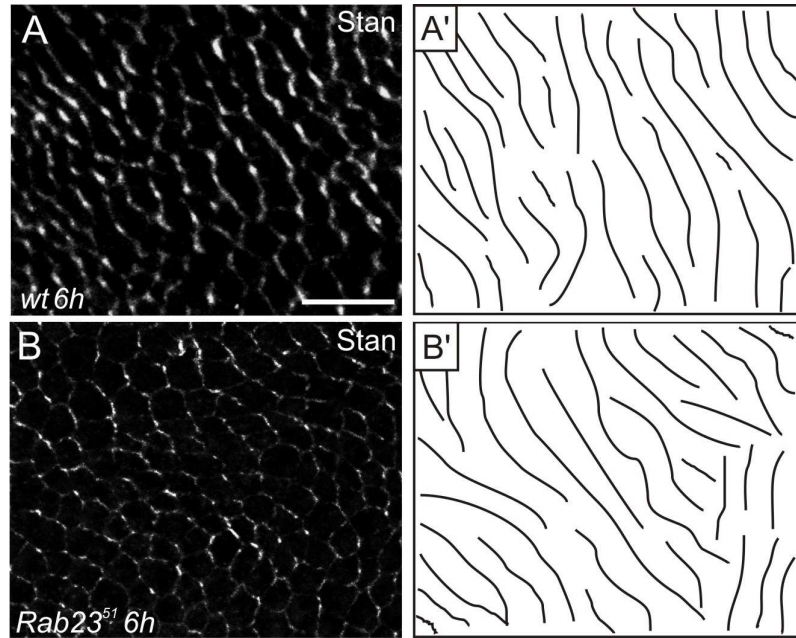


Figure 23. *Rab23* is not required for the early polarization of Fmi. (A-A') Wild type pupal wing cells display a partial polarization of Fmi distribution (white) at 6 hours APF (A), schematized on panel A'. (A') Black lines are drawn between cells with coherent Fmi polarity. (B-B') Fmi distribution (white) in *Rab23*⁵¹ mutant pupal wing cells displays a similar level of polarization at 6 hours APF as in wild type. Scale bar: 10 μm. Proximal is on the left distal is on the right on all panels.

As we pointed out above, *Rab23* is also required for hexagonal packing of the wing epithelium therefore it was necessary to clarify if the abnormal- looking PCP protein localization is not simply the consequence of irregular packing. In order to address this issue, we carefully examined Pk localization in wild type and *Rab23* mutant wings in such hexagonal cells, whose all six neighbours were hexagonally shaped as well. This analysis revealed that a *Rab23* mutant hexagonal cell has significantly higher (about twice as high) chance to display impaired PCP protein localization than a wild type cell (Figure 24. C). Because impaired PCP protein localization is also associated with cellular packing defects in the core PCP mutants, as a comparison, we applied this approach to *dsh*¹ mutant hexagonal wing cells. In agreement with previous work that provided a general assessment of Pk localization in *dsh* mutants, we found that *dsh* strongly impairs the asymmetric accumulation of Pk in hexagonal cells (Figure 24. C). Hence, it appears that the core PCP mutations have a stronger effect on PCP protein polarization than that of *Rab23*. Since asymmetric accumulation of the PCP proteins is likely to serve as a critical cue for cell polarization, the subtle but significant alterations in wing hair polarity probably produced by *Rab23* are best explained by the similarly moderate effect on PCP asymmetries.

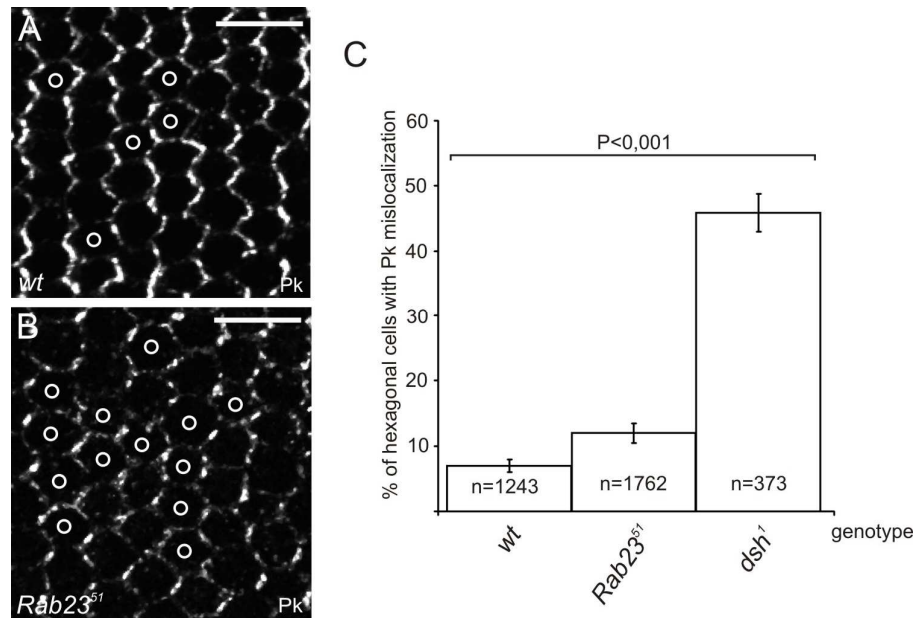


Figure 24. Pk is mislocalized in hexagonally packed *Rab23* and *dsh* mutant wing cells. (A-B) Pk staining (white) on wild type (A) and *Rab23⁵¹* mutant wings (B). Pk localization was examined in those hexagonally shaped cells whose all neighbors were hexagonal as well, white circles represent cells with impaired Pk localization. Note that *Rab23⁵¹* mutant wings exhibit a higher ratio of cells with localization defects than wild type. (C) Quantification of hexagonal cells with impaired Pk localization in wild type, *Rab23⁵¹* mutant and *dsh¹* mutant wings. 6-15 wings were analyzed for each genotype. To test for significance we applied the *t*-test as a statistical method, P indicates probability. Scale bars 5 μ m. Proximal is on the left distal is on the right on all panels.

Taken together, *Rab23* is required for the late (24-30 hours APF) apical cortical polarization of the core PCP proteins and In. However, *Rab23* does not appear to be involved in core PCP protein polarization during the early pupal life. These results suggest that, similarly to Dsh and Pk, *Rab23* plays a role only in the late phase of PCP protein polarization, and thus, consistent with its cell autonomous mode of action, *Rab23* is likely to be involved in the establishment of intracellular asymmetries without major contribution to intercellular PCP signaling prior to the establishment of intracellular asymmetries (Srutt and Strutt, 2007).

The subcellular localization of *Rab23* in developing pupal wing cells

To gain insight into the mechanism whereby *Rab23* contributes to core PCP protein localization, we examined the subcellular localization of *Rab23* in developing pupal wings. During the first set of experiments we used an anti-*Rab23* serum raised in our laboratory. However, this antibody was not suitable for immunohistochemical analyses because of

background problems. To get around this problem, we expressed a YFP::Rab23 fusion protein to assess localization in wing cells. As a control, we first tested the YFP::Rab23 fusion construct in rescue experiments. Because YFP::Rab23 fully rescued the *Rab23* mutant phenotypes (Figure 17. L), we considered it fully functional. We found that between 24 and 32 hours APF, when the core PCP proteins repolarize, the YFP::Rab23 protein expressed uniformly in the wing exhibits a strong plasma membrane association in the junctional zone and also in the basolateral zone (Figure 25. A- B''), and a weak staining is evident in the cytoplasm with occasional accumulation in punctate structures in the sub-apical region (Figure 25. A- B''). We detected a very similar localization pattern before 24 hours APF (not

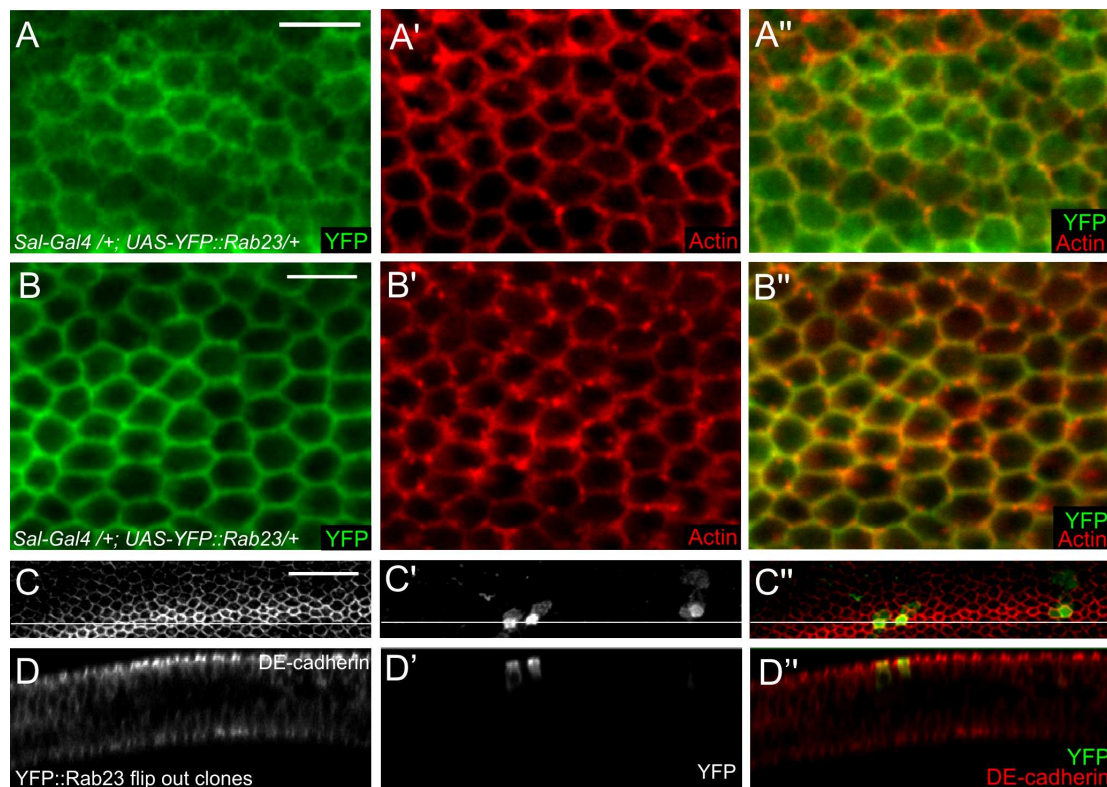


Figure 25. The subcellular distribution of YFP::Rab23 in pupal wing cells. (A-A'') In the junctional zone the YFP::Rab23 protein (in green) is enriched in the plasma membrane of pupal wing cells and displays a diffuse staining in the cytoplasm. In the basolateral zone (B-B'') YFP::Rab23 is also enriched in the plasma membrane, but staining in the cytoplasm is much weaker than in the junctional zone. Pupal wings depicted on A-B'' were stained at 39 hours APF at 22°C (corresponding to 31 hours APF at 25°C), actin is labeled in red in these panels. (C-D'') The subcellular localization of YFP::Rab23 (green) expressed in flip-out clones. DE-cadherin (red) labels the junctional zone. Note the lack of any obvious proximal-distal polarization (C-C''), and the strong co-localization with DE-cadherin in the junctional zone (D-D''). D-D'' display a Z section of the wing along the white line indicated on C-C''. Proximal is on the left, distal is on the right on each panel. Scale bars: 5 μ m in A-B and 20 μ m in C.

shown) and at 36 hours APF. The expression of the YFP::Rab23 fusion protein in flip-out clones also led to similar observations and importantly, it confirmed the lack of any apparent proximal-distal polarization (Figure 25. C- D”). Thus, Rab23 itself does not appear to display a proximo-distally polarized distribution from the onset of pupal development till shortly after trichome placement.

As a comparison, we examined the localization pattern of YFP::Rab23^{Q96L}, a constitutively active (CA) (Figure 26. C) and YFP::Rab23^{S51N}, a dominant negative (DN) form of Rab23 (Figure 26. B). The overall patterns were similar to wild type YFP::Rab23, but the activated form displayed stronger membrane association, whereas the DN exhibited higher accumulation in the cytoplasm than wild type. This is in agreement with the membrane cycle model for Rab GTPases (Behnia and Munro, 2005). We concluded that although the localization studies are based on overexpression, they are likely to reflect the normal localization of Rab23 to a grate extent.

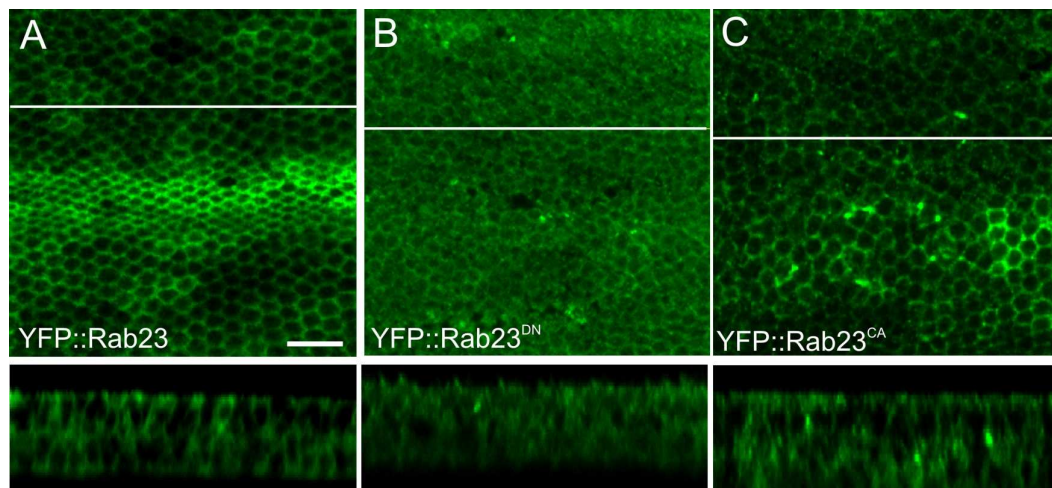


Figure 26. The subcellular distribution of DN and CA YFP::Rab23 in pupal wing cells. (A) In the junctional zone the wild type YFP::Rab23 protein (in green) is enriched in the plasma membrane of pupal wing cells and displays a weak diffused staining in the cytoplasm as well. (B) The dominant negative (DN) form of YFP::Rab23 (in green) is partly membrane associated, but displays a stronger accumulation in the cytoplasm than the wild type protein. (C) The constitutively active (CA) form of YFP::Rab23 (in green) is enriched in the plasma membrane, whereas the cytoplasmic staining is somewhat weaker than that of the wild type protein. A-C displays apical sections, while Z axis reconstructions (made along the white lines indicated on A-C) are shown below these panels. Scale bar: 10 μ m.

Next, we addressed the question whether increased amounts of Rab23 would affect wing development and PCP protein localization. However, overexpression of YFP::Rab23 had no effect on wing development and the protein did not impair PCP protein localization. Similarly, overexpression of EGFP::Rab23^{Q96A}, a constitutively active form of Rab23, had no effect on pupal wing development either (not shown), while the DN induced a weak multiple hair phenotype that was much weaker than that of *Rab23*⁵¹ (not shown). Therefore this allele was not used for further studies.

Rab23 associates with the Pk protein

As *Rab23* seems to be required for PCP protein polarization, we wondered whether core proteins might be directly regulated by, or associated with Rab23. Because YFP::Rab23 displays a strong, uniform membrane association when expressed in pupal wing cells, and the core PCP proteins are also enriched in membrane complexes, our initial colocalization studies in pupal wings were not informative with regard to the identification of potential Rab23 partners. To address this question, we used *Drosophila* S2 cells in which Rab23 and the core proteins are normally not expressed or only expressed at a moderate level (Bhanot et al., 1996). We analysed the subcellular distribution of the core proteins in S2 cells in the presence of Rab23. We examined if protein localization was altered by Rab23 in Fz/Dsh and Stbm/Pk co-transfected cells (data not shown). These studies led to the conclusion that the presence of Rab23 does not modify the subcellular pattern of the core proteins including the membrane localization of Fz (Figure 27. A- C) and Fz/Dsh. However, we noticed that while Fz, Dsh and Dgo do not exhibit a significant degree of colocalization with Rab23 (Figure 27. A-B", and not shown) (for Fz 0% of the cells exhibited colocalization, n=29), the Stbm and Pk proteins partly colocalize with Rab23 (Figure 27. C-D"). The degree of colocalization is higher between Rab23 and Pk (96% of cells, n=54) than Rab23 and Stbm (compare Figure 27. C" to D"). Because the Stbm and Pk proteins did not show cell membrane localization when expressed alone or together (not shown), it was not possible to test directly if Rab23 dependent endocytosis affects the subcellular distribution of Stbm and Pk. Nonetheless, these results suggest that Rab23 might affect core protein localization by regulating Stbm and/or Pk distribution.

Consistently, the activated form of Rab23 (Rab23Q96A) displayed a strong colocalization with Pk (Figure 27. E-E"), whereas the T69A mutant version of Rab23 (Rab23T69A, corresponding to *Rab23*^{T69A}) exhibited a significantly lower level of colocalization with Pk (Figure 27. F-F") (in 1 out of 26 cells).

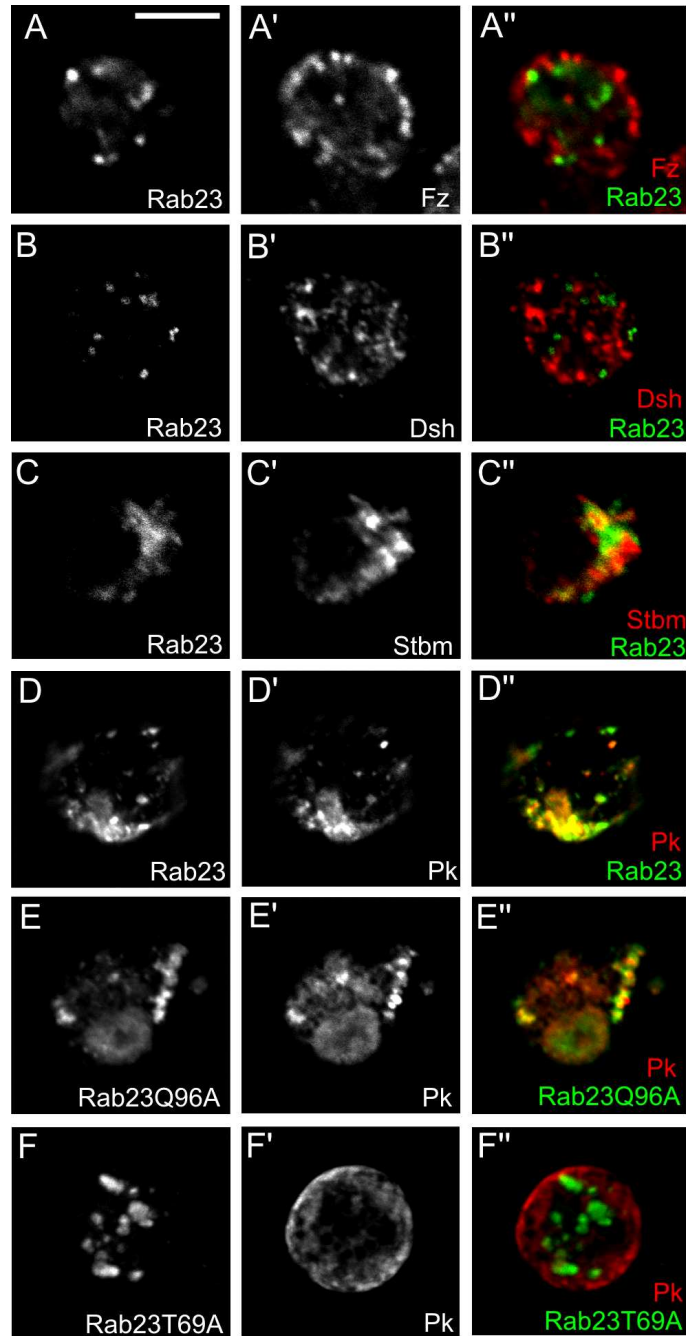


Figure 27. Rab23 colocalizes with Pk in S2 cells. (A-F'') S2 cells cotransfected with Rab23 and Fz (A-A''), Rab23 and Dsh (B-B''), Rab23 and Stbm (C-C''), Rab23 and Pk (D-D''), Rab23Q96A and Pk (E-E'') and Rab23T69A and Pk (F-F''). Rab23 is labeled in green, core PCP proteins are labeled in red. Fz and Dsh do not show a significant colocalization with Rab23 (A'', B''), whereas Stbm and Pk display a partial overlap with that of Rab23 (C'', D''). Rab23Q96A, the activated form of Rab23, exhibits a strong colocalization with Pk (E-E''), while the Rab23T69A mutation reduces colocalization with Pk (F-F''). Scale bar: 5 μ m.

To support the relevance of the observations made in S2 cells, and to verify whether Rab23 associates with Stbm and Pk *in vivo*, coimmunoprecipitation experiments were carried out. Western-blot analysis of S2 cells transfected with HA-tagged Rab23 demonstrated that HA-Rab23 is specifically recognized by our anti-Rab23 serum, but not by the pre-immune serum (Figure 28. A). The same was true for the purified His-tagged protein (not shown), therefore the anti-Rab23 serum appeared suitable for biochemical experiments. Indeed, anti-Rab23 co-immunoprecipitated Pk from wild type but not from *Rab23*⁵¹ mutant pupal protein extracts (28-30 hours APF) (Figure 28. B). In parallel, we were unable to detect Stbm or Fmi

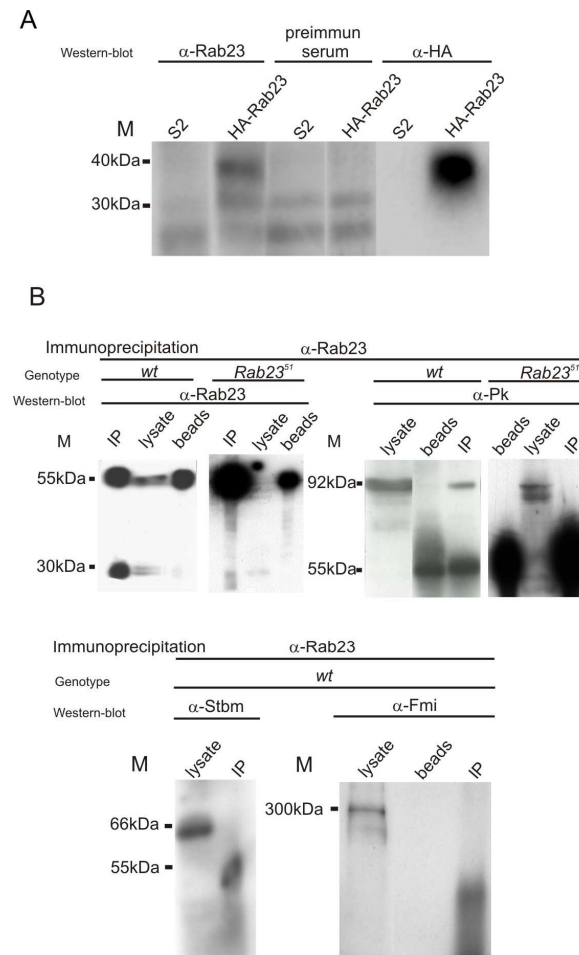


Figure 28. Rab23 associates with Pk in immunoprecipitation experiments. (A) Western-blot analysis of non-transfected S2 cells, and S2 cells transfected with HA-tagged Rab23. Rab23-HA is specifically recognized by anti-Rab23 and anti-HA, but not by the pre-immune serum. The predicted molecular weight of wild type Rab23 is 30kDa, whereas HA-Rab23 is about 40kDa. (B) Immunoprecipitations from lysates of wild type and *Rab23*⁵¹ homozygous mutant 30 hours pupae using anti-Rab23 and probed with anti-Rab23 (upper left), anti-Pk (upper right), anti-Stbm (lower left) and anti-Fmi (lower right). Rab23 co-immunoprecipitates Pk but not Stbm and Fmi from wild type pupae, whereas Rab23 and Pk could not be precipitated from *Rab23*⁵¹ mutants.

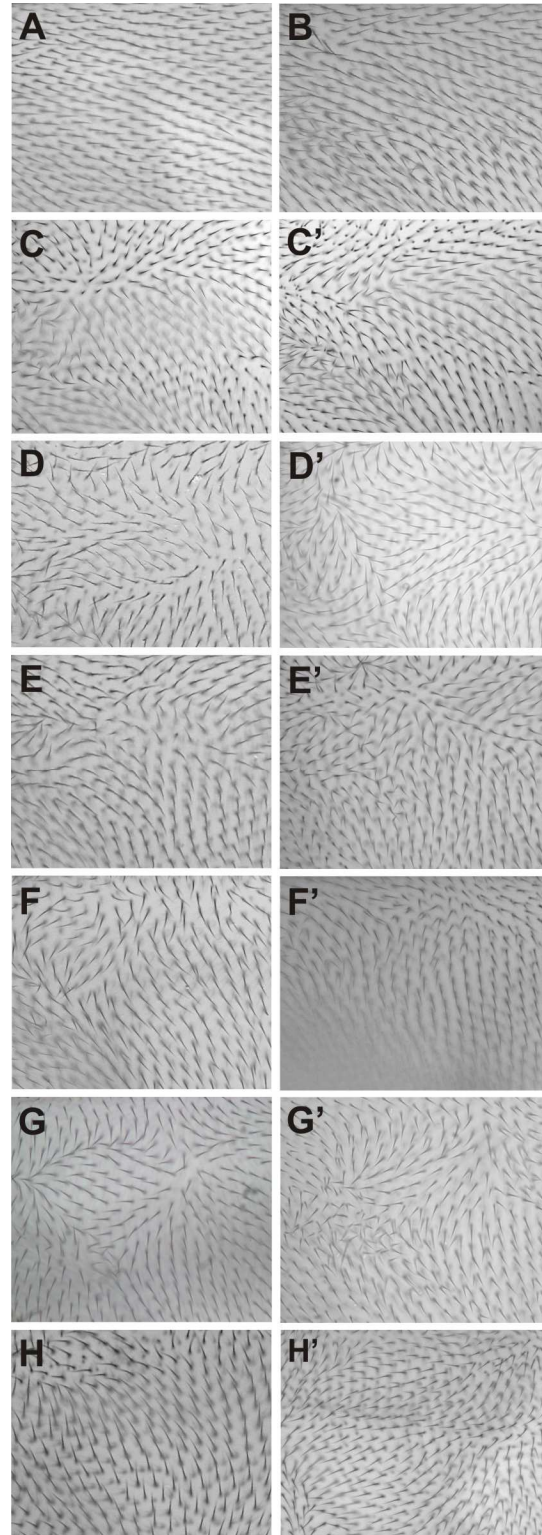
in the Rab23 complex (Figure 28. B), despite the fact that Stbm is known to bind Pk (Bastock et al., 2003; Jenny et al., 2003). Thus, our data suggest that *Rab23* interacts with Pk that could explain the localization problems of Pk and, indirectly, the other core PCP proteins. However, because the PCP complexes might be sensitive to biochemical manipulations or might undergo very dynamic changes, we can not exclude that Rab23 directly regulates the distribution of Stbm or some of the other PCP proteins as well.

Dominant genetic interactions between *Rab23* and other PCP genes

If the sole function of *Rab23* would be to promote the cortical polarization of Pk, and may be some other core PCP proteins, one would expect that *Rab23* mutants would exhibit similar phenotypic effects as *pk* mutants or mutations of the core group. However, we observed that the strong multiple hair phenotype of *Rab23* is markedly different from the orientation defects exhibited by the core PCP mutants. Thus, it appears that *Rab23* has two distinct (albeit not necessarily independent) activities during the establishment of tissue polarity in the wing. The first is a role in late PCP protein polarization, while the second is to restrict actin accumulation and prehair initiation to a single site. Consistent with a specific role in the restriction of prehair formation, we found that *Rab23* dominantly enhances the weak multiple hair phenotype of the core mutations *fz*²¹, *dsh*¹, *fmi*^{fz3}, *stbm*⁶, *pk*^{pk-sple13} and *pk*^{pk30} without affecting the hair orientation defects (Figure 29. and Figure 31. B). We also observed that the *Rab23* homozygous mutant phenotype is sensitive to the gene dose of the In group (Figure 30. and Figure 31. E) which is known to play a role in the regulation of wing hair number. Quantification of wing hair numbers in mutant combinations that were homozygous for *Rab23* and heterozygous for In group mutations have shown that *frtz*¹ and *fy*³ dominantly enhance the number of multiple wing hairs exhibited by *Rab23*⁵¹. The *in*¹, *Rab23*^{T69A}/*Rab23*⁵¹ combination does not exhibit larger number of multiple hairs in the A sector of the wing (Figure 31. E) than the *Rab23* single mutants, but increased multiple hair number was evident in the D region (Figure 30. B, C'). In contrast, *RhoA* and *Drok* mutations, affecting two cytoskeletal regulators of trichome placement, do not exhibit genetic interaction with *Rab23* (Figure 31. E). Moreover, we found that the multiple hair phenotype induced by late *hs-Fz* overexpression (Krasnow and Adler, 1994) is enhanced by *Rab23* (Figure 31. F). This is again similar to the effect of In group mutations (Lee and Adler, 2002) but opposite to the one of *RhoA* and *Drok* (Strutt et al., 1997; Winter et al., 2001). Hence, the dominant

interaction studies suggest that *Rab23* cooperates with the core and In group of genes but not with the Rho pathway during the regulation of wing hair number.

Figure 29. Genetic interaction studies with *Rab23* and the core PCP mutations. (A) Wild type wing with single distally pointing hairs. (B) *Rab23*⁵¹ mutant wing exhibiting multiple hairs in a moderately strong density. *fz*²¹ (C), *dsh*¹ (D), *fmi*^{fz3} (E), *stbm*⁶ (F), *pk*^{pk-sple13} (G) and *pk*^{pk30} (H) wings displaying very few, if any multiple hairs and strong hair orientation defects. *Rab23* significantly increases the number of multiple hairs in the *fz*²¹/*fz*²¹; *Rab23*⁵¹ (C'), *dsh*¹/*dsh*¹; *Rab23*⁵¹/+ (D'), *fmi*^{fz3}/*fmi*^{fz3}; *Rab23*⁵¹/+ (E'), *stbm*⁶/*stbm*⁶; *Rab23*⁵¹/+ (F'), *pk*^{pk-sple13} *pk*^{pk-sple13}/+; *Rab23*⁵¹/+ (G') and *pk*^{pk30}/*pk*^{pk30}; *Rab23*⁵¹/+ (H') mutant combinations. Photomicrographs were taken from the D wing region and were positioned in the same way like in Figure 17. Quantification of wing hair number is presented in Figure 31. Proximal is on the left, distal is on the right on each panel.



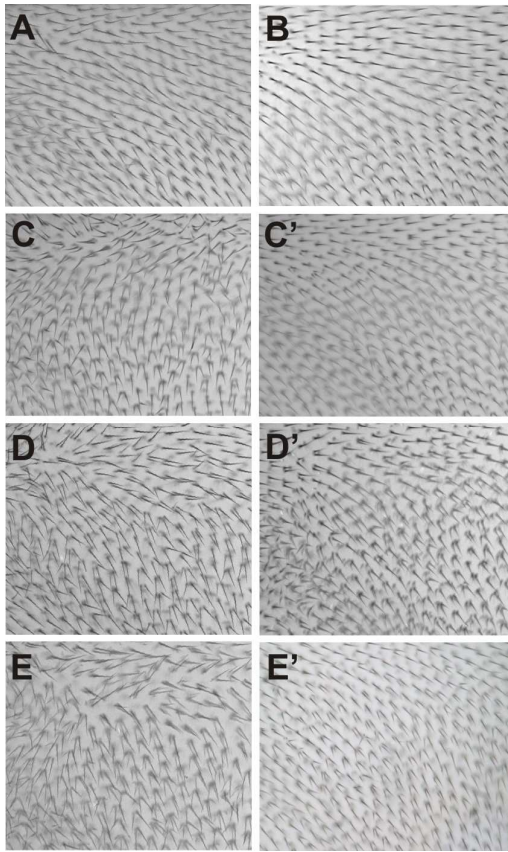


Figure 30. Genetic interaction studies with *Rab23* and *in*, *frtz* and *mwh¹* mutations. (A) *Rab23⁵¹* mutant wing exhibiting multiple hairs in moderately strong density, like the *Rab23⁵¹/Rab23^{T69A}* mutant combination in (B). *in¹* (C), *frtz¹* (D) and *mwh¹* (E) mutant wings exhibiting a large number of multiple hairs and orientation problems. The *in¹/+; Rab23⁵¹/Rab23⁵¹* (C'), *frtz¹/+; Rab23⁵¹/Rab23⁵¹* (D') and *mwh¹/+; Rab23⁵¹/Rab23⁵¹* (E') combinations exhibit larger number of multiple hairs than *Rab23* (A or B). Photomicrographs were taken from the D wing region and were positioned in the same way like in Figure 17. Proximal is on the left, distal is on the right on each panel.

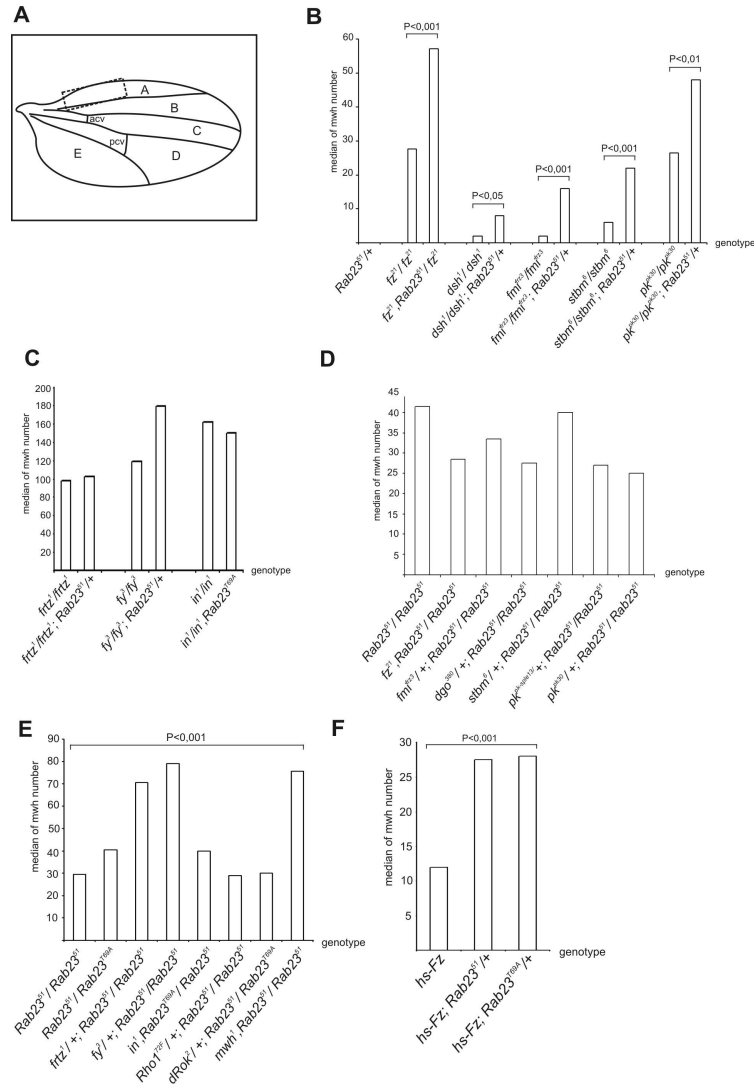


Figure 31. Quantification of wing hair numbers in different *Rab23* and PCP mutant combinations. (A) Schematized wing, multiple wing hairs were counted in the proximal half of the A region on the dorsal side of each wing (a square with dashed lines indicates the area). (B) Quantification of wing hair numbers in mutant combinations that were homozygous for a core PCP mutation and heterozygous for *Rab23*. *Rab23* dominantly enhanced the number of multiple wing hairs exhibited by core PCP mutations. (C) Quantification of wing hair numbers in mutant combinations that were homozygous for an In group mutation and heterozygous for *Rab23*. (D) Quantification of wing hair numbers in mutant combinations that were homozygous for *Rab23* and heterozygous for a core PCP mutation. The number of multiple wing hairs exhibited by *Rab23*⁵¹ is not sensitive to the gene dose of the core PCP genes. (E) Quantification of wing hair numbers in mutant combinations that were homozygous for *Rab23* and heterozygous for an In group mutation or a mutation of the Rho pathway. *frtz*¹, *fy*³ and *mwh*¹ dominantly enhance the number of multiple wing hairs exhibited by *Rab23*⁵¹, whereas *dRok*² and *RhoA*^{72F} had no significant effect. The *in*¹ allele also had no effect in this wing region but in other wing regions it significantly enhanced the number of multiple hairs exhibited by *Rab23*⁵¹/*Rab23*^{769A}. (F) Quantification of wing hair numbers in wings that express hs-Fz. Note that both *Rab23* alleles increase the number of multiple hairs produced. We examined 10-22 wings for each genotype. To test for significance we applied the *t*-test as a statistical method, P indicates probability.

Double mutant analysis of *Rab23* with core genes, In group genes and *mwh*

After the dominant genetic interaction assays, to further probe the relationship between *Rab23* and the PCP genes, we examined double mutant combinations of *Rab23* and mutations of the core PCP group, the In group and *mwh*. Such an analysis has previously been successfully used to determine the epistatic relationship between the different PCP mutation groups (Wong and Adler, 1993), therefore we wondered about the position of *Rab23* as compared to the described hierarchy of PCP regulators. We constructed double mutants of *Rab23*⁵¹ with *fz*²¹, *dsh*¹, *stbm*⁶, *pk*^{pk30}, *in*¹, *frtz*¹, and *mwh*¹. This double mutant analysis revealed that the *dsh*¹; *Rab23* double mutant exhibited a combination of hair orientation defects essentially identical to the ones visible in *dsh*¹ and a multiple hair phenotype resembling the *Rab23* single mutant (Figure 32. D, D') and thus, this is an example of an additive interaction. The double mutants with *fz*²¹ and *stbm*⁶ displayed the type of hair

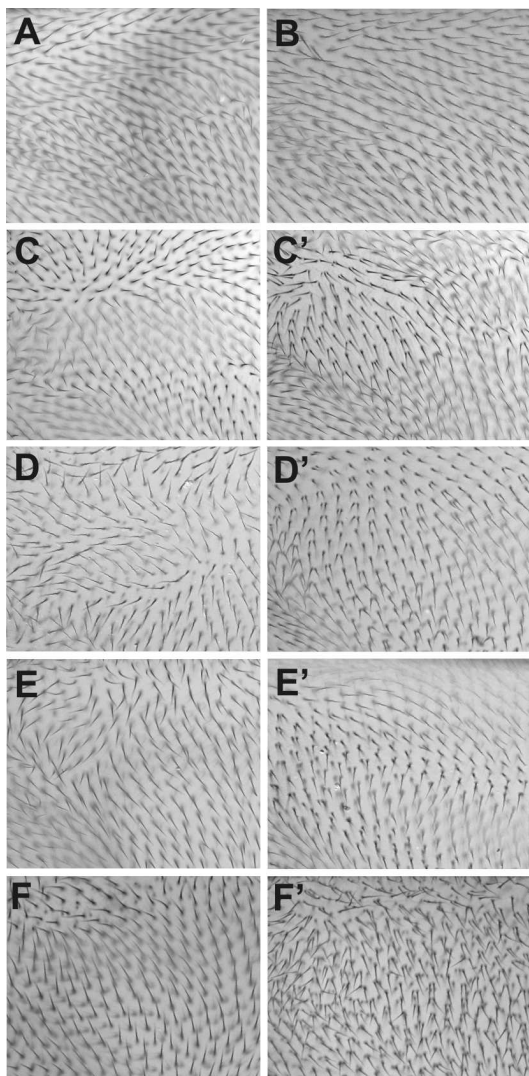


Figure 32. Double mutant analysis with *Rab23* and core PCP mutations. (A) *Rab23*^{T69A} and (B) *Rab23*⁵¹ mutant wings exhibiting multiple wing hairs in a moderately strong density. *fz*²¹ (C), *dsh*¹ (D), *stbm*⁶ (E), and *pk*^{pk30} (F) wings displaying very few if any multiple hairs, and strong hair orientation defects. The double mutant combinations of *fz*²¹, *Rab23*⁵¹ (C'), and *stbm*⁶, *Rab23*⁵¹ (E') display very high number of multiple hairs. (D') *dsh*¹, *Rab23*⁵¹ wing exhibits a similar number of multiple hairs as *Rab23*⁵¹ homozygotes (compare D' to B). In *pk*^{pk30}, *Rab23*⁵¹ (F') double mutants the number of multiple hairs is increased compared to single mutants, while the hair orientation defects are weaker than in *pk*^{pk30} (F). Photomicrographs were taken from the D wing region and were positioned in the same way like in Figure 17. Proximal is on the left, distal is on the right on each panel.

orientation defects found in the corresponding single core PCP mutants (Figure 32. C, C', E, E'). However, they exhibited a synergistic interaction with regard to their multiple hair phenotype, which is stronger than the sum of the individual mutants (quantified in Figure 35. A). In the $pk^{pk30}; Rab23$ combination we noted a partial suppression of the very strong and stereotyped hair orientation defects typically exhibited by the pk^{pk30} single mutant (Figure 32. F, F'). Additionally, with respect to wing hair number, we observed an even stronger synergistic effect than with fz and $stbm$, since the $pk^{pk30}; Rab23$ double mutant exhibited a very high number of multiple hairs (Figure 35. A). Overall, the phenotype was almost identical to that of $frtz^1$ or in^1 (Figure 33. C, D).

The $frtz^1; Rab23^{51}$ and $in^1, Rab23^{T69A}$ double homozygous combinations displayed essentially identical PCP defects as the $frtz^1$ or in^1 homozygotes (Figure 33. C, D'), except that the average trichome number per cell was somewhat higher in the double mutants than in the corresponding single mutant (Figure 34.). Finally, the $mwh, Rab23$ double mutants displayed an identical PCP phenotype with that of mwh single mutants (Figure 33. E, E').

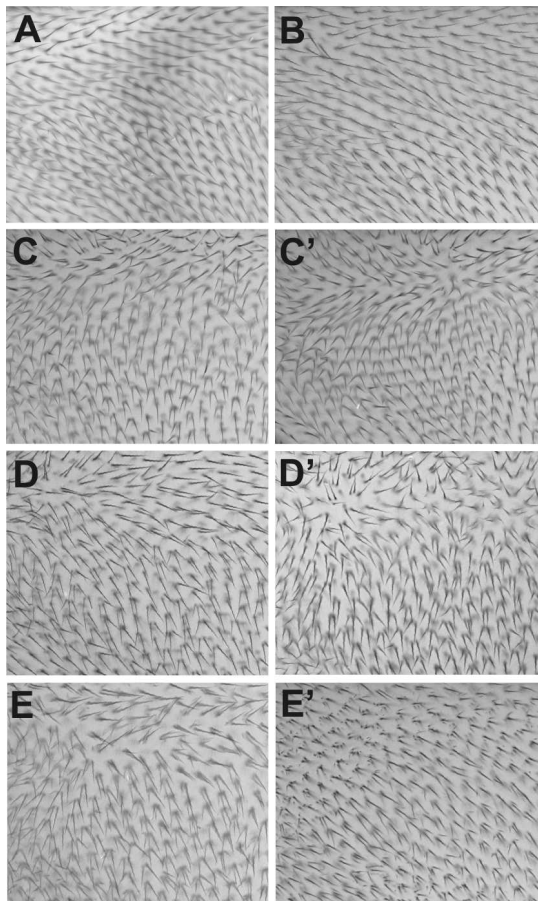
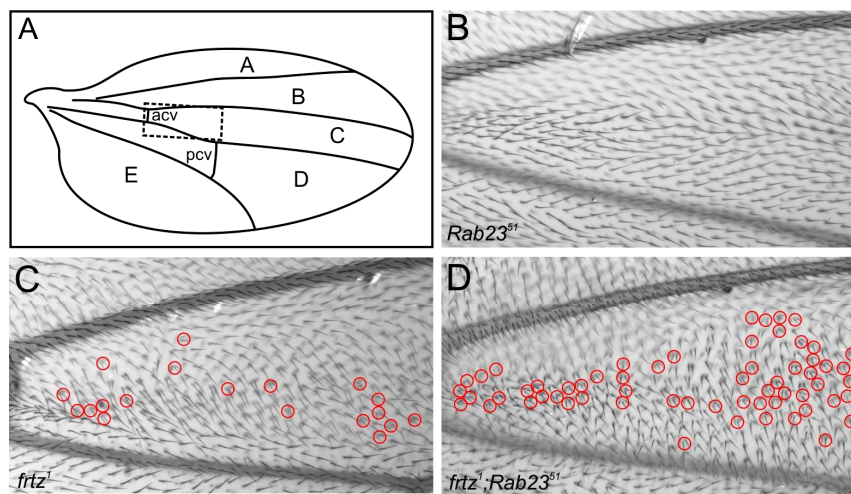


Figure 33. Double mutant analysis with *Rab23* and *In* group and *mwh*¹ mutations. (A) *Rab23*^{T69A} and (B) *Rab23*⁵¹ mutant wings exhibiting multiple wing hairs in a moderately strong density. *in*¹ (C), *frtz*¹ (D) and *mwh*¹ (E) wings show a strong multiple wing hair phenotype with orientation defects. *in*¹, *Rab23*^{T69A} (C'), *frtz*¹, *Rab23*⁵¹ (D'), and *mwh*¹, *Rab23*⁵¹ (E') double mutant combinations display identical PCP phenotypes as the corresponding *in* (C), *frtz* (D) or *mwh* (E) mutations. Photomicrographs were taken from the same wing region and were positioned in the same way like in Figure 17. Proximal is on the left, distal is on the right on each panel.

With respect to the determination of prehair initiation site, the double mutant analysis revealed that *in*, *frtz* and *mwh* are epistatic to *Rab23*, and therefore they are likely to act downstream of, or later than *Rab23*. However, the core PCP proteins appear to cooperate with *Rab23* in a more complex manner. In the double mutant assay they exhibit an additive or a synergistic interaction in regard of wing hair number, suggesting that they act in parallel and/or redundant signaling pathways. Yet, the core PCP mutations not only exhibit a dominant genetic interaction with that of *Rab23*, but *Rab23* seems to bind Pk and appears to play a role in cortical polarization of the PCP proteins, which makes it unlikely that they only act through completely independent pathways.



E

Genotype	Cell No.	Trichome No.	Trichome/Cell
<i>Rab23</i> ⁵¹	1712	1916	1.119
<i>Rab23</i> ^{T69A}	1471	1781	1.21
<i>in</i> ¹	1806	2932	1.623
<i>in</i> ¹ ; <i>Rab23</i> ^{T69A}	1495	2732	1.827
<i>frtz</i> ¹	1589	2277	1.432
<i>frtz</i> ¹ ; <i>Rab23</i> ⁵¹	1702	3002	1.763

Figure 34. Quantification of the average number of trichomes per cell in *Rab23*, *in* and *frtz* mutant combinations. (A) Schematized wing, trichomes were counted in the C region (area bordered by dashed lines) immediately distal to the anterior cross vein (acv) until the line of the posterior cross vein (pcv). (B) *Rab23*⁵¹, (C) *frtz*¹ and (D) *frtz*¹; *Rab23*⁵¹ mutant wings. Wing cells with more than two hairs are indicated with red circles. Note that the number of such cells is higher in the double homozygous mutant combination than in the single mutants. (E) Quantification of the average number of trichomes per cell in *Rab23* and *In* group mutant combinations. In double mutant wings the average number of trichomes per cell is always higher than in the appropriate single mutants. Proximal is on the left, distal is on the right on each panel.

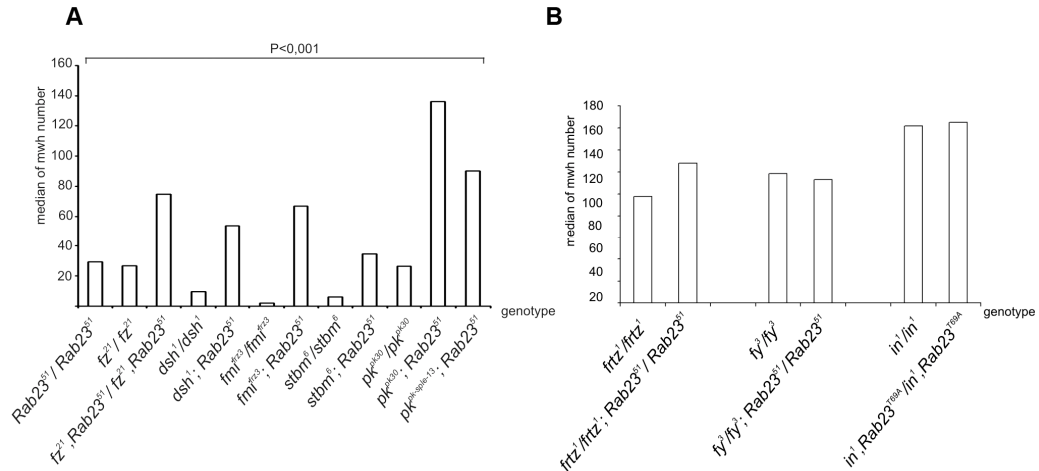


Figure 35. Quantification of wing hair numbers in different *Rab23* and PCP gene double mutants.

(A) Quantification of wing hair numbers in double homozygous mutant combinations of *Rab23* and a core PCP mutation. Additive and synergistic effects are both seen. **(B)** Quantification of *Rab23* and In group double homozygous mutant combinations. During the quantitative analysis hairs were counted in the proximal half of wing sector A, we examined 10-22 wings for each genotype. To test for significance we applied the *t*-test as a statistical method, P indicates probability.

DISCUSSION

The analysis of PCP establishment has recently become an important field of research in many different organisms from plants to vertebrates. During the course of my Ph.D. studies, we were analyzing PCP establishment in *Drosophila* by trying to find some of the missing elements of the pathway that is responsible for this process, and thus, to contribute to a deeper understanding of this conserved phenomenon. In order to isolate new PCP genes, we performed a large scale, two generation mutagenesis screen on three major autosomal chromosomal arms (2R, 2L and 3R) by taking advantage of the FRT/Flp mosaic recombination system. This system proved to be a powerful tool for our purpose and resulted in the isolation of 28 new PCP genes. Out of the 28 novel PCP complementation groups, we have successfully mapped two; the *Kul* (*Kuzbanian like*) and the *Rab23* genes. Subsequently, we have focused on the detailed analysis of one of these genes, *Rab23*.

We have shown that one of the newly identified PCP complementation group on 3R with five members exhibit PCP phenotype in all tissues examined, which is similar to that of the primary polarity genes. These alleles carry a point mutation in the *Drosophila Kul* gene. *Kul* encodes an ADAM10 family transmembrane metalloprotease that has been shown to play a role in Notch/Delta signaling in *Drosophila* (Sapir et al., 2005). It is known that Notch/Delta signaling is required for correct R3/R4 cell fate determination, and as a consequence, PCP establishment in the compound eye (Cooper and Bray, 1999; Adler, 2002), and that the impairment of this pathway in the eye usually leads to the formation of symmetrical ommatidia. However, our *Kul* mutants induced mainly ommatidial rotation defects, and the Notch/Delta pathway is not known to regulate PCP establishment in the wing (Jenny and Mlodzik, 2006). Thus, it seems likely that the PCP defects induced by *Kul* are not related to its well described function in Notch/Delta signaling. Instead, we propose that during PCP signaling *Kul* acts through the regulation of an unidentified substrate that is distinct from Delta. This hypothesis is in good agreement with the knowledge that ADAM10 family metalloproteases are not dedicated exclusively to Delta processing but are able to cleave many other proteins as well (Lamieux et al., 2007; Kohutek et al., 2009). With regard to PCP signaling, the substrate of *Kul* can be an already known component of the pathway or it might be a novel PCP protein. The identification of this substrate and the detailed analysis of the relationship between *Kul* and the other elements of the PCP pathway could provide interesting information about the molecular mechanism of PCP establishment in flies.

The other new PCP gene we identified corresponds to *Drosophila Rab23*. Mutations in the *Drosophila Rab23* orthologue result in abnormal trichome orientation and the formation of multiple hairs on the wing, leg and abdomen. We show that *Rab23* impairs hexagonal packing of the wing cells, and that it plays a role in cortical polarization of the PCP proteins. We found that *Rab23* is able to associate with the proximally accumulated Prickle protein, although *Rab23* itself does not appear to display a polarized subcellular distribution in wing cells. The absence of *Rab23* leads to increased actin accumulation in the sub-apical region of the pupal wing cells that fail to restrict prehair initiation to a single site. Moreover, our results indicate that, unlike the vertebrate orthologues, *Drosophila Rab23* is not an essential gene and does not appear to regulate Hh signaling.

Careful comparison of the *Rab23* mutant wing and abdomen phenotype with that of the other PCP mutations revealed that the *Rab23* effect differs from all the others. Most notably, *Rab23* has a specific requirement in the development of one particular type of sub-cellular structure (cuticular hair) in every body region we examined, however it does not appear to play any role in the planar orientation of multicellular units such as ommatidia in the eye or the sensory bristles of the adult epidermis. On *Rab23* mutant wings, the weak trichome orientation defects and the medium strong multiple hair (mostly double hair) phenotype is clearly different from the core PCP phenotypes (hair orientation problems and few multiple hairs), or the phenotypes induced by the In group (strong multiple hair effect and orientation defects), or *mwh* typically displaying 4-5 hairs per cell and clear hair orientation defects. As compared to *Rho1* and *Drok*, *Rab23* displays a similar adult wing hair phenotype in mutant clones in respect of multiple hairs, while the orientation defects are less clear in *Rho1* and *Drok* mutants (Strutt et al., 1997; Winter et al., 2001). Moreover, a significant difference exists at the molecular level because unlike *Rab23*, *RhoA* and *Drok* do not play a role in cortical polarization of the core PCP proteins (our unpublished results). Given that our *Rab23* alleles genetically behave as strong LOF or null alleles, it appears that *Rab23* identifies a unique class of PCP genes employed for the regulation of trichome planar polarization.

The analysis of *Drosophila Rab23* indicated further that although this small GTPase family is structurally well conserved during evolution, the functional conservation between the vertebrate and insect members is much less obvious. Notably, unlike in the case of its vertebrate orthologues, we found that *Drosophila Rab23* is not an essential gene and does not appear to regulate Hedgehog signaling. In flies, *Rab23* is not expressed in the embryonic CNS and CNS defects were not detected in *Rab23* mutant embryos, therefore *Rab23* is unlikely to play a role in neural development. Similarly, we found no evidence for a *Rab23* requirement

in other Hh dependent developmental processes, since the embryonic cuticle pattern or anterior-posterior patterning of the wing remained normal in *Rab23* mutants. Moreover, if *Drosophila Rab23* would be a negative regulator of Hh signal transduction in flies - like its mouse orthologue (Eggenschwiler et al., 2001) -, the loss of *Drosophila Rab23* should activate the Hh pathway (e.g. the loss of *patched*) and would show phenotypic effects similar to the overexpression of Hh. However, in case of the abdominal cuticle, Hh overexpression induces reversed hair polarity (Srtuhl et al., 1997; Lawrence et al., 1999) that is clearly distinct from the effect of *Rab23* which induces randomized polarity and multiple hair outgrowth. These findings suggest that although the Rab23 protein is highly conserved throughout evolution (Guo et al., 2006), its role in Hh signaling is likely to be restricted to vertebrates.

It is generally thought that the polarized activity of the core PCP proteins is a key determinant of hair polarity. *Rab23* mutant wing cells display both cortical polarization and hair orientation defects, and additionally, we found that Rab23 is able to associate with Pk which shows a polarized localization. The simplest model explaining these observations is that *Rab23* plays a role in the proximal accumulation of Pk. Given that Rab proteins are known to control membrane trafficking, our results provide further support for models suggesting that polarized membrane transport is an important mechanism for the asymmetric accumulation of the PCP proteins. Until now, there are several evidences arguing for endocytosis playing role in PCP signaling. Yu et al. described an interaction between Dishevelled2 (Dvl2) and the clathrin adaptor AP-2 in *Xenopus*. They show that direct interaction of Dvl2 with AP-2 is important for Fz internalization and Fz/PCP signaling (Yu et al., 2007). Another interesting observation was made by Shimada and co-workers. They observed that internalized Fz is transported in vesicles along a planar microtubule array in *Drosophila* pupal wing cells in a polarized manner (Shimada et al., 2006). These are nice evidences for the role of vesicular transport in the polarized translocation of PCP proteins. Based on our data, Rab23 could be an additional factor that influences these transport processes. Given that Pk, found to be associated with Rab23, is enriched at the proximal side of the wing cells, it is possible that Rab23 promotes transport towards the proximal direction.

The Rab23 protein itself was first linked to vesicular trafficking and endocytosis in 2003 by Evans and coworkers. They revealed that Rab23 in HeLa cells is localized to the plasma membrane and shows colocalization with the early endosomal marker Rab5, but not with the late endosomal marker LBPA (Evans et al., 2003). During our studies we have also observed a partial colocalization of Rab23 with Rab5- positive endosomes in *Drosophila* S2

cells (data not shown). This pattern let us to speculate about the possibility that Pk transport to the proximal membrane domain in wing cells is accomplished by its association with early endosomes through the Rab23 molecule.

Although Rab23 showed a specific interaction with Pk, technical limitations might have prevented the detection of interactions with other core PCP proteins, and hence it is possible that the mechanism whereby Rab23 contributes to cortical polarization is not limited to Pk regulation. One additional candidate is the transmembrane protein Stbm that partly colocalizes with Rab23 in S2 cells (this work) and has been shown to bind Pk (Bastock et al., 2003; Jenny et al., 2003). Thus, through binding to Pk, Rab23 might affect Stbm localization or signaling capacity. Irrespective of whether *Rab23* directly affects the localization of only one or more PCP proteins, in the wing *Rab23* has a relatively modest effect on protein localization, and on hair orientation, indicating that *Rab23* has a minor or largely redundant role in this tissue. Interestingly, however, *Rab23* induces much stronger trichome orientation defects on the abdominal cuticle than in the wing. Although it is not proven formally, genetic analysis suggests that asymmetric PCP protein accumulation (or at least polarized activation) is likely to occur in the abdominal histoblast cells as well. Hence, with respect to protein polarization *Rab23* may act in a tissue-specific manner playing a largely dispensable role in the wing, but having a critical role in the abdominal epidermis.

Besides our work that suggests a role for Rab23 in actin cytoskeleton regulation through Pk, recent works demonstrated the role of another intracellular trafficking molecule in localized actin assembly. It has been shown that Rab35 regulates the assembly of actin filaments during bristle development in *Drosophila* and filopodia formation and neurite outgrowth in cultured cells (Zhang et al., 2009; Chua et al., 2010). These effects were mediated by the actin binding protein fascin, which directly associated with active Rab35. Inadequate Rab35 function leads to bends and kinks in the bristles (Zhang et al, 2009). Although we could not detect similar phenotypes in *Rab23* mutants, it would be interesting to investigate if beyond its role in PCP signaling, Rab23 is directly associated with actin binding molecules.

Correct trichome placement at a single distally located site is clearly a crucial step in planar polarization of the wing cells. Current models suggest that prehair initiation is controlled by an inhibitory cue localized proximally in a Stbm-dependent manner, and by a Fz-dependent cue that positively regulates hair formation at the distal vertex (Strutt and Warrington, 2008). Whereas it is not clear how the distal cues work, with regard to the proximal cues it is known that Stbm and Pk colocalize with the effector proteins In, Fy and

Frtz that controls the localization and activity of Mwh, which is thought to regulate prehair initiation directly by interfering with actin bundling in the sub-apical region of cells (Strutt and Warrington, 2008; Yan et al., 2008). We found that *Rab23* severely impairs trichome placement in the wing leading to the formation of multiple hairs, which indicates a role in the repression of ectopic hair initiation. Where does *Rab23* fit into the regulatory hierarchy of trichome placement? Our double mutant analysis suggests that *Rab23* is upstream of the In group and Mwh, and acts at the same level as the core PCP genes. The additive and synergistic genetic interactions between *Rab23* and the core PCP mutations indicate that they function in parallel and/or partly overlapping pathways during the restriction of prehair initiation. Remarkably, the *pk^{pk}; Rab23* double mutants exhibit an almost identical phenotype to mutations of the In group, suggesting that, unless we assume the existence of an In independent restriction system, Pk and *Rab23* together are both necessary and sufficient to fully activate the In complex. In *pk* single mutants the proximal accumulation of In protein is severely impaired, yet multiple hairs rarely develop, indicating that proper In localization plays only a minor role in the restriction mechanism. Conversely, in *Rab23* single mutants In protein localization is weakly affected, but multiple hairs often form, suggesting that the major function of *Rab23* is related to In activation. Thus, it appears that the proximally restricted activation of In on the one hand is ensured by Pk, that mainly plays a role in proper In localization, and on the other hand by *Rab23*, that seems to be required for In activation. At present, the molecular function of the In system is unknown, and it is therefore also unclear how *Rab23* might contribute to the activation of the In complex. Nevertheless, because *Rab23* has a weaker multiple hair phenotype than *in*, but the *pk^{pk}; Rab23* double mutant is nearly as strong as *in*, it is conceivable that In activation is not exclusively *Rab23* dependent but, beyond a role in protein localization, Pk has a partial requirement as well. Because the molecular basis of the establishment of the properly polarized cortical domains is poorly understood, and the machinery that prevents hair formation at ectopic positions is almost completely elusive, future analysis of *Rab23* will help to gain deeper insights into these two critical aspects of planar polarization in the *Drosophila* wing and abdomen.

The regulation of cellular packing is an interesting, yet only lately appreciated aspect of wing development. It has been reported by Classen et al., (2005) that the wing epithelium is irregularly packed throughout larval and prepupal stages, but shortly before hair formation it becomes a quasi-hexagonal array of cells. Hexagonal repacking depends on the activity of the core PCP proteins (Classen et al., 2005) although defects in packing geometry do not appear to directly perturb hair polarity in core PCP mutant wing cells. The possible exception

to this rule is *pk* that exhibits very strong hair orientation defects and induces the strongest packing defects within the core PCP group (Classen et al., 2005; Lin and Gubb, 2009). Additionally, another study revealed that irregularities in cell geometry are associated with polarity defects in the case of *fat* mutant clones (Ma et al., 2008). Thus, cell geometry is not the direct determinant of cell polarity, but in some instances cell packing seems to impact on PCP signaling and hair orientation. Here we have shown that in the wing *Rab23* is predominantly involved in the regulation of wing hair number, and it is also required for hexagonal packing of the wing epithelium. Do these packing defects correlate with the severity of the multiple hair phenotype? Our data argue against this idea for the case of *Rab23*, and also for the cases of other strong multiple hair mutants, such as *in*, *frtz* and *mwh*. Therefore, cell shape has no direct effect on the regulation of the number of prehair initiation sites, and *Rab23* appears to regulate hexagonal packing and hair number independently.

As *Rab23* and *Pk* are both required for cellular packing, and *Rab23* associates with *Pk* in pupal protein extracts, it is possible that they cooperate during the regulation of packing. This alternative is in agreement with the observation that *pk^{pk}; Rab23* double mutant wings do not show stronger packing defects than a *pk^{pk}* single mutant (not shown). However, other interpretations are also possible, hence further investigations will be required to understand how *Rab23* and *Pk* regulates cellular packing, and to clarify the impact of packing geometry on PCP establishment in the wing.

Given that the Rab GTPases are thought to regulate vesicular transport, and consistently, localization studies linked mouse *Rab23* to endosomes (Evans et al., 2003), it was expected that *Rab23* regulates the trafficking of vesicle-associated Hedgehog signaling components. However, mouse *Rab23* does not appear to regulate the subcellular localization of the tested Hedgehog signaling elements (Evans et al., 2003; Eggenschwiler et al., 2006), hence in the mammalian systems it has remained obscure what does *Rab23* traffic (Wang et al., 2006a). Our finding that *Drosophila* *Rab23* associates with *Pk* suggests that *Rab23* might be directly involved in the regulation of *Pk* trafficking, and therefore *Pk* could be the first known direct target of *Rab23*. Interestingly, there is a significant overlap reported in the embryonic expression domains of the vertebrate *Pk* and *Rab23* genes in the region of the dorsal neural ectoderm, the somites and the limb buds (Eggenschwiler et al., 2001; Wallingford et al., 2002b; Takeuchi et al., 2003; Veeman et al., 2003; Li et al., 2008; Cooper et al., 2008). Moreover, it is also known that blocking of *Rab23* or *Pk* function in vertebrate embryos can both lead to a *spina bifida* phenotype (Eggenschwiler et al., 2001; Wallingford et al., 2002b; Takeuchi et al., 2003; Li et al., 2008). These observations raise the possibility that,

unlike the Rab23 involvement in Hedgehog signaling, the Rab23-Pk regulatory connection might be evolutionarily conserved.

LIST OF ABBREVIATIONS

- A- anterior
A-P- anterior-posterior
APF- after puparium formation
arr- *arrow*
ato- *atonal*
atro- *atrophin*
- BMP- bone morphogenetic protein
BSA- bovine serum albumine
- CA- constitutive active
CE- convergent extension
CNS- central nervous system
- D- dorsal
DFz2- *Drosophila* Frizzled 2
dgo- *diego*
DI- Delta
DN- dominant negative
dpp- *decapentaplegic*
dRok- *Rho-kinase*
ds- *dacshsous*
dsh- *dishevelled*
D-V- dorso-ventral
dvl- *dishevelled*
- E16- 16 days old
EMS- ethyl-metanolsulphonate
ENU- N-ethyl-N-nitrosourea
ER- endoplasmic reticulum
- FBS- fetal bovine serum

FH3- formin homology 3

fj- four-jointed

fmi- flamingo

frtz- fritz

fry- furry

ft- fat

FTase- farnesyl transferase

fy- fuzzy

fz- frizzled

GAP- GTPase activating protein

GDI- GDP dissociation inhibitor

GDP- guanosin diphosphate

GEF- guanine nucleotide exchange factor

GGTase-geranylgeranyl transferase

grh- grainy head

GTP- guanosine triphosphate

HCC- hepatocellular carcinoma

Hh- hedgehog

HRPO- horseradish peroxidase

lamA- *lamininA*

in- inturned

JNK- Jun N-terminal kinase

Kul- Kuzbanian-like

Kuz- Kuzbanian

LBPA-lysobisphosphatidic acid

LOF- loss of function

msn- *misshapen*
mwh- *multiple wing hairs*

N- Notch
nmo- *nemo*

ON- overnight
opb- *open brain*

P- posterior
PBS- phosphate buffered saline
PCP- planar cell polarity
P-D- proximo-distal
pk- *prickle*
ptch- *patched*

R- rhabdomere
Rab- Ras associated binding
Rce1- Ras converting enzyme
REP- Rab escort protein
rlt- *roulette*
RNAi- RNA- interference
RT- room temperature

sca- *scabrous*
Shh- *Sonic- hedgehog*
smo- *smoothened*
SOP- sensory organ precursor
stan- *starry night*
stbm- *strabismus*
svp- *sevenup*

trc- *tricornered*

Vang- Van Gogh

VDRC- Vienna Drosophila RNAi Center

wdb- *widerborst*

V- ventral

wg- *wingless*

wt- wild-type

REFERENCES

1. **Adler, P. N. (2002).** Planar signaling and morphogenesis in *Drosophila*. *Dev Cell* 2, 525-535.
2. **Adler, P. N., Taylor, J., Charlton, J. (2000).** A domineering non-autonomy of frizzled and Van Gogh clones in the *Drosophila* wing is a consequence of a disruption in local signaling. *Mech Dev* 96, 197-207.
3. **Adler, P. N., Zhu, C., Stone, D. (2004).** Inturned localizes to the proximal side of wing cells under the instruction of upstream planar polarity proteins. *Curr Biol* 14, 2046-2051.
4. **Adler, P. N., Charlton, J., Liu, J. (1998).** Mutations in the cadherin superfamily member gene *dachsous* cause a tissue polarity phenotype by altering Frizzled signaling. *Dev* 125, 959-968.
5. **Ali, B. R., Seabra, M. C. (2005).** Targeting of Rab GTPases to cellular membranes. *Biochem Soc Trans* 33, 652-656.
6. **Amillet, J. M., Ferbus, D., Real, F. X., Antony, C., Muleris, M., Gress, T. M., Goubin, G. (2006).** Characterization of human Rab20 overexpressed in exocrine pancreatic carcinoma. *Hum Pathol* 37, 256-263.
7. **Axelrod, J. D. (2001).** Unipolar membrane association of Dishevelled mediates Frizzled planar cell polarity signaling. *Genes Dev* 15, 1182-1187.
8. **Bai, C. B., Stephen, D., Joyner, A. L. (2004).** All mouse ventral spinal cord patterning by hedgehog is Gli-dependent and involves activator function of Gli3. *Dev Cell* 6, 103-115.
9. **Baonsa, A., Garcia-Bellido, A. (2000).** Notch signalling directly controls cell proliferation in the *Drosophila* wing disc. *Proc Natl Acad Sci U.S.A.* 14, 2609-2614.
10. **Bardin, A. J., Le Borgne, R., Schweisgut, F. (2004).** Asymmetric localization and function of cell fate determinants: a fly's view. *Curr Opin Neurobiol* 14, 6-14.
11. **Bastock, R., Strutt, H., Strutt, D. (2003).** Strabismus is asymmetrically localized and binds Prickle and Dishevelled during *Drosophila* planar polarity patterning. *Dev* 130, 3007-3014.
12. **Behnia, R., Munro, S. (2005).** Organelle identity and the signposts of membrane traffic. *Nature* 438, 597-604.
13. **Bhanot, P., Brink, M., Samos, C. H., Hsich, J. C., Wang, Y., Macke, J. P., Andrew, D., Nathans, J., Nusse, R. (1996).** A new member of the frizzled family from *Drosophila* functions as a Wingless receptor. *Nature* 382, 225-230.

14. **Bock, J. B., Matem, H. T., Peden, A. A., Scheller, R. H. (2001).** A genomic perspective on membrane compartment organization. *Nature* 409, 839-841.
15. **Buvelot, F. S., Rahl, P. B., Nussbaum, M., Briggs, B. J., Calero, M., Janecko, S., Regan, A. D., Chen, C. Z., Barral, Y., Wittaker, G. R., Collins, R. N. (2006).** Bioinformatic and comparative localization of Rab proteins reveals functional insights into the uncharacterized GTPases YPT10p and YPT11p. *Mol Cell Biol* 26, 7299-7317
16. **Casal, J., Struhl, G., Lawrence, P. A. (2002).** Developmental compartments and planar polarity in *Drosophila*. *Curr Biol* 12, 1189-1198.
17. **Casal, J., Struhl, G., Lawrence, P. A. (2006).** Two separate molecular systems. Dachshous/Fat and Starry night/Frizzled, act independently to confer planar cell polarity. *Dev* 133, 4561-4572.
18. **Chae, J., Kim, M. J., Goo, J. H., Collier, S., Gubb, D., Charlton, J., Adler, P. N., Park, W. J. (1999).** The *Drosophila* tissue polarity gene starry night encodes a member of the protocadherin family. *Dev* 126, 5421-5429.
19. **Chavier, P. and Goud, B. (1999).** The role of ARF and Rab GTPases in membrane transport. *Curr Opin Cell Biol* 4, 466-475.
20. **Chen, W., Ten Berge, D., Brown, J., Ahn, S., Hu, L. A., Miller, W. E., Caron, M. G., Barak, L. S., Nusse, R., Lefkowitz, R. J. (2003).** Disheveled 2 recruits beta-arrestin 2 to mediate Wnt5A-stimulated endocytosis of Frizzled 4. *Sci* 301, 1391-1394.
21. **Cheng, K. W., Lahad, J. P., Kuo, W. L., Lapuk, A., Yamada, K., Auesperg, N., Liu, J., Smith-McCune, K., Lu, K. H., Fishman, D., Gray, J. W., Mills, G. B. (2004).** The RAB25 small GTPase determines aggressiveness of ovarian and breast cancers. *Nat Med* 10, 1251-1256.
22. **Classen, A, K., Anderson, K, I., Marois, E., Eaton, S. (2005).** Hexagonal packing of *Drosophila* wing epithelial cells by the planar polarity pathway. *Dev Cell* 9, 805-17.
23. **Choi, K. W., Benzer, S. (1994).** Rotation of photoreceptor clusters in the developing *Drosophila* eye requires the nemo gene. *Cell* 78, 125-136.
24. **Chou, J. H., Chien, C. T. (2002).** Scabrous controls ommatidial rotation in the *Drosophila* compound eye. *Dev Cell* 3, 839-850.
25. **Chua, C., Lim, Y. I., Tang, B. L. (2010).** A vesiculat trafficking small GTPase with actin modulating roles. *Febs Lett* 584, 1-6.
26. **Collier, S., Gubb, D. (1997).** *Drosophila* tissue polarity requires the cell-autonomous activity of the fuzzy gene, which encodes a novel transmembrane protein. *Dev* 124, 4029-4037.

27. Collier, S., Lee, H., Burgess, R., Adler, P. (2005). The WD40 repeat protein fritz links cytoskeletal planar polarity to frizzled subcellular localization in the *Drosophila* epidermis. *Genetics* 169, 2035-2045.
28. Cooper, O., Sweetman, D., Wangstaff, L., Munsterberg, A. (2008). Expression of avian prickles during early development and organogenesis. *Dev Dyn* 237, 1442-1448.
29. Cooper, M. T., Bray, S. J. (1999). Frizzled regulation of Notch signaling polarizes cell fate in the *Drosophila* eye. *Nature*, 397, 526-530.
30. Copp, A. J., Greene, N. D., Murdoch, J. N. (2003). The genetic bases of mammalian neurulation. *Nat Rev Gen* 4, 784-793.
31. Corbeel, L., Ferson, L. (2008). Rab proteins and Rab-associated proteins: major actors in the mechanism of protein-trafficking disorders. *Eur J Pediatr* 167, 723-729.
32. Dabdoub, A., Donohue, M. J., Brennan, A., Wolf, V., Montcouquiol, M., Sassoon, D. A., Hsieh, J. C., Rubin, J. S., Salinas, P. C. and Kelley M. W. (2003). Wnt signaling mediates reorientation of outer hair cell stereociliary bundles in the mammalian cochlea. *Dev* 130, 2375-2384.
33. Das, G., Jenny, A., Klein, T. J., Eaton, S., Mlodzik, M. (2004). Diego interacts with Prickle and Strabismus/Van Gogh to localize planar cell polarity complexes. *Dev* 131, 4467-4476.
34. Eaton, S., Simons, K. (1995). Apical, basal and lateral cues for epithelial polarization. *Cell* 82, 5-8.
35. Eaton, S., Wepf, R. Simons, K. (1996). Roles for Rac1 and Cdc42 in planar polarization and hair outgrowth in the wing of *Drosophila*. *J Cell Biol* 135, 1277-1289.
36. Echard, A., Opdam, F. J., de Leeuw, H. J., Jolliver, F., Savelkoul, P., Hendriks, W., Voorberg, J., Goud, B., Fransen, J. A. (2000). Alternative splicing of human Rab6A gene generates two close but functionally different isoforms. *Mol Biol Cell* 11, 3819-3833.
37. Eggenchwiler, J. T., Bulgakov, O. V., Oin, J., Li, T., Anderson, K. V. (2006). Mouse Rab23 regulates hedgehog signaling from smoothed to Gli proteins. *Dev Biol* 290, 1-12.
38. Eggenchwiler, J. T., Espinoza, E., Anderson, K. V. (2001). Rab23 is an essential negative regulator of the mouse Sonic hedgehog signaling pathway. *Nature* 412, 194-198.
39. Eggenchwiler, J. T and Anderson, K. V. (2000). Dorsal and lateral fates in the mouse neural tube require the cell-autonomous activity of the open brain gene. *Dev Biol* 227, 648-660.
40. Emery, G., Hutterer, A., Berdnik, D., Meyer, B., Witz-Peitz, F., Gaitan, M G., Knoblick, J. A. (2005). Asymmetric Rab11 endosomes regulate delta recycling and specify

cell fate in *Drosophila* nervous system. *Cell* 122, 763-773.

- 41. Evans, T. M., Ferguson, C., Wainwright, B. J., Parton, R. J., Wicking, B. J. (2003).** Rab23, a negative regulator of hedgehog signaling, localizes to the plasma membrane and the endocytic pathway. *Traffic* 4, 869-884.
- 42. Evans, T. M., Simpson, F., Parton, R., Wicking, C. (2005).** Characterization of Rab23, a negative regulator of sonic hedgehog signaling. *Methods Enzymol* 403, 759-777.
- 43. Fabre, C., Casal, J., Lawrence, P. (2008).** The abdomen of *Drosophila*: does planar polarity orient the neurons of mechanosensory bristles? *Neural Dev* 3, 1-14.
- 44. Fanto, M., Clayton, R., Meredith, J., Hardiman, K., Chartoux, B., Kerridge, S., McNeill, H. (2003).** The tumor suppression and cell adhesion molecule Fat controls planar polarity via physical interactions with Atrophin, a transcriptional co-repressor. *Dev* 130, 763-774.
- 45. Fanto, M., McNeill, H. (2004).** Planar polarity from flies to vertebrates. *J Cell Sci* 117, 527-533.
- 46. Fanto, M., Mlodzik, M. (1999).** Asymmetric Notch activation specifies photoreceptors R3 and R4 and planar polarity in the *Drosophila* eye. *Nature* 397, 523-526.
- 47. Feguin, F., Hannus, M., Mlodzik, M., Eaton, S. (2001).** The ankyrin repeat protein Diego mediates Frizzled-dependent planar polarization. *Dev Cell* 1, 93-101.
- 48. Fischer, U., Ikeda, Y., Ljung, K., Serralbo, O., Singh, M., Heidstra, R., Palme, K., Scheres, B., Grebe, M. (2006).** Vectorial information for *Arabidopsis* planar polarity is mediated by combined Aux1, Eln2, and GNOM activity. *Curr Biol* 16, 2143-2149.
- 49. Gao, F. B., Kohwi, M., Brenman, J. E., Jan, L. Y., Jan, Y. N. (2000).** Control of dendritic field formation in *Drosophila* the roles of flamingo and competition between homologous neurons. *Neuron* 28, 91-101.
- 50. Grebe, M. (2004).** Ups and downs of tissue and planar polarity in plants. *Bioessays* 26, 719-729.
- 51. Grosshans, D. L., Ortiz, D., Novick, P. (2006).** Rabs and their effectors: achieving specificity in membrane traffic. *PNAS* 8, 11821-11827.
- 52. Gubb, D. (1993).** Genes controlling cellular polarity in *Drosophila*. *Dev Suppl* 269, 277.
- 53. Gubb, D., Garcia-Bellido, A. (1982).** A genetic analysis of the determination of cuticular polarity during development in *Drosophila melanogaster*. *J Embryol Exp Morphol* 68, 37-57.
- 54. Guo, A., Wang, T., Ng, L., Aulia, S., Chong, K. H., Teng, F. Y., Wang, Y., Tang, B. L. (2006).** Open brain gene product Rab23: expression pattern in the adult mouse brain and functional characterization. *J Neurosci Res* 83, 1118-1127.

- 55. Hartley, J. L., Temple, G. F., Brasch, M. A. (2000).** DNA cloning using in vitro site specific recombination. *Genom Res* 10, 1788-1795.
- 56. Henchcliffe, C., Garcia-Alonso, L., Tang, J., Goodman, C. S. (1993).** Genetic analysis of laminin A reveals diverse functions during morphogenesis in *Drosophila*. *Dev* 103, 299-300.
- 57. Ikeda, Y., Fischer, U., Stepanova, A. N., Alonso, J. M., Ljung, K., Grebe, M. (2009).** Local auxin biosynthesis modulates gradient-directed planar polarity in *Arabidopsis*. *Nat Cell Biol* 11, 731-738.
- 58. Ingham, P. W., McMahon, A. P. (2001).** Hedgehog signaling in animal development: paradigms and principles. *Genes Dev* 15, 3059-3087.
- 59. Jenny, A., Darken, R. S., Wilson, P. A., Mlodzik, M. (2003).** Prickle and Strabismus form a functional complex to generate a correct axis during planar cell polarity signaling. *EMBO J* 22, 4409-4420.
- 60. Jenny, A., Mlodzik, M. (2006).** Planar cell polarity signaling: a common mechanism for cellular polarization. *The Mount Sinai J of Med* 73, 738-750.
- 61. Jordens, I., Marsman, M., Kuijl, C., Neefjes, J. (2005).** Rab proteins, connecting transport and vesicle fusion. *Traffic* 6, 1070-7.
- 62. Kartberg, F., Elsner, M., Fröderberg, L., Asp, L., Nilsson, T. (2005).** Commuting between Golgi cisternae-Mind the GAP! *Biochimica et Biophysica Acta* 1744, 351-363.
- 63. Kohutek, Z. A., diPietro, C. G., Redpath, G. T., Hunaini, I. M. (2009).** ADAM-10-mediated N-cadherin cleavage is protein kinase C-alpha dependent and promotes glioblastoma cell migration. *J Neurosci* 29, 4605-4615.
- 64. Krasnow, R. E. and Adler, P. (1994).** A single frizzled protein has a dual function in tissue polarity. *Dev* 120, 1883-1893.
- 65. Lai, L. S., Chien, A. J., Moon, R. T. (2009).** Wnt/Fz signaling and the cytoskeleton: potential roles in tumorigenesis. *Cell Research* 19, 532-545.
- 66. Lamieux, G. A., Blumenkron, F., Yeung, N., Zhou, P., Williams, J., Grammer, A. C., Petrovich, R., Ripsky, P. E., Moss, M. L., Werb, Z. (2007).** The low affinity IgE receptor (CD23) is cleaved by the metalloprotease ADAM-10. *J Biol Chem* 282, 14836-14844.
- 67. Lanzetti, L., Rybin, V., Malabarba, M. G., Christoforidid, S., Scita, G., Zerial, M., Di Fiore, P.P. (2000).** The Eps8 protein coordinates EGF receptor signaling through Rac and trafficking through Rab5. *Nature* 405, 374-377.
- 68. Lawrence, P. A., Casal, J., Struhl, G. (1999).** The hedgehog morphogene and gradients of cell affinity in the abdomen of *Drosophila*. *Dev* 126, 2441-2449.
- 69. Lawrence, P. A., Casal, J., Struhl, G. (2004).** Cell interactions and planar polarity in the

abdominal epidermis of *Drosophila*. *Dev* 131, 4651-4664.

70. Lawrence, P. A., Struhl, G., Casal, J (2007). Planar cell polarity: one or two pathways? *Nat Rev Genet* 8, 555-563.

71. Lawrence, P. A., Shelton. P. M. J. (1975). The determination of polarity in the developing insect retina. *J Embryol Exp Morph* 33, 471-486.

72. Le Borgne, R., Schweisguth, F. (2003). Unequal segregation of Neuralized biases Notch activation during asymmetrical cell division. *Dev Cell* 5, 139-148.

73. Lee, H., Adler, P. N. (2002). The function of the frizzled pathway in the *Drosophila* wing is dependent on inturnd and fuzzy. *Genetics* 160, 1535-1547.

74. Li, N., Volff, J-N., Wizenmann, A. (2008). Rab23 GTPase is expressed asymmetrically in Hensen's node and plays a role in the dorsoventral patterning of the chick neural tube. *Dev Dyn* 236, 2983-3006.

75. Lim, J., Choi, K, W. (2004). *Drosophila* eye disc margin is a center for organizing long range planar polarity. *Genesis* 39, 26-37.

76. Lin, Y., Gubb, D. (2009). Molecular dissection of *Drosophila* Prickle isoforms distinguishes their essential and overlapping roles in planar cell polarity. *Dev Biol* 325, 386-399.

77. Ma, D., Amonlirdviman, K., Raffard, R. L., Abate, A., Tomlin, C. J., Axelrod, J. D. (2008). Cell packing influences planar cell polarity signalling. *Proc Natl Acad Sci USA* 105, 18800-5.

78. Ma, D., Yang, C. H., McNeill, H., Simon, M. A., Axelrod, J. D. (2003). Fidelity in planar cell polarity signaling. *Nature* 421, 543-547.

79. Marcos, I., Borrego, S., Antinolo, G. (2003). Molecular cloning and characterization of human Rab23, a member of the group of Rab GTPases. *Int J of Molec Med* 12, 983-987.

80. Marois, E., Mahmoud, A., Eaton, S. (2005). The endocytic pathway and formation of Wingless morphogene gradient. *Dev* 133, 307-317.

81. Matakatsu, H., Blair, S. (2004). Interactions between Fat and Dachshous and the regulation of planar cell polarity in the *Drosophila* wing. *Dev* 131, 3785-3794.

82. Meggouh, F., Bienfait, H. M., Weterman, M. A., Visser, M., Baas, F. (2006). Charcot-Marie-Tooth disease due to a de novo mutation of the Rab7 gene. *Neurology* 67, 1476-1478.

83. Mihály, J., Matusek., T., Pataki, Cs. (2005). Diego and friends play again. *FEBS J* 272, 3241-3252.

84. Montcouquiol, M., Sans, N., Huss, D., Kach, J., Dickman, J. D., Forge, A., Rachel, R. A., Copeland, N. G., Jenkins, N. A., Bogani, D., Murdock, J., Warchol, M. E., Wenthold,

- R. J., Kelley, M. W. (2006).** Asymmetric localization of Vangl2 and Fz3 indicate novel mechanism for planar cell polarity in mammals. *J Neurosci* 26, 5265-5275.
- 85. Mori, Y., Yin, J., Sato, F., Sterian, A., Simms, L. A., Selaru, F. M., Schulmann, K., Xu, Y., Olaru, A., Wang, S., Deacu, E., Abraham, J. M., Young, J., Legett, B. A., Meltzer, S. J. (2004).** Identification of genes uniquely involved in frequent microsatellite instability colon carcinogenesis by expression profiling combined with epigenetic scanning. *Cancer Res* 64, 2434-2348.
- 86. Newsome, T., Asling, B., Dickson, B. J. (2000).** Analysis of *Drosophila* photoreceptor axon guidance in eye specific mosaics. *Dev* 127, 851-860.
- 87. Nishimura, N., Sasaki, T. (2008).** Regulation of epithelial cell adhesion and repulsion: role of endocytic recycling. *The J of Med Inv* 10.
- 88. Ng, L. E., Tang, B. L. (2008).** Rab GTPases and their roles in brain neurons and glia. *BRESR* 101622.
- 89. O'Hare K., Rubin, G. (1983).** Structures of P transposable elements and their sites of insertion and excision in the *Drosophila melanogaster* genome. *Cell* 34, 25-36.
- 90. Olkkonen, V M., Peterson, J. R., Dupree, P., Lutcke, A., Zerial, M., Simons, K. (1994).** Isolation of mouse cDNA encoding Rab23, a small novel GTPase expressed predominantly in the brain. *Gene* 138, 207-211.
- 91. Ostermeier, C., Brunger, A. T. (1999).** Structural basis of Rab effector specificity: crystal structure of the small G protein Rab3A complexed with the effector domain of Rabphilin-3A. *Cell* 96, 363-374.
- 92. Park, T. J., Haigo, S. L., Wallingford, J. B. (2006).** Ciliogenesis defects in embryos lacking inturned or fuzzy function are associated with failure of planar cell polarity and Hedgehog signaling. *Nat Genet* 38, 303-311.
- 93. Pechlivanis, M., Kuhlmann, J. (2006).** Hydrophobic modifications of Ras proteins by isoprenoid groups and fatty acids-More than just membrane anchoring. *Biochemica et Biophysica Acta* 1764, 1914-1931.
- 94. Pereira-Leal, J. B., Hume, A. M., Seabra, M. C. (2001).** Prenylation of Rab GTPases: molecular mechanisms and involvement in genetic disease. *FEBS Lett* 498, 197-200.
- 95. Pfeffer, S. (2005).** A model for Rab GTPase localization. *Biochem Soc Trans* 33, 627-30.
- 96. Pfeffer, S. R. (2001).** Rab GTPases: specifying and deciphering organelle identity and function. *Trends Cell Biol* 11, 487-491.
- 97. Pfeffer, S., Aivazian, D. (2004).** Targeting Rab GTPases to distinct membrane compartments. *Nat Rev Mol Cell Biol* 5, 886-896.

- 98. Pirrotta, V., Chan, C. S., McCabe, D., Qian, S. (1995).** Distinct parasegmental and imaginal enhancers and the establishment of the expression pattern of the Ubx gene. *Genetics* 141, 1439-1450.
- 99. Rawls, A. S., and Wolff, T. (2003).** Strabismus requires Flamingo and Prickle function to regulate tissue polarity in the Drosophila eye. *Dev* 130, 1877-1887.
- 100. Rives, A. F., Rochlin, K. M., Wehrli, M., Schwatz, S. L., DiNaro, S. (2006).** Endocytic trafficking of Wingless and its receptors Arrow and Dfrizzled-2, in the Drosophila wing. *Dev Biol* 293, 268-283.
- 101. Roegiers, F., Younger-Shepherd, S., Jan, L. Y., Jan, Y. N. (2001).** Two types of asymmetric division in the Drosophila sensory organ precursor cell lineage. *Nat Cell Biol* 3, 58-67.
- 102. Roskoski, R., Ritchie, P. (1998).** Role of the carboxyterminal residue in peptide binding farnesyltransferase and protein geranylgeranyl transferase. *Arch Biochem Biophys* 356, 164-176.
- 103. Roszko, I., Sawada, A., Krezel, L. S. (2009).** Regulation of convergence and extension movements during vertebrate gastrulation by Wnt/PCP pathway. *Semin Cell Dev* 10-1016.
- 104. Salminen, A., Novick, P. J. (1987).** A Ras-like protein is required for a post-Golgi event in yeast secretion. *Cell* 49, 527-538.
- 105. Santos, E., Nebreda, A. R. (1989).** Structural and functional properties of ras proteins. *FEBS J* 3, 2151-2163.
- 106. Sapir, A., Assa-Kunik, E., Tsruya, R., Schejter, E., Shilo, B. Z. (2005).** Unidirectional Notch signaling depends on continuous cleavage of Delta. *Dev* 132, 123-132.
- 107. Seabra, M. C., Mules, E. H., Hume, A. N. (2002).** Rab GTPases, intracellular traffic and disease. *Trends Mol Med* 8, 23-30.
- 108. Seifert, J. and Mlodzik, M. (2007).** Frizzled/PCP signaling: a conserved mechanism regulating cell polarity and directing motility. *Nature Rev* 6, 126-138.
- 109. Shimada, Y., Usui, T., Yanagawa, S., Takeichi, M., Uemura, T. (2001).** Asymmetric colocalization of Flamingo a seven-pass transmembrane cadherin, and Dishevelled in planar cell polarization. *Curr Biol* 11, 859-863.
- 110. Shimada, Y., Yonemura, S., Ohkura, H., Strutt, D. (2005).** Polarized transport of Frizzled along the planar microtubule array in Drosophila wing epithelium. *Dev Cell* 10, 209-222.
- 111. Simon, M. A. (2004).** Planar cell polarity in the Drosophila eye is directed by graded Four-jointed and Dachshous expression. *Dev* 131, 6175-6184.

- 112. Simons, M., Mlodzik, M. (2008).** Planar cell polarity signaling: from fly development to human disease. *Annu Rev Genet* 42, 517-540.
- 113. Smith, A C., Won Do Heo., Braun, V., Jiang, C., Casanova, J E., Scidmore, A M., Grinstein, S., Brumell, J. (2007).** A network of Rab GTPases controls phagosome maturation and is modulated by *Salmonella enterica* serovar Typhomurium. *J Cell Biol* 176, 263-268.
- 114. Stenmark, H., Olkkonenn, V. (2001).** The Rab GTPase family. *Genome Biology* 2, 3007.1-3007.7.
- 115. Struhl, G., Barbash, D. A., Lawrence, P. A. (1997).** Hedgehog organizes the pattern and polarity of epidermal cells in the *Drosophila* abdomen. *Dev* 124, 2143-2154.
- 116. Strutt, D. J. (2002).** The asymmetric localisation of components of the planar polarity pathway. *Semin Cell Dev Biol* 13, 225-231.
- 117. Strutt, D. J. (2001).** Asymmetric localization of frizzled and the establishment of cell polarity in the *Drosophila* wing. *Mol Cell* 7, 367-375.
- 118. Strutt, D., Weber, U., Mlodzik, M. (1997).** The role of RhoA in tissue polarity and Frizzled signaling. *Nature* 387, 292-295.
- 119. Strutt, H., Mundy, J., Hofstra, K., Strutt, D. (2004).** Cleavage and secretion is not required for Four-jointed function in *Drosophila* patterning. *Dev* 131, 881-890.
- 120. Strutt, H., Strutt, D. (2002).** Nonautonomous planar polarity patterning in *Drosophila*, Dishevelled independent functions of frizzled. *Dev Cell* 3, 851-863.
- 121. Strutt, H., Strutt, D. (2005).** Long-range communication of planar polarity in *Drosophila*. *BioEssay* 27, 1218-1227.
- 122. Strutt, D., Strutt, H. (2007).** Differential activities of the core planar polarity proteins during *Drosophila* wing patterning. *Dev Biol* 302, 181-194.
- 123. Strutt, D and Warrington, S. (2008).** Planar polarity genes in the *Drosophila* wing regulate the localization of the FH3-domain protein Multiple Wing Hairs to control the site of hair production. *Dev* 135, 3103-30111.
- 124. Sullivan, W., Ashburner, M., Hawley, R. S. (2000).** *Drosophila* protocols. In: Sullivan, W., Ashburner, M., Hawley, R. S. eds, Cold Spring Laboratory Press 728p.
- 125. Takeuchi, M., Nakabayashi, J., Sakaguchi, T., Yamamoto, T. S., Takahashi, H., Takeda, H., Ueno, N. (2003).** The prickle related gene in vertebrates is essential for gastrulation cell movements. *Curr Biol* 13, 674-679.
- 126. Taylor, J., Abramova, N., Charlton, J. (1998).** Van Gogh: a new *Drosophila* tissue polarity gene. *Genetics* 150, 199-210.

- 127. Touchot, N., Chardin, P., Tavitian, A. (1987).** Four additional members of the ras gene superfamily isolated by an oligonucleotide strategy: molecular cloning of YPT-related cDNAs from a rat brain library. *Proc Nat Acad Sci USA* 84, 8210-8214.
- 128. Tree, D. R., Ma, D., Axelrod, J. D. (2002a).** A three-tiered mechanism for regulation of planar cell polarity. *Semin Cell Dev Biol* 13, 217-224.
- 129. Tree, D. R., Shulman, J. M., Rousset, R., Scott, M. P., Gubb, D., Axelrod, J. D. (2002b).** Prickle mediates feedback amplification to generate asymmetric planar cell polarity signaling. *Cell* 109, 371-381.
- 130. Usui, T., Shima, Y., Shimada, Y., Hirano, S., Burgess, R. W., Schwarz, T. L., Takeichi, M., Uemura, T. (1999).** Flamingo, a seven-pass transmembrane cadherin, regulates planar cell polarity under the control of Frizzled. *Cell* 98, 585-595.
- 131. Van der Heuvel, M., Nusse, R., Johnston, P., Lawrence, P. (1989).** Distribution of the wingless gene product in *Drosophila* embryos, a protein involved in cell-cell communication. *Cell* 59, 739-749.
- 132. Veeman, M. T., Slusarski, D. C., Kaykas, A., Lojue, S. H., Moon, R. T. (2003).** Zebrafish prickle, a modulator of noncanonical Wnt/Fz signaling, regulates gastrulation movements. *Curr Biol* 13, 680-685.
- 133. Vetter, I. R. and Wittinghofer, A. (2001).** The guanine nucleotide-binding switch in three dimensions. *Science* 294, 1299-1304.
- 134. Vidricaire, G., Tremblay, M. J. (2005).** Rab5 and Rab7, but not ARF6, govern the early events of HIV-1 infection in polarized human placental cells. *J Immunol* 175, 6517-6530.
- 135. Vinson, C. R., Adler, P. N. (1987).** Directional non-cell autonomy and the transmission of polarity information by the frizzled gene of *Drosophila*. *Nature* 329, 549-551.
- 136. Vinson, C. R., Conover, S., Adler, P. N. (1989).** A *Drosophila* tissue polarity locus encodes a protein containing seven potential transmembrane domains. *Nature* 338, 263-264.
- 137. Wallingford, J. B. and Harland, R. M. (2001).** *Xenopus* Dishevelled signaling regulates both neural and mesodermal convergent extension parallel forces elongating the body axis. *Dev* 128, 2581-2592.
- 138. Wallingford, J. B. and Harland, R., M (2002).** Neural tube closure requires Dishevelled dependent convergent extension of the midline. *Dev* 129, 5815-5825.
- 139. Wallingford, J. B., Goto, T., Keller, R., Harland, R. M. (2002b).** Cloning and expression of *Xenopus* Prickle, an orthologue of a *Drosophila* planar cell polarity gene. *Mech Dev* 116, 183-186.

- 140. Wallingford J. B., Fraser, S. E., Harland, R., M. (2002a).** Convergent extension the molecular control of polarized cell movement during embryonic development. *Dev Cell* 2, 695-706.
- 141. Wang, Y., and Nathans, J. (2007).** Tissue/planar cell polarity in vertebrates: new insights and new questions. *Dev* 134, 647-658.
- 142. Wang, J., Hamblet, N. S., Mark, S., Dickinson, M. E., Brinkman, B. C., Segil, N., Fraser, S. E., Chen, P., Wallingford, J. B., Wynshaw-Boris, A. (2006).** Dishevelled genes mediate a conserved mammalian PCP pathway to regulate convergent extension during neurulation. *Dev* 133, 1767-1778.
- 143. Wang, X., Kumar, R., Navarra, J., Casanova, J. E., Goldenring, J. R. (2000).** Regulation of vesicle trafficking in Madin-Derby canine kidney cells by Rab11a and Rab25. *J Biol Chem* 275, 29138-29146.
- 144. Wang, Y., Badea, T., Nathans, J. (2006b).** Order from disorder: self organization in mammalian hair patterning. *Proc Nat Acad Sci USA* 103, 19800-19805.
- 145. Wang, Y., Ng, E. L., Tang, B. L. (2006a).** Rab23: What Exactly Does it Traffic? *Traffic* 7, 746-750.
- 146. Winter, C. G., Wang, B., Ballew, A., Royou, A., Karess, R., Axelrod, J. D., Luo, L. (2001).** Drosophila Rho/associated kinase (Drok) links Frizzled/mediated planar cell polarity signaling to the actin cytoskeleton. *Cell* 105, 81-91.
- 147. Wolff, T., Ready, D. F. (1993).** Pattern formation in *Drosophila* retina. The development of *Drosophila melanogaster* (Bate, A. and Martinet-Aria, A eds.) pp. 1277-1326. Cold Spring Harbor Press, Cold Spring Harbor, NY.
- 148. Wolff, T., Rubin, G. (1998).** Strabismus, a novel gene that regulates tissue polarity and cell fate decisions in drosophila. *Dev* 125, 1149-1159.
- 149. Wong, H. C., Bourdelas, A., Krauss, A., Lee, H. J., Shao, Y., Wo, D., Mlodzik, M., Shi, D. L., Zheng, J. (2003).** Direct binding of the PDZ domain of Dishevelled to a conserved internal sequence of the C-terminal region of Frizzled. *Mol Cell* 12, 1251-1260.
- 150. Wong, L. L., Adler, P. N. (1993).** Tissue polarity genes of *Drosophila* regulate the subcellular location for prehair initiation in pupal wing cells. *J Cell Biol* 123, 209-221.
- 151. Wootton, R. (1992).** Functional morphology of insect wings. *Annu Rev Entomol* 37, 113-140.
- 152. Xu, T., Rubin, C. M. (1993).** Analysis of genetic mosaics in developing and adult *Drosophila* tissues. *Dev* 117, 1223-1237.
- 153. Yan, J., Huen, D., Morely, T., Johnson, G., Gubb, D., Rootie, J., Adler, P N. (2008).**

The multiple-wing-hairs gene encodes a novel GBD-FH3 domain-containing protein that functions both prior and after hair initiation. *Genetics* 180, 219-228.

154. Yang, C. H., Axelrod, J. D., Simon, M. A. (2002). Regulation of Frizzled by fat-like cadherins during planar polarity signaling in the *Drosophila* compound eye. *Cell* 108, 675-688.

155. Yoshida, N. (1999). Stereociliary anomaly in the guinea pig effects of hair bundle rotation on cochlear sensitivity. *Hearing Res* 131, 29-38.

156. Yu, A., Rual, J. F., Tamai, K., Harada, Y., Vidal, M., He, X., Kirchhausen, T. (2007). Association of Dishevelled with the Clatrin AP-2 adaptor is required for Frizzled endocytosis and planar cell polarity. *Dev Cell* 12, 129-141.

157. Zallen, J. A. (2007). Planar polarity and tissue morphogenesis. *Cell* 129, 1050-1063.

Zeidler, M. P., Perrimon, N., Strutt, D. (1999). The four-jointed gene is required in the *Drosophila* eye for ommatidial polarity specification. *Curr Biol* 9, 1363/1372.

158. Zeidler, M. P., Perrimon, N., Strutt, D. (2000). Multiple roles for four-jointed in planar polarity and limb patterning. *Dev Biol* 228, 181-196.

159. Zerial, M., McBride, H. (2001). Rab proteins as membrane organizers. *Nat Rev Moll Cell Biol* 2, 107-117.

160. Zhang, J., Schulze, K. L., Hiesinger, P. R., Suyama, K., Wang, S., Fish, M., Acar, M., Hoskins, R. A., Bellen, H. J., Scott, M.P. (2007). 31 flavors of *Drosophila* Rab proteins. *Genetics* 176, 1307-1322.

161. Zhang, J., Fonovic, M., Suyama, K., Bogoy, M., Scott, P. M. (2009). Rab35 controls actin bundling by recruiting fascin as an effector protein. *Science* 325, 1250-1254.

162. Zhang, F. L., Casey, P. J. (1996). Protein prenylation- Molecular mechanisms and functional consequences. *Annu Rev Biochem* 65, 241-269.

163. Zhang, M., Chen, L., Wang, S., Wang, T. (2009). Rab7: roles in membrane trafficking and disease. *Biosci Rep* 29.

164. Zheng, L., Zhang, J., Carthew, R. W. (1995). Frizzled regulates mirror-symmetric pattern formation in the *Drosophila* eye. *Dev* 121, 3045-3055.

LIST OF PUBLICATIONS

1. Mihály, J., Matusek, T., **Pataki, C.** (2005). Diego and friends play again. *FEBS Lett* 272, 3241-3252. **IF= 3,3**
2. Rus, F., Kurucz, É., Márkus, R., Sinenko, S. A., Laurinyecz, B., **Pataki, C.**, Gausz, J., Hegedüs, Z., Udvardy, A., Hultmark, D., Andó, I. (2006). Expression pattern of Filamin-240 in *Drosophila* blood cells. *Gene Expr. Patterns* 6, 928-934. **IF= 2,1**
3. **Pataki, C.** (2006). Isolation of new planar polarity genes in *Drosophila melanogaster*. *Acta Biol Szegediensis* 50, 3-4.
4. Weber, U., **Pataki, C.**, Mihály, J., Mlodzik, M. (2008). Combinatorial signaling by the Frizzled/PCP and Egfr pathways during planar cell polarity establishment in the *Drosophila* eye. *Dev Biol* 316, 110-123. **IF= 5,234**
5. Matusek, T., Gombos, R., Szécsényi, A., Sanchez-Soriano, N., Czibula, Á., **Pataki, C.**, Gedai, A., Prokop, A., Raskó, I., Mihály, J. (2008). Formin proteins of the DAAM subfamily play a role during axon growth. *J Neurosci* 28, 13310-13319. **IF= 7,5**
6. **Pataki, C.**, **Matusek, T.**, Kurucz, É., Andó, I., Jenny, A., Mihály, J. (2009). *Drosophila* Rab23 is involved in the regulation of the number and planar polarization of the adult cuticular hairs. Published ahead of print in February 1, 2010 in *Genetics*. **IF= 4**

ACKNOWLEDGEMENTS

First of all I would like to express my gratitude to my supervisor Dr. József Mihály for giving me the possibility to work in his laboratory and for his contributions that initiated my interest to the subject and his suggestions and advises that affected my scientific point of view. The experience I obtained in his group will always help me in the future. Further, I thank to my colleague Tamás Matusek for all his help and teaching and to all the members of the group - Rita Gombos, Imre Molnár, Anita Mihály-Gedai, Ede Migh, Tibor Kalmár, and our assistants: Anikó Berente, Edina Ördög, Csendes Tiborné and Szilvia Bozsó- for their help, discussions, and for creating a pleasant friendly atmosphere during work.

Special thanks to all members of the Drosophila Molecular Genetics Group for their help and advises, to Dr. István Andó for his help in antibody generation, to Dr. Andor Udvardy (Institute of Biochemistry) for his help in purifying the antibody, to Dr. Margit Pál (Institute of Biochemistry) for injecting the embryos, and to the Institute of Genetics for financial support.

Finally, I am thankful to my family and my friends for their valuable help, moral support and friendship I will never forget.

SUMMARY

Epithelial cells commonly become polarized within the plane of the cell layer during development, a property referred to as planar cell polarity (PCP) or tissue polarity. This phenomenon is evident in many vertebrate tissues (such as the ordered arrangement of scales on fish or feathers of birds, hairs of mammalian skin, the cilia of the respiratory tract or oviduct or stereocilia of the sensory epithelium in the organ of Corti). Although recent reports demonstrated that PCP regulation is highly conserved throughout the animal kingdom, such polarity patterns are perhaps best studied in *Drosophila*. PCP in flies is most evident in the wing, which is covered by uniformly polarized, distally pointing hairs, in the epidermis where sensory bristles and trichomes point to the posterior, and in the eye where PCP is manifest in a mirror symmetric arrangement of ommatidia.

Genetic and molecular studies of *Drosophila* led to identification of a set of genes, called PCP genes that are directing the establishment of PCP. Mutations in a number of genes result in abnormal wing hair polarity patterns without major effects on other aspects of tissue morphogenesis. Based on their cellular phenotypes, initial studies placed PCP genes into four groups. Mutations in the first group including *ft* (*fat*), *ds* (*dachsous*) and *fj* (*four-jointed*) (referred to as the Ft/Ds group), display wing hairs with reversed polarity derived from prehairsts that form at the cell edges (Adler et al., 1998; Strutt and Strutt, 2002). The second group (core group) includes *fz* (*frizzled*), *dsh* (*disheveled*), *fmi* (*flamingo*), *stbm* (*strabismus*), *pk* (*prickle*) and *dgo* (*diego*), mutants of which impair hair orientation to a various degree, some cells display double hairs, and prehairsts typically form in the center of the cells (Wong and Adler, 1993). The third group consists of *in* (*inturned*), *fy* (*fuzzy*), *fritz* (*fritz*) (In group) and causes the formation of multiple (mostly two) hairs per cell that are roughly equal in size, slightly misoriented, and derive from prehairsts from around the cell cortex in abnormal positions. Finally the fourth group includes *mwh* (*multiple wing hairs*) that is characterized by the presence of four or more hairs equal in size in each cells initiated from periphery. Double mutant analysis demonstrated that these phenotypic groups also represent epistatic groups from which *mwh* is epistatic to all the other groups, the In group is epistatic to Ft/Ds group and core group and the core group is epistatic to Ft/Ds group. These data together suggest that PCP genes act in a regulatory hierarchy where the Ft/Ds group is on the top followed downstream by core, In and *mwh* groups. Although the existence of such a linear hierarchy is debated (Casal et al., 2006; Lawrence et al., 2007) it is clear that PCP genes regulate (1) wing hair orientation, (2) the place of hair formation, and (3) the number of trichomes formed.

Whereas, the molecular mechanism that restricts prehair formation to the distal vertex of the wing cells is still elusive, it has been demonstrated that the core proteins adopt an asymmetrical subcellular localization when prehair forms. This localization appears to be critical for proper trichome placement (Mihály et al., 2005; Seifert and Mlodzik, 2007). The core PCP proteins are first recruited to the apical cell surface and subsequently segregate into complementary apical sub domains before the onset of hair formation. Fmi localizes to proximal and distal surfaces (Ursui et al., 1999; Shimada et al., 2001), Fz, Dsh and Dgo localizes specifically to the distal surface (Axelrod, 2001; Strutt, 2001; Das et al., 2004) while Pk and Stbm localizes on the proximal surface (Tree et al., 2002b; Bastock et al., 2003). Subsequent work revealed that, in addition to the core proteins, In protein also displays an asymmetrical pattern with accumulation to the proximal zone (Adler et al., 2004). Significantly, the absence of any of the core PCP proteins prevents the asymmetric localization of the other PCP proteins and that of In. However, in agreement with the epistatic data, asymmetric core PCP protein localization does not depend on *in* function (Adler et al., 2004). Very recent findings demonstrate that Fy and Frtz also show a proximal enrichment, and, together with In, activate Mwh that is enriched on the proximal side of the wing cells as well (Yan et al., 2008; Strutt and Warrington, 2008).

It has been shown that the core PCP proteins are found in symmetric complexes until 24 hours APF, when they relocalize and become asymmetrically enriched until prehair formation begins at 30-32 hours APF, but then, by 35 hours APF, they again fail to display an asymmetrical pattern.

How exactly these elements act together to polarize tissues properly, is still an unsolved problem. A model or working hypothesis that is consistent with most of the experimental data is as follows. First a directional clue that is provided by the Fj, Ds and Ft proteins determines the axis of polarization. This somehow initiates the asymmetric relocalization of the core PCP proteins that is enlarged by feedback mechanisms between the core elements themselves. This will lead to high Fz signaling activity on the distal side of the cell, which will subsequently activate (an as yet unidentified) effector proteins in the distal vertex where they initiate prehair formation. Additionally, it is believed that the In complex prevents hair formation on the proximal side of the cell. Although this model explains many observations, the mechanistic details on protein localization are largely missing or poorly understood, the link between Fz signaling and asymmetric localization is not understood and it remains a mystery how upstream elements are coupled to the asymmetric enrichment of PCP proteins.

Furthermore the tissue specific downstream components or their way of action is still an open problem.

The aim of this work was to answer a part of these questions by isolating new PCP genes, and by studying their role in PCP signaling and development. In order to do so, we employed the FRT/Flp mosaic system to induce homozygous mutant clones on the wing and notum by Ubx-Flp. After chemical mutagenesis of the 2L, 2R and 3R chromosomal arms, we have isolated 33 new PCP mutants, 3 on 2L, 3 on 2R and 27 on 3R. Complementation analysis and genetic mapping of our mutants revealed that one of the new complementation groups (consisting of five members) identifies *Kuzbanian-like (Kul)*. This gene behaves like a core polarity gene because it affects PCP on the notum, wing and eye. The new alleles carry amino acid changes in the metalloprotease domain of the Kul protein, four of them in the C481, and one of them in the V603 position. Deeper analysis of these mutants is subject of future investigations.

Genetic mapping of another new PCP mutant from 3R, has led to the conclusion that this allele carries a point mutation in the Switch 1 region of the GTPase domain of the *Rab23* gene. The mutation affects an aminoacid residue (T69, corresponding to T35 of Ras) that is conserved in the whole small GTPase superfamily. This point mutant (named *Rab23^{T69A}*) is semilethal and displays a strong multiple wing hair phenotype, and mild hair orientation defects.

Because no other *Rab23* alleles were available, we generated independent alleles by P-element remobilization. One of these alleles, *Rab23⁵¹* is homozygous viable and displays a strong multiple wing hair phenotype. *Rab23^{T69A}* and *Rab23⁵¹* maintain their phenotype over deficiency chromosomes uncovering the gene, behaving as strong LOF or functionally null mutants. We were able to fully rescue the phenotype of these mutants by providing one copy of the wild type *Rab23* gene. Silencing of *Rab23* by *RNAi* using ubiquitously expressed drivers resulted in a moderately strong multiple hair phenotype but neither viability nor the morphogenesis of tissues other than the wing were affected. The *Rab23* mutants exhibit trihome orientation defects and multiple hairs on the abdomen and legs as well, without affecting bristle polarity. Together these data suggest that *Rab23* is a peculiar PCP gene that has a role in determination of trichome orientation and number without affecting the polarity pattern multicellular structures, such as bristles or unit eyes.

It has been shown that the mouse *Rab23* orthologue is an essential negative regulator of the Shh (Sonic-hedgehog) pathway during neuronal patterning of the embryo (Eggenchwiler et al., 2001). Therefore we analyzed *Rab23* homozygous mutant embryos and

adult tissues, but we failed to find any evidence for a *Rab23* involvement in *Drosophila* Hedgehog signaling. *Rab23* is not expressed in the *Drosophila* embryonic CNS and no CNS defects were detected in *Rab23* mutant embryos either, therefore most likely *Rab23* has no role in neuronal development in flies indicating that the role of *Rab23* gene in Shh signaling is restricted to the vertebrates. In agreement with this, the embryonic cuticle hair pattern of *Rab23* mutants shows no sign of *Rab23*'s involvement in Hh pathway in *Drosophila*.

To investigate *Rab23* function at the cellular level, we examined prehair initiation in *Rab23*⁵¹ homozygous mutant pupal wing cells, and in *Rab23*^{T69A} mutant clones. We found that in the absence of *Rab23* apical actin accumulation is not restricted to the distal vertex, instead, the actin network was diffused and many cells developed multiple hairs in abnormal positions at the cell periphery. Additionally, prehair initiation is somewhat delayed in the *Rab23* mutant tissue. Since the multiple hairs were always restricted to the mutant area, *Rab23* acts cell autonomously.

Recent studies revealed that the wing epithelial cells are irregularly shaped throughout larval and early pupal stages, but most of them become hexagonally packed shortly before prehair formation (Classen et al., 2005). We noticed that some of the *Rab23* mutant wing cells fail to adopt a hexagonal shape at around 30-32 hours APF. We quantified this effect and found that in the *Rab23*^{T69A} point mutant the ratio of the non-hexagonally shaped cells is significantly higher compared to wild type wing cells. As a comparison we measured the packing defects in two core PCP mutants, *stbm*⁶ and *dsh*¹ too. Because the strength of the *Rab23* induced packing defects is comparable to the effect of the core mutations, this data suggest that *Rab23* might also be an important determinant of cellular packing.

Next we addressed if the packing defects revealed in *Rab23* mutant wings correlate with hair orientation defects and /or the formation of multiple hairs also exhibited upon loss of *Rab23*. However, we found that *Rab23* regulates cellular packing, and hair orientation and number, independently. To extend this analysis, we investigated the packing defects of other mutations causing multiple hairs, like *in*, *frtz* and *mwh*. These mutants exhibit somewhat weaker packing defects than *Rab23*, but in the same way, the formation of multiple hairs does not appear to correlate with irregular cell shape in these cases either. These results demonstrate that cell packing has no direct effect on the number of prehair initiation sites in the wing epithelial cells. In regard of hair orientation our data support the same conclusion, that is similar to the findings of Classen et al., 2005 for the case of the core PCP mutations, but opposite to the case of *fat* (*ft*) mutant clones (Ma et al., 2008).

It has been recently shown that asymmetric accumulation of the core PCP proteins depends on hexagonal packing, and because in our mutants packing was altered, we were curious if Rab23 has any effect on core PCP protein localization in different stages of development. To address this issue, first we examined the localization pattern of Fmi in early, 6 hours APF, *Rab23*⁵¹ mutant wings, but we failed to detect any localization defects in this stage of development. Next, we examined the localization pattern of the PCP proteins in later stages (24-32h APF) in *Rab23*⁵¹ homozygous wings and *Rab23*^{T69A} clones. We found that at this stage the core proteins and In fail to polarize properly in a *Rab23* mutant tissue, although they still accumulate into apico-lateral complexes. From these experiments we concluded that *Rab23* plays a role only during the late phase of PCP protein localization.

To understand the mechanism whereby Rab23 contributes to core PCP protein localization, we examined the subcellular distribution of YFP::Rab23 in developing pupal wings. We found that at 24-32 hours APF the Rab23 protein is predominantly enriched in the cell membrane in the apico-lateral zone. This pattern was detected before and after this developmental stage, and it seems that Rab23 has no polarized distribution during pupal development. These observations were strengthened with results from examining flies expressing the YFP::Rab23 in flip-out clones or the constitutively active and dominant negative form of Rab23.

Since Rab23 is localized mainly to the plasma membrane in pupal wings and core PCP protein asymmetric localization is also linked to the membrane, it was not informative to check the colocalization between Rab23 and core elements in this system. However, we were curious to know which core protein(s) might be directly regulated by Rab23, therefore we compared the subcellular distribution of different core proteins (Fz, Dsh, Dgo, Stbm, Pk) with Rab23 in S2 cells. We observed that Pk and Stbm show a partial colocalization with Rab23. Because Pk or Stbm did not show membrane localization when expressed alone or together in S2 cells, it was not possible to test directly if Rab23 affects Pk or Stbm endocytosis. Nonetheless these results indicated that Rab23 might affect core protein distribution by regulating Pk or Stbm. This hypothesis was strengthened by the observation that in cells transfected with Rab23T69A (corresponding to the point mutant) the degree of colocalization between Rab23T69A and Pk was much lower. Unfortunately, a similar experiment was not possible in the wing because of the low quality of the available Rab23 antibody but we were able to show that Rab23 and Pk can be coimmunoprecipitated from pupal wing protein extracts, indicating that they may act in the same protein complex.

If the sole function of Rab23 would be to promote the cortical polarization of Pk, and may be some other core proteins, it would be expected that *Rab23* mutants have similar phenotype as *pk* or mutations of the core group. However, the strong multiple hair phenotype of *Rab23* is different from the orientation defects shown by core group mutants. Thus, it seems that *Rab23* has two distinct, albeit not necessarily independent, roles during the establishment of tissue polarity in wing. The first role is in PCP protein polarization, the second is to restrict actin accumulation to a single site. Consistent with the second role, we found that *Rab23* dominantly enhances the weak multiple hair phenotype of the core mutants without affecting their hair orientation defects, while the *Rab23* homozygous mutant phenotype is sensitive to the gene dose of the In group that has role in the regulation of wing hair number.

Further, we were wondering what is the position of *Rab23* in the hierarchy of known PCP genes, therefore we initiated double mutant analysis of *Rab23* with *fz²¹*, *dsh¹*, *pk^{pk30}*, *stbm⁶*, *in¹*, *frtz¹* and *mwh¹*. Our results have shown that in respect of the regulation of hair orientation, *Rab23* has minor or no function there, which is entirely consistent with the single mutant phenotype of *Rab23*. In respect of the determination of the prehair initiation site, the In group and *mwh* clearly appears to function downstream of or later than *Rab23*. Conversely, the core PCP proteins and Rab23 function in parallel pathways during the restriction of trichome placement.

Taken the Rab23 multiple wing hair phenotype and the effect on PCP protein localization together with the dominant genetic interactions and double mutant analysis, these results suggest that Rab23 links cortical PCP polarization to a mechanism that is more directly involved in the repression of hair initiation at ectopic sites. In the simplest model, Rab23 would contribute to the proximal accumulation of Pk, and would also play a role in linking In activation to the proximal cell domain.

ÖSSZEFOGLALÁS

Az egyedfejlődés folyamán az epitéliális sejtek gyakran a szövetek síkjában is polarizálódnak. Ezt a jelenséget planáris vagy szöveti polaritásnak (SZP) nevezzük. A SZP jelensége számos gerinces állat szöveiben is megfigyelhető, ilyenek a halak pikkelyei, a madarak tollai, az emlősök szőrmintázata, a légső vagy a petevezeték csillói vagy a belső fül érzékhámjában a Corti-féle szerv sztereocilliumainak elrendeződése. Habár az utóbbi időben kimutatták, hogy a polaritás kialakulása egy, az egész állatvilágban konzervált szabályozási folyamat eredménye, e jelenséget mindeztáig az ecetmuslicában (*Drosophila melanogaster*) tanulmányozták legbővebben. Az ecetmuslicában a SZP a szárnyon a legfeltűnőbb, mivel minden egyes szárnysejtből egy apró szőr (ún. trichóma) nő ki és ezek mindegyike a disztális irányba mutat, de nyilvánvaló az epidermiszen is amelyet egységesen hátrafelé mutató érzékszőrök borítanak, illetve az összetett szemben, amelyet tükör szimmetrikusan elhelyezkedő elemi szemek alkotnak.

Az ecetmuslicán végzett genetikai és molekuláris biológiai kísérletek elvezettek a SZP-t meghatározó gének azonosításához, ezeket polaritási géneknek nevezték el. Ezen gének egy részének mutációja hibás szárnyászőr mintázatot eredményez anélkül, hogy befolyásolná a szöveti fejlődés egyéb aspektusait. A sejt fenotípusuk alapján ezeket a géneket négy csoportba sorolták. Az első csoport génjeinek mutációi, a *ft* (*fat*), *ds* (*dachsous*) és *ff* (*four-jointed*) avagy a Ft/Ds csoport, fordított polaritású szőrmintázatot mutatnak, a szőrkezdemenyek a sejtek szélén alakulnak ki (Adler és mtsai., 1998; Strutt és Strutt, 2002). A második csoport tartalmazza a *fz* (*frizzled*), *dsh* (*dishevelled*), *fmi* (*flamingo*), *stbm* (*strabismus*), *pk* (*prickle*) és *dgo* (*diego*) (core csoport) géneket, amelyek mutációja megváltoztatja a tüskék kinövési irányát, sokszor örvényes fenotípust eredményez, ritkán kettős szőrkinövések is előfordulnak és a tüskék a sejtek közepéből nőnek ki (Wong és Adler, 1993). A harmadik csoport (In csoport) tartalmazza az *in* (*inturned*), *fy* (*fuzzy*) és *frtz* (*fritz*) géneket. Ezek mutációja többes, elsősorban kettős szőrkinövéseket eredményez, amelyek egyforma hosszúságúak, orientációs hibákat mutatnak és az iniciáció nem a sejtek disztális csúcsából hanem a az apikális sejtmembrán mentén random pozícióból történik. Végül a negyedik csoport tartalmazza az *mwh* (*multiple wing hairs*) gént, amelynek mutánsaira jellemző, hogy sejtenként négy vagy több egyforma tüskét növesztenek sejtenként. A kettős mutáns elemzések kimutatták, hogy ezek a fenotípus csoportok episztatikusak egymáshoz képest, mégpedig az Mwh csoport episztatikus az összes többihez, az In csoport a Ft/Ds csoporthoz és a core csoporthoz, míg a core csoport a Ft/Ds csoporthoz képest. Ezek az

adatok azt sugallták, hogy ezek a gének egy lineáris hierarchikus szabályozás elemei, ahol a Ft/Ds csoport van legfelül és ezt követik a core, In és Mwh csoportok. Habár egy ilyen lineáris hierarchia létezése még vitatott (Casal és mtsai., 2006; Lawrence és mtsai., 2007), az világos, hogy a SZP gének szabályozzák a (1) szárnyszőr orientációját, (2) a kinövés helyét és (3) a sejtenkénti szőrök számát.

Habár még nem ismert az a molekuláris mechanizmus, amely meghatározza az aktin tüske kinövési helyét, kimutatták, hogy a core fehérjék aszimmetrikus sejten belüli mintázatot mutatnak az aktin tüske kialakulásakor. Ez a lokalizáció kritikusnak tűnik a szőrkinövés helyének meghatározásában (Mihály és mtsai., 2005; Seifert és Mlodzik, 2007). A core fehérjék előbb kihorgonyozódnak a sejtek apikális felszínén majd polarizált komplexekben halmozódnak fel a szőriniciáció előtt. A Fz, Dsh és Dgo fehérjék jellegzetesen a disztális oldalon halmozódnak fel (Axelrod, 2001; Strutt, 2001; Das és mtsai., 2004), a Pk és a Stbm a proximális oldalra vándorol (Tree és mtsai., 2002; Bastock és mtsai., 2003), míg a Fmi a proximális és a disztális oldalon egyaránt kimutatható (Usui és mtsai., 1999; Shimada és mtsai., 2001). Későbbi munkákból kiderült, hogy az In fehérje is aszimmetrikus mintát mutat ebben a fejlődési stádiumban, és a proximális oldalon halmozódik fel (Adler és mtsai., 2004). Megfigyelték, hogy bármely core fehérje hiánya befolyásolja a többi core elem és az In fehérje aszimmetrikus lokalizációját és az episztázis analízisnek megfelelően, a core fehérjék aszimmetrikus lokalizációja nem függ az *in* funkciójától (Adler és mtsai., 2004). A legfrissebb adatok alapján a Fy és Frtz fehérjék ugyancsak a proximálisan halmozódnak fel és az In-el együtt aktiválják az ugyancsak proximálisan feldúsuló Mwh-t (Yan és mtsai., 2008; Strutt és Warrington, 2008).

Ismert, hogy a bebábozódás utáni (BU) 24 óráig a fent említett fehérjék szimmetrikus komplexeket alkotnak, majd relokalizálódnak és aszimmetrikusan halmozódnak fel a membrán megfelelő oldalán, amíg a szőrkinövés elkezdődik (30-32 óra BU). Később, a bebábozódás után 35 órával, újra felbomlik ez az aszimmetrikus mintázat.

Mindmáig nem tisztázott, hogy a fenti elemek pontosan hogyan befolyásolják a megfelelő szöveti polaritás kialakulását. Egy model vagy munkahipotézis, ami megfelel a kísérleti megfigyelések nagy részének, a következő. Előbb egy, a Fj, Ds és Ft fehérjék által meghatározott irányadó jel, kijelöli a polarizáció irányát. Ez valamilyen módon elindítja a core fehérjék aszimmetrikus relokalizációját, amit egy közöttük lévő visszacsatolós mechanizmus erősít. Ez egy magasabb Fz aktivitást eredményez a sejtek disztális oldalán, ami aktiválja a disztális oldalon lévő végrehajtó fehérjéket (amelyek még ismeretlenek) és ez által

elindítja a szőrkinövést ezen az oldalon. Másrészt elterjedt az a nézet miszerint az In komplex szerepe, hogy megakadályozza a szőrkinövést a sejtek proximális oldalán. Annak ellenére, hogy ez a model számos megfigyelést megmagyaráz számos kérdés tisztázatlan maradt. Nem ismeretesek azok a mechanizmusok, amelyek a fehérjék lokalizációjáért felelősek, ismeretlen a Fz jelátvitel és a fehérjék aszimmetrikus felhalmozódása közti kapcsolat, nem tudjuk, hogy a felső elemek hogyan befolyásolják a core fehérjék aszimmetrikus felhalmozódását, valamint nem ismeretes az összes szövetspecifikus végrehajtó elem és a hatásmechanizmusuk sem.

Ezen munka célkitűzése az volt, hogy olyan új, a SZP kialakításában résztvevő elemeket azonosítsunk és tanulmányozzunk, amelyekkel választ adhatnánk a fenti kérdések egy részére. Ennek megvalósítására egy nagy léptékű mutagenézis kísérletet hajtottunk végre, amelyben az FRT/Flp mozaik rendszert használtuk arra, hogy az Ubx-Flp segítségével nagyméretű mutáns klónokat hozzunk létre a muslicák szárnyán és notumán. Kémiai mutagenézisnek vetettük alá a második kromoszóma jobb és bal karját, valamint a harmadik kromoszóma jobb karját és így 33 új SZP mutánst azonosítottunk. Ebből 3 a második kromoszóma bal karjára, 3 a jobbra és 27 a harmadik kromoszóma jobb karjára térképeződött. A kapott jelöltek komplementációs analízise és genetikai térképezése kimutatta, hogy öt közülük, amelyek SZP fenotípussal rendelkeztek a notumon, szárnyon és szemben, egy komplementációs csoportot alkotnak és a *Kul* (*Kuzbanian-like*) gén pontmutánsai. Ezek az allélek a *Kul* fehérje matalloproteáz doménjében hordozzák az aminósav cserét, négyben a C481-es, egyben a V603-as aminósav érintett. Ezen allélek behatóbb jellemzése, csoportunk jövőbeni tervei közé tartozik.

Egy másik új, a harmadik kromoszóma jobb karjára térképeződő mutáns genetikai jellemzése azt mutatta, hogy ez az allél egy pontmutációt hordoz a *Drosophila Rab23* gén GTPáz doménjének első kapcsoló régiójában. A 69-es pozícióban található mutáció, a kis GTPázok családjában nagymértékben konzervált Threonin aminósavat érintette. Ez a pontmutáns (amelyet *Rab23^{T69A}*-nak neveztünk el) szemilevális és közepes erősségű többes szőrkinövéses fenotípust, illetve szőr orientációs hibákat mutat.

Mivel ezen a pontmutánson kívül nem állt rendelkezésünkre más *Rab23* allél, a további vizsgálatokhoz P-elem ugrasztás segítségével független alléleket hoztunk létre. Az ily módon létrehozott egyik deléciós mutáns, a *Rab23⁵¹*, homozigóta életképes és erős többes szőrkinövéses fenotípust mutat. A *Rab23^{T69A}* és *Rab23⁵¹* mutánsok megőrzik fenotípusukat a gént kitakaró deléció fölött is, funkcióvesztéses vagy funkcionálisan null mutánsként viselkednek. A teljes hosszúságú vad típusú *Rab23* gén egy példányát tartalmazó konstrukció

segítségével sikerült teljes mértékben menekítenünk a mutáns fenotípust. A *Rab23* funkció csendesítése RNS interferenciával különböző driverek felhasználásával, moderált többes szőrkinövéses fenotípust okozott a szárnyon, de más szövetet és az életképességet nem érintette. A *Rab23* mutánsok a szárnyfenotípuson túlmenően, az abdomen kutikulát és a lábat érintő többes trichómakinövéseket is mutatnak anélkül, hogy az érzékszőrök polaritását befolyásolnák. Összesítve, ezek az eredmények azt sugallják, hogy a *Rab23* egy olyan egyedi SZP gén, melynek szerepe van a trichómák sejtenkénti számának és orientációjának a meghatározásában, anélkül, hogy befolyásolná a többsejtű képződmények-pl. az érzékszőrök és az elemi szemek polaritását.

Korábbi kísérletekben kimutatták, hogy a *Rab23* egér ortológ a Shh (Sonic hedgehog) jelátviteli út negatív szabályozója az embrionális idegrendszer fejlődése során (Eggenschwiller és mtsai., 2001). Ezért mi is megvizsgáltuk a Shh jelátviteli út aktivitását homozigóta mutáns *Rab23*⁵¹ embriókban és felnőtt szövetekben, de nem találtunk arra bizonyítékot, hogy ecetmuslicában a *Rab23* ezen útvonalon keresztül hat. A *Rab23* fehérje nincs jelen a *Drosophila* embrionális idegrendszerben és nem észleltünk idegrendszeri hibákat a mutáns embriókban sem. Tehát valószínűleg a *Rab23* nem játszik szerepet a *Drosophila* embrionális idegrendszerének fejlődésében, utalva arra, hogy a *Rab23* gén szerepe az Shh jelátvitelben a gerincesekre korlátozódik. Ezzel összhangban, a *Rab23* mutánsok abdomen fenotípusa sem hordozza jelét annak, hogy a *Rab23* szerepelne a Hh jelátviteli útban, muslicában.

Hogy betekintést nyerjünk a *Rab23* sejtszinten játszott szerepébe, megfigyeltük a szőr iniciációt *Rab23*⁵¹ homozigóta mutáns, illetve *Rab23*^{T69A} mutáns klónokat hordozó szárnyakon. Azt láttuk, hogy *Rab23* hiányában az apikális aktin felhalmozódás nem korlátozódik a sejtek disztális csúcsára, hanem az apikális régióban mindenhol kimutatható egy diffúz aktin hálózat, és később nagy számban jelentek meg többes szőrök a sejtek perifériáján. Ezetül, a szőrkinövés időpontja késett a vad típushoz képest, de a többes szőrkinövések mindig a mutáns szövetre korlátozódtak, ami arra utal, hogy a *Rab23* sejtautonóm módon hat.

Korábbi megfigyelések szerint a szárnysejtek rendezetlen alakúak a lárva stádiumban és a bábfejlődés elején, de többségük a szőriniciáció előtt hatszögűvé válik (Classem és mtsai, 2005). Megfigyeltük, hogy a *Rab23* mutáns sejtek egy része nem veszi fel a hatszögű alakot 30-32 órával a BU. Ezt a hatást számszerűsítettük és kiderült, hogy a *Rab23*^{T69A} pont mutánsban szignifikánsan nagyobb a nem megfelelően csomagolódott sejtek száma a vad

típushoz képest. Összehasonlítás képpen megvizsgáltuk a szárnysejtek csomagolódását *stbm*⁶ és *dsh*¹ core mutánsokban is. Mivel a *Rab23* mutáció okozta csomagolódási hibák összehasonlíthatóak a core mutációk hatásával, ezen eredmények azt sugallják, hogy a *Rab23*-nak meghatározó szerepe van a fejlődés során a szárnyszövet csomagolódásában.

Kíváncsiak voltunk arra, hogy van-e valamilyen összefüggés a sejtek alakja és a *Rab23* mutáns orientációs hibákat és többes szőrkinövéseket mutató fenotípusa között. Azt találtuk, hogy a *Rab23* függetlenül befolyásolja a sejtek csomagolódását, illetve a többes szőrkinövést és szőr orientációt. Hogy kiszélesítsük megfigyeléseinket, megvizsgáltuk a sejtalakot más, többes szőrkinövést mutató mutánsban (*in*, *frtz*, *mwh*) és habár ezek valamivel gyengébb csomagolódási fenotípust mutattak, itt sem találtunk összefüggést a sejtenkénti szőrszám és a sejtek alakja között. Ezen eredmények azt mutatják, hogy a szárnyszövet csomagolódásának nincs közvetlen hatása a szőriniciációs helyek számának meghatározására a szárnyszövetben. A szőr orientáció és sejtalak közti összefüggést illetően, megfigyeléseink alátámasztják Classen és mtsai. (2005) core génekre vonatkozó eredményeit, és ellentmondanak a *fat* mutáns klónokban tapasztalt megfigyeléseknek (Ma és mtsai, 2008).

Nemrég kimutatták, hogy a szárnysejtek a szőr iniciációt megelőzőleg válnak hatszögűvé és ez a folyamat befolyásolja a core SZP fehérjék aszimmetrikus elrendeződését. Mivel a mi mutánsainkban a hexagonális csomagolódás hibás volt, kíváncsiak voltunk arra, hogy a *Rab23*-nak van-e valamilyen szerepe a core SZP fehérjék lokalizációjára a fejlődés különböző szakaszaiban, de a Fmi fehérje eloszlása a bábfejlődés kezdetén (6 órával a BU) a *Rab23* mutáns szárnyakban normális volt. A következőkben megvizsgáltuk a fehérjék lokalizációját későbbi fejlődési stádiumokban (24-32 órával a BU) *Rab23*⁵¹ homozigóta és *Rab23*^{T69A} klónos szárnyakon. Azt találtuk, hogy ebben a fejlődési szakaszban a core és In fehérjék lokalizációs hibát mutatnak a *Rab23* mutáns szövetben, habár az apiko-laterális zónában történő feldúsulásuk nem sérül. Ezen kísérletekből levonhatjuk azt a következtetést, hogy a *Rab23* csak a késői SZP fehérje lokalizációban játszik szerepet.

Hogy megértsük azt a mechanizmust mely segítségével a Rab23 hozzájárul a core fehérjék lokalizációjához, megvizsgáltuk a YFP::*Rab23* tarnszgént hordozó legyek szárnyát. Azt láttuk, hogy 24-30 órával a BU után a Rab23 az apiko-laterális övezetben dúsul fel, de a membrán minden területén megtalálható. Ez a mintázat megfigyelhető volt a korábbi és későbbi fejlődési stádiumokban is tehát a Rab23 nem mutat polarizált felhalmozódást a bábfejlődés folyamán. Ezen eredményeket alátámasztották az YFP::*Rab23* flip-out klónon kísérletben vézett megfigyelések, illetve a CA Rab23 mintázata.

Mivel a *Rab23* bábszárny mintázata átfedést mutatna a core fehérjék lokalizációjával, nem lett volna informatív a fehérjék lokalizációjának átfedését ebben a rendszerben vizsgálni. Ezért ahhoz, hogy megnézzük, mely SZP fehérjéket szabályozhatja a *Rab23*, összehasonlítottuk a különböző core fehérjék (*Fz*, *Dsh*, *Dgo*, *Stbm*, *Pk*) lokalizációját *S2* sejtekben *Rab23* jelenlétében és hiányában. Azt láttuk, hogy a *Pk* és a *Stbm* részleges átfedést mutatott a *Rab23*-al. Mivel a *Pk* vagy a *Stbm* nem mutatott membrán lokalizációt, nem volt lehetséges annak tesztelése, hogy a *Rab23* befolyásolja-e a *Pk* vagy *Stbm* endocitózist. Ezek az eredmények azt mutatták, hogy a *Rab23* a *Pk* és/vagy a *Stbm* fehérjén keresztül befolyásolhatja a core fehérjék eloszlását. Ezt a feltevésünket az is alátámasztotta, hogy azokban a sejtekben, amelyek a *Rab23T69A* fehérjét termelték, sokkal alacsonyabb volt az átfedés a mutáns *Rab23* és a *Pk* között. Sajnos hasonló kísérletek elvégzése nem volt lehetséges a szárnyon, a gyenge minőségű *Rab23* ellenanyag miatt, de a *Rab23* és a *Pk* fehérjék koimmunoprecipitálhatók voltak bábszárnyakból készített fehérje kivonatokban, ami arra utal, hogy egy fehérje komplexben található.

Ha a *Rab23* egyetlen szerepe az volna, hogy szabályozza a *Pk* lokalizációt és ezáltal más core fehérjékét, azt várnánk, hogy a *Rab23* mutánsok fenotípusa a *pk* mutánsok fenotípusához vagy a core gének mutáns fenotípusához hasonlítson. De a *Rab23* erős többes szőrkinövéses fenotípusa eltér a core mutációk okozta orientációs hibáktól. Tehát feltehetően a *Rab23*-nak két különböző, de nem feltétlenül független szerepe van az SZP kialakításában, a szárnyban. Az első a fehérjék polarizált elosztása, a második az aktin felhalmozódás és ezáltal a szőrkinövés helyének meghatározása. A másodiknak említett szerepével egybeesik az a megfigyelésünk, hogy a *Rab23* dominánsan erősíti a core gének gyenge többes szőrkinövéses fenotípusát, de nincs erős hatása a szőrök orientációjára, míg a homozigóta mutáns fenotípus érzékeny az *In* csoport génjeire, amelyek szerepet játszanak a sejtenkénti szőrszám meghatározásában.

A következőkben kettős mutáns analízist végeztünk, hogy meghatározzuk a *Rab23* helyét a polaritási jelátviteli útban. Ennek érdekében elvégeztük a *Rab23* kettős mutáns elemzését a *fz²¹*, *dsh¹*, *pk^{pk30}*, *stbm⁶*, *in¹*, *frtz¹* és *mwh¹* allélekkel. Eredményeink azt mutatták, hogy a szőrorientáció szabályozása szempontjából, a *Rab23*-nak kevés szerepe van ebben a folyamatban, ami megfelel a *Rab23* egyes mutáns fenotípusának. A szőriniciáció helyének meghatározása szempontjából az *In* csoport és az *mwh* downstream/ vagy később hat a *Rab23*-hoz képest. Ezzel ellentétben, a core fehérjék és a *Rab23* párhuzamos útvonalban hatnak a szőrkinövés helyének meghatározásakor.

Összegezve, a *Rab23* mutáns többes szőrkinövéses fenotípusát a SZP fehérjék lokalizációjára kifejtett hatását, a domináns genetikai interakciók és a kettős mutáns analízis eredményeit, azt mondhatjuk, hogy a szárnysejtekben a *Rab23* összeköti a fehérjék kortikális lokalizációját az ektopikus szőrkinövés megakadályozásával. Egy nagyon egyszerűsített modellben a *Rab23* szerepet játszhat a Pk proximális felhalmozódásában és összekötheti az In aktivációt a proximális sejt doménnel.